Doctoral dissertation (Shinshu University)

Mechanical properties of CFRPs enhanced by carbon film using magnetron sputtering technology

マグネトロンスパッタ炭素膜強化 CFRPs の力学特性に関する研究

March　2023

YANG LI

Abstract

Carbon fiber-reinforced polymer (CFRP) composites are widely used in many industries because of their excellent properties, e.g., high specific strength, high specific stiffness, electromagnetic shielding, and good electrical and thermal conductivity. However, the carbon fibers in the original filament have defects, affecting their mechanical properties, and their surface is smooth and chemically inert, making it difficult to form a strong interfacial bond with resin; thus, it is difficult for carbon-fiber composite materials to meet the needs of higher fields with regard to comprehensive performance. Therefore, researchers have improved the defects of carbon fibers by improving the spinning process and increasing the fineness of the raw filaments. Surface treatment of carbon fibers has been performed to increase the interfacial bonding strength of carbon fibers and resins using physical and chemical methods, e.g., increasing the fiber surface roughness, surface energy, and chemical bonding strength. Although the current modification methods for carbon fibers can improve the defects of carbon fibers, which can enhance their tensile properties, they increase the production cost, reduce the production efficiency, and limit the applicability of carbon fibers. The modification methods for improving the performance of the interface between the carbon fibers and the resin matrix have problems such as sacrificing the strength of the carbon fibers, polluting the environment, and cumbersome steps. In this study, I aimed to improve the interfacial bonding strength of a CFRP composite by modifying its characteristics and the interfacial microstructure without reducing the strength of the carbon fibers or polluting the environment. Using magnetron-sputtering technology, a carbon film was deposited on the surface of the carbon fibers to repair defects by exploiting the homogeneity of the sputtering target and carbon fibers. Additionally, the interfacial properties of the carbon fibers and resin matrix were improved using the nanoscale property of magnetron-sputtering deposition.

To investigate the effects of the magnetron-sputtering process on the morphology and structure of deposited carbon films, carbon-film deposition was performed on two substrates: silicon wafer and carbon fibers. The effects of the magnetron-sputtering process on the surface morphology, microstructure, and phase composition of the carbon fibers were analyzed with the magnetron-sputtering time and power as variables. To evaluate the structural properties of

the magnetron-sputtered carbon films, the carbon films deposited on silicon wafers were heat-treated at 800–1200 °C. The structural properties of the magnetron-sputtered carbon films were analyzed, with a focus on the effects of magnetron sputtering on the properties of the carbon-fiber body and the mechanism underlying the effects on the mechanical properties of the CFRP composites. The most significant results of this study are presented below.

(1) The carbon film deposited via magnetron sputtering was made of carbon nanoparticles. There were microcracks on the surface of the film and a columnar structure in the cross-section of the film. The thicknesses of the carbon films deposited on the silicon wafers and carbon fibers deposited via the same magnetron-sputtering process were comparable. The surface roughness of the carbon fibers was increased after modification by magnetron sputtering, and the degree of increase depended on the scanning conditions. The magnetron-sputtering modification treatment had no effect on the microstructures or material compositions of the carbon fibers and did not affect the intrinsic properties of the carbon fibers and CFRP composites. The surface morphology and microstructure of the magnetron sputtering-deposited carbon film were changed after heat treatment. The heat treatment transformed the particle stacking structure of the original magnetron-sputtered carbon film into a continuous layer structure, and the surface changed from a surface morphology with microcracks to a carbon stacking structure with a lamellar crystal morphology. As the heat-treatment temperature increased, the lamellar crystal structure on the surface of the carbon fibers transformed into a rheological yarn-like stacking structure. The heat treatment enhanced the ordered structure of the carbon film and increased the surface roughness. Additionally, it improved the mechanical properties of the carbon film: the hardness, Young's modulus, and friction resistance increased, and the wear rate of the carbon film after heat treatment at 1000 ℃ was reduced by 28% compared with that before heat treatment.

(2) The mechanical properties of the carbon fibers were improved by magnetron-sputtering modification. The tensile breaking strengths of single and multifilament carbon fibers were increased by 9.93% and 6.9%, respectively, after the magnetron sputtering. Additionally, the magnetron sputtering significantly improved the dispersion of the tensile breaking strength of the carbon fibers; the CV value of the tensile breaking strength of single carbon fibers decreased by 57.5% at maximum, and that of multifilament carbon fibers decreased by 31% at maximum.

The tensile fracture toughness of the modified carbon fibers was significantly improved through the crack effect mechanism in the tensile process. The tensile fracture work of the single and multifilament carbon fibers was increased by 19.73% and 23%, respectively, after 250 W, 50 min magnetron-sputtering modification treatment.

(3) The mechanical properties of the CFRP composites modified by magnetron sputtering were significantly improved, including the in-plane shear strength, tensile strength, bending strength, and toughness. Owing to the deposition of the carbon film on the surface of the carbon fibers, a composite interface layer was created between the interface layers of the CFRP composite, and the load-transfer effect of the composite interface layer was used to meet the delayed failure of carbon-fiber composite damage.

CONTENTS

Chapter 1

General introduction

Chapter 1: General introduction

1.1 Introduction

With the progress of science and technology and continuous human exploration of new fields, new materials for aerospace, marine exploration, and other high-end fields have been emerging. Material compounding has gradually become the main trend in material science research to maintain pace with the development of science and production technology and the increasing demand for new materials. Compared with single-component materials, composite materials combine the excellent properties and functions of multiple materials, providing better flexibility to meet the needs arising from many aspects of production and life [1-4]. Resin-matrix composites are the most representative in the field of composite materials because of their high specific strength, light weight, and high modulus, among other characteristics. Moreover, because of their good fatigue resistance, high temperature resistance, corrosion resistance, and adaptability to extreme environments, resin-matrix composites are widely used in many fields, such as automotive, energy, sports supplies, and electronic devices [5-9].

Carbon fiber reinforced polymer (CFRP) composites have been the leading composites due to their high specific strength, high specific modulus, good fatigue resistance, and strong designability. Carbon fiber (CF) has a series of excellent properties, such as high strength, high modulus, low coefficient of thermal expansion, high temperature resistance, chemical resistance, and good electrical conductivity, and also exhibits flexibility and processability as a textile material; thus, it has become an important part of the high-end materials field since its introduction in the 1960s [10-12]. However, some issues in the production process of CFs have led to gaps between their actual and theoretical performance. Moreover, due to the influence of the carbonization process, the surface of CFs is smooth and inert and the surface energy is low, which is not conducive to resin infiltration into fiber or chemical bonding, resulting in more defects at the interface of CF composites, whereby the stress cannot be effectively transferred in the interface phase, thus affecting the comprehensive performance of the overall CF composite [13]. Therefore, it has become an important

research direction in the field of CFs and CF composites to modify the CF and its surface by various means to improve the properties of CFs, enhance the physical and chemical effects at the interface between the CF and matrix, and conduct research on the relationship between the interfacial microstructure and macroscopic mechanical properties [14-19].

In recent years, surface modification of CFs using nanotechnology has been an important means to reduce CF defects and enhance the interfacial bonding performance of CF composites, achieved by using the characteristics of small particle size and large specific surface area of nanomaterials to improve the interfacial bonding performance between the CF and resin matrix and the multi-scale structure of nanomaterials to change the load transfer to ultimately improve the mechanical properties of CF composites [20-27]. However, in practice, these modification methods are complicated, difficult to operate, and environmentally unfriendly, restricting the development and use of nanostructured interfaces in CF composites.

Presently, magnetron sputtering, a form of physical vapor deposition (PVD), is an important method to prepare nanofilm materials. Compared with other deposition technologies, it has the characteristics of fast sputtering speed, dense film layer, and good adhesion, among other characteristics. In addition, it has the advantages of suitability for a variety of target materials, availability of different variants, easy control of the preparation process, and high film quality [28-31]. Therefore, this study uses magnetron sputtering to construct a nanocarbon film on the surface of CFs. Homogeneity between the film and CF allows for repairing defects on the surface of the CF without changing its physical composition CF; simultaneously, the nano property of the film, deposited by magnetron sputtering, enables improving the interfacial bonding between the CF and resin and the mechanical properties of CFRP composites.

1.2 Composite interface theory and bonding types

1.2.1 Interface theory of composite

The composite interface is a discontinuous region between the reinforcement and

matrix phases, which plays the role of a bridge connecting the reinforcing material and matrix, thus making it an important part of the composite material. The composite interface controls the overall mechanical properties of the composite, and its presence effectively and uniformly transmits stress and prevents crack propagation, while significantly affecting the overall properties of the composite, such as the interfacial shear strength, interlaminar shear strength, and fracture toughness. As research on interfacial layers continues to advance, various interface theories have been proposed. Currently, the widely recognized interface theories include mainly chemical bonding, infiltration, meshing, diffusion, and transition layer theories [35-37].

1.2.1.1 Chemical bonding theory

The chemical bonding theory is the most widely recognized interface theory for composite materials and the most thoroughly researched. The main core of this theory is the use of chemical bonding to achieve a good combination between fibers and resins wherein the high binding energy of chemical bonds prevents the free movement of the matrix molecules in the interface area more effectively than physical effects such as the Van Der Waals force [38]. According to this theory, the interfacial bond between the fiber and resin can be effectively increased by constructing several active functional groups on the fiber surface or the resin matrix. For example, coating a coupling agent on the reinforcement material is one of the methods for the interfacial modification of composite materials based on chemical bonding theory. Choi et al [39]. used nitric acid and nitric acid combined with a glutaric dialdehyde coupling agent to modify CFs to form chemical bonds between the fibers and phenolic resin, resulting in CF composites with higher electrical conductivity and mechanical properties. In addition, chemical grafting is also an important method to modify the interface of composite materials using the chemical bonding theory [40,41]. The chemical bonding theory is used to modify the interface to ensure that as many chemical reactions as possible occur between the fiber and resin to form chemical bonds to realize the interface efficiency of composite materials. Although the chemical bonding theory is widely applicable, some disputes remain. Some scholars believe that although chemical bonds are stronger

than physical interactions, such as Van Der Waals forces and mechanical engagement, these physical interactions play an important role in the bond strength of composite interfaces. Simultaneously, only a limited number of chemical bonds can be generated in the interfacial region. Therefore, when studying the structure and interfacial interactions of the reinforcement, several factors should be considered: in addition to covalent bonds, hydrogen bonds, acid-base interactions, and other broad chemical bonds should also be considered.

1.2.1.2 Interface infiltration theory

Infiltration theory, proposed by Zisman in 1963, emphasizes that the interfacial bond strength is affected by infiltration [42]. This theory suggests that the solid–liquid interface is necessary for establishing excellent interfacial phases; the bonding between the matrix resin and the reinforcement depends on the wettability between the two phases. Due to factors such as unsmooth surface and air, some holes are formed when the fiber or reinforcement is soaked with the resin, creating defects at the material interface, resulting in stress concentration, and thereby easy cracking during loading, thus leading to poor interface performance. If good wettability exists between the two phases, the liquid phase matrix can be immersed in the defects and cavities on the surface of the CF, increasing the contact area between the two phases, excluding the gas adsorbed on the fiber surface, and slowing the generation of voids, thus improving the interfacial bond strength between the two phases. Sun et al [43]. treated the surface of CFs using oxygen plasma and observed higher reactivity between the fiber surface and matrix and a decrease from 75 to 61° in the contact angle between water and CFs. Similarly, Jang and Yang [44] modified the CF surface by plasma and found more interpenetration between the CF and PBZ matrix, which improved the interfacial properties between the CF and matrix. However, interfacial bonding is a relatively complex process, and the infiltration theory cannot explain all interfacial phenomena, e.g., the fiber wettability may deteriorate after modification; however, the interfacial bonding strength is significantly improved. Therefore, the infiltration theory needs to be improved.

1.2.1.3 Meshing theory

The mechanical meshing theory suggests that the existence of fine pores and surface grooves on the surface of the fiber reinforcement can significantly increase the fiber's specific surface area and roughness to produce stronger friction and mechanical engagement between the fiber and resin during the composite molding process, thereby increasing the interfacial bond strength between the matrix and reinforcement [45]. For example, Han Rui et al [46]. used nano-silica to roughen the surface of basalt fibers and increase the molecular wettability between basalt fibers and PP melt. They also used a mechanical meshing mechanism to enhance the mechanical friction between the basalt fibers and PP matrix, thereby improving the interfacial bonding performance between the basalt fibers and PP matrix.

1.2.1.4 Transition layer theory

Transition layer theory assumes the existence of a transition layer between the fiber reinforcement and resin matrix in the composite material that can relieve the internal stress during the molding process. The theory introduces the "deformation layer" and "inhibition layer" theories to account for the role and shape of the filter layer. The "deformation layer" theory assumes that the composite material produces additional stress between the fibers and matrix resin during the preparation process due to the large difference in the expansion coefficients, the internal stress generated during molding leads to the degradation of the composite material performance, and the existence of the transition layer plays a role in relaxing or eliminating the stress. The "inhibition layer" theory assumes that, because of the large difference in modulus between the reinforcement and matrix, the transition layer balances the modulus between the reinforcement and matrix and ensures a uniform and effective stress transfer [47,48].

1.2.1.5 Diffusion theory

Diffusion theory suggests that the interfacial layer between two-phase polymers is formed by the mutual diffusion, penetration, and entanglement of macromolecules. This diffusion is an intermolecular interaction caused by hydrogen bonding or Van Der Waals forces. However, this theory cannot appropriately explain the interfacial bonding

between polymers and inorganic materials, making this theory inapplicable to CF composites.

Although additional interface theories, such as friction, electrostatic, and acid-base theories, have gained some theoretical support and experimental basis for different fibers and resins, simultaneously more than one interfacial mechanism of action may be present. Based on the above composite interface reinforcement theory, the types of interfacial bonding of CF composites can be classified into two categories, namely mechanical and chemical bonding

1.2.2 Types of interfacial bonding of composite materials

1.2.2.1 Mechanical connection

Mechanical bonding is also called mechanical engagement or mechanical interlocking, implying that the reinforcement and matrix are meshed and interlocked through the rough structure of the surface; this mechanism is shown in Figure 1-1. Two main factors affect the degree of mechanical engagement: the first is related to the surface roughness of the reinforcing fiber; generally, the greater the roughness, the more conducive to the formation of mechanical engagement. Second, when the matrix resin undergoes a curing reaction, it shrinks, firmly binding the reinforcement to achieve a closer fit with the matrix resin. However, in practice, no separate mechanical bonding can exist between the reinforcement and matrix, with generally a weak Van Der Waals force present between the two; thus, mechanical bonding usually refers to the bonding where mechanical bonding plays a dominant role.

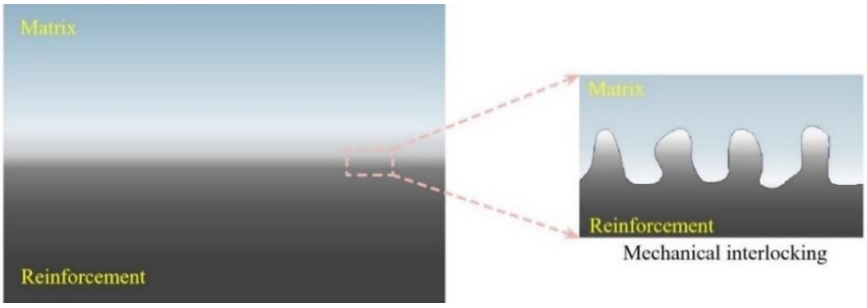

Fig. 1-1 Schematic diagram of mechanical connection

1.2.2.2 Chemical bonding

Chemical bonding refers to the chemical reaction between the fiber and matrix

resin, which and the interface is bonded by chemical bonding, as shown in Figure 1-2. Two prerequisites must be guaranteed to achieve chemical bonding: first, the fiber and resin must contain reactive groups that can participate in the chemical reaction. Second, a good wetting state should exist between the fiber and matrix to provide the conditions for chemical reactions.

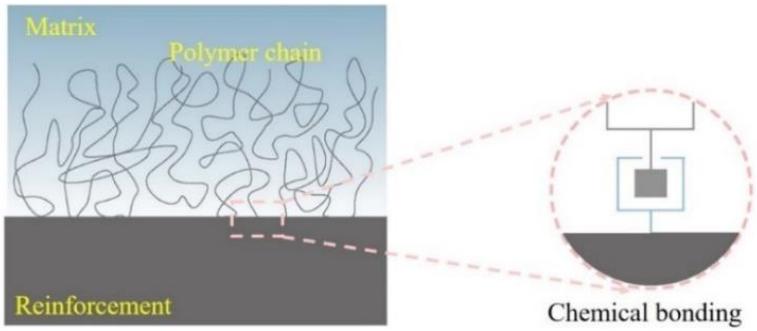

Fig. 1-2 Schematic diagram of chemical bonding

1.3 Carbon fiber surface modification technology

1.3.1 Carbon fiber structure characteristics

CF, an inorganic fiber material with a carbon content of more than 92%, has excellent properties such as high strength, low density, stable chemical properties, low expansion coefficient, good electrical and thermal conductivity [49,50], etc. As a result, it is known as the most vital high-performance fiber material of the 21st century. At present, the commercially produced CFs can be divided into viscose-based, pitch-based, and polyacrylonitrile (PAN)-based CFs according to the types of precursors. Among them, the production of viscose-based CFs, mainly used as ablative and heat-resistant composite materials, is less than 1% of the total world output of CF materials due to the high production cost, complex process, and low carbonization yield, among other reasons. Although asphalt fiber is rich in raw materials and cheap, due to the complex production technology of asphalt-based CFs and poor mechanical properties and repeatability of products, there is unbalanced development in technology development and market application. Polyacrylonitrile is the most promising precursor for preparing high-performance CFs. PAN-based CFs prepared from PAN have simple production processes, high carbon yields, and good overall performance, with their output exceeding 90% of the world's total output of CF materials, thus occupying a mainstream

position in the current industrial production of CFs [51-53].

CF, a kind of fibrous polymer carbon material with a disordered graphite structure, is made of organic fibers carbonized at high temperatures in an inert atmosphere. The CF has a typical “skin-core” structure (shown in Fig. 1-3), and presents a gradually ordered graphite layer structure from the core to the skin layer [54-56]. The innermost part of the CF is called the core. Due to the gas generated during the carbonization process, many gaps exist in the fiber, forming defects. Thus, the core layer has the structural characteristics of several small and scattered microcrystal-size, poorly oriented, loose, and porous folds. The transition zone from the core layer to the skin layer is the transition layer, and the graphite microcrystals show an orderly layered structure arranged axially along the fiber, and the structure tends to be uniform. The skin layer is a compact and orderly arrangement layer enriched with carbon elements formed on the surface of the CF after non-carbon elements escaped during high-temperature carbonization and graphitization. It is characterized by an increased crystallite size, gradually dense structure, and fewer defects. Therefore, this "skin-core" structure of CFs leads to a smooth and dense surface, low surface energy, and few active carbon atoms, impeding good infiltration with the resin matrix during the composite process and producing chemical bonding and mechanical locking cooperation between the two phases, ultimately leading to deteriorated interface performance and comprehensive performance of the composite material [57,58].

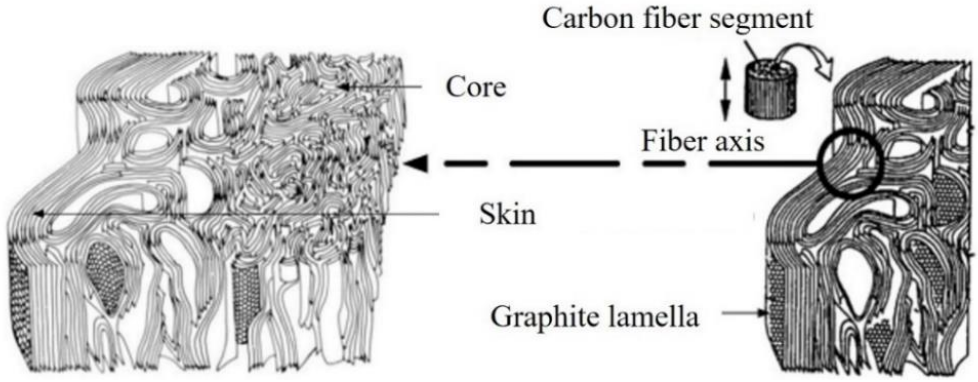

Fig. 1-3 Diagram of carbon fiber structure

1.3.2 Carbon fiber surface modification technology

The poor bonding performance between the CF and resin matrix considerably

limits the application of CFs in the field of composite materials. To fully exploit the excellent performance of the CF as a composite reinforcement, surface modification of CFs is required. The surface modification of CFs includes physical property and chemical property modification. Physical property modification refers to changing the surface roughness, specific surface area, and other microstructure morphology of the CF, increasing the mechanical engagement center to enhance the mechanical bonding between the CFs and matrix resin. Chemical property modification refers to the introduction of active functional groups on the surface of CFs to increase the surface energy, improve the wettability of CFs in the matrix resin, cause a chemical reaction between the CFs and matrix resin, and enhance the chemical bonding between the two phases, thereby improving the interfacial and overall mechanical properties of the composite material. At present, the relatively mature CF surface modification technologies include mainly oxidation, high-energy radiation, plasma treatment, coating, and surface grafting technologies [60-68].

1.3.2.1 Oxidation method

Oxidation, one of the most common methods of CF surface modification, includes mainly liquid-phase, gas-phase, and electrochemical oxidation. This method is mainly used to effectively increase the interfacial bond strength by etching the fiber surface under oxidizing conditions, thereby increasing the fiber surface roughness and simultaneously activating the fiber surface [69,70].

Liquid phase oxidation involves surface etching of CFs using liquid oxidants such as sulfuric acid, nitric acid, hydrochloric acid, and hydrogen peroxide. Simultaneously, several oxygen-containing functional groups are introduced into the fiber surface, which enhances the chemical interaction between the fibers and matrix resin, improves their wettability, and increases the bonding strength of the composite material interface. The method requires mild conditions and is easy to operate, and the oxidation degree of the CF surface can be controlled by adjusting the oxidation time and temperature to avoid the performance degradation of the CF caused by excessive etching. Yu et al. [71] oxidized CFs in an $AgNO_3/K_2S_2O_8$ oxidation system at 70 °C and in an inert atmosphere

for 1 h, and several polar oxygen-containing functional groups (carboxyl and hydroxyl groups) were introduced on the surface of the CFs. These polar functional groups significantly improved the wettability of CFs in the matrix and were able to react chemically with the matrix resin to form a chemical bonding interaction, thus improving the interfacial bonding properties of the composite.

The vapor phase oxidation uses oxygen-containing gases such as air, ozone, and carbon dioxide, to oxidize CFs under high temperature and pressure or under catalyst conditions to introduce oxygen-containing functional groups such as hydroxyl and carboxyl groups on the surface of CFs, increasing the polarity and improving the interfacial bonding between the fibers and the resin. For example, Hao et al [72]. used hot air to oxidize CFs. After treatment, several active groups were generated on the surface of the treated fibers. The interfacial properties of the composite were enhanced, with the tensile strength increased by 34.5%, tensile modulus increased by 43.4%, flexural strength increased by 23%, flexural modulus increased by 30%, impact strength increased by 54.7%, and creep decreased by 10%.

Electrochemical oxidation, also known as anodic oxidation, mainly uses CF conductivity as the reaction anode plate, and graphite, stainless steel, or nickel as the cathode plate. The oxidation etching of CF is performed in an acid, alkali, or salt electrolyte medium. The surface roughness of the CF increases after the electrochemical oxidation, the number of active carbon atoms increases, and the surface hydroxyl content increases, resulting in a substantial improvement in the interfacial properties of the CF composites. Liu et al [73]. used ammonium bicarbonate/ammonium oxalate mixture as an electrolyte for the continuous oxidation of PAN-based CFs, which considerably improved the roughness and specific surface area of the fiber surface, enhanced the bond strength between the two phases of CFs and matrix resin, and increased the interlaminar shear strength of the composite by more than 20%.

CF surface oxidation is simple and can directly increase the hydroxyl, carboxyl, and other oxygen-containing active functional groups on CF surfaces to ensure that the wettability between the fiber and the resin can be improved; however, it is also

accompanied by stringent conditions for oxidation treatment, high energy consumption, difficult operation control, and degradation of the mechanical properties of the CF itself due to excessive oxidation.

1.3.2.2 Surface grafting technology

The surface grafting technology involves using the surface reactive functional groups of the CF and grafted macromolecules to react, introduce a variety of reactive functional groups, and improve the wettability properties of CFs on the resin matrix, thus improving the interfacial bond strength of carbon-fiber-reinforced composites. At present, the main methods for surface grafting modification of CFs include chemical, radiation, and plasma grafting. Among them, chemical grafting is widely used because of its simple operation, mild reaction conditions, and absence of disadvantages such as low grafting rate, uneven grafting, and monomer deactivation after grafting is completed.

The chemical grafting method is mainly used to introduce reactive functional groups on the surface of CFs by chemical modification, and then use these reactive functional groups to graft macromolecules on the surface of CFs. For example, F.S. Verini et al [74]. oxidized the CFs in ammonia and triggered a chemical polymerization grafting of tetracyanoethylene with maleic anhydride on the CF surface to introduce amine groups to the CF surface.

In recent years, with the rapid development of nanoscience and nanotechnology, researchers chemically grafted excellent nano components (CNTs, GO, TiO_2, and SiO_2) as reinforcement onto the surface of CFs to prepare multi-scale reinforcement of nano components/CFs. The introduction of interfacial phases with excellent performance into the composite considerably improved the interface performance of the composite. He et al [75]. prepared carbon nanotubes/CF (CNTs/CF) multiscale reinforcement using chemical grafting; the multi-walled carbon nanotubes (MWCNT) were first functionalized with hexamethylene diamine (HMD) end caps and then grafted onto the surface of chloroformed CFs by chemical reaction. The test results confirmed that the carbon nanotubes were grafted onto the CF surface by chemical bonding and uniformly

distributed along the outer edge of the grooves on the fiber surface.

Plasma grafting is a CF modification method that introduces specific functional groups on the surface of CFs under the action of plasma-activated particles; cross-linked structural layers and surface radicals are formed, thus causing the CF surface to be activated by plasma and triggering the grafting polymerization of monomer molecules on the CF surface. For example, Jia et al [76]. used plasma to treat the surface of CFs, and then grafted aryl acetylene on the surface of CFs; the results showed that the microcrystal size of the grafted CF surface was reduced, and the interlaminar shear strength of CF-reinforced composites increased by 51.27%, thus effectively improving the mechanical properties of the CF composites.

Radiation grafting technology involves using high-energy rays, such as electron beams, γ-rays, and β-rays emitted particles, to bombard the surface of CFs, thereby producing free radicals, triggering the polymerization of monomer molecules on the surface of CFs to increase the wettability and chemical reactions between the two phases of CF and the matrix resin and promote the chemical bonding of the CF and matrix. Moderate etching changes the surface microstructure of CFs and increases the roughness, thus enhancing the mechanical engagement between the fibers and matrix and ultimately improving the interfacial properties of the composite. Li et al [77]. used 60Co γ-radiation to irradiate CFs and studied the morphological and structural changes of the CF surface after irradiation with absorbed doses ranging from 0～1000 kGy. The results showed that the interlaminar shear strength of the CF-reinforced epoxy resin composites increased by more than 27% at an absorbed dose of 30 kGy.

Surface grafting technology has an obvious modification effect on CFs, which improves the toughness of CF and interfacial shear strength of the CF composites; however, this method has a complicated process and long reaction time, which cannot achieve continuous preparation. Moreover, damage to the mechanical properties of CFs is still difficult to avoid. Therefore, surface grafting modification is only applicable in theoretical research of composite materials, and it is difficult to achieve industrial continuous processing.

1.3.2.3 Surface coating technology

Surface coating technology involves coating an interface layer of a certain thickness on the CF surface to wet the fiber and matrix and protect the CF. This interface layer releases the stress and absorbs the energy produced by fiber pull-out to the maximum extent; thereby, it plays a role in passivating the crack growth and increasing the material surface energy. Different coating structures can be designed for different reinforcing fibers and resin substrates. Common surface coating technologies mainly include sizing, polymer, and coupling agent coating technologies.

Sizing is the most commonly used method to modify CFs; it involves using sizing agents to modify the surface of the CF. Sizing improves the interfacial bonding of the composite material and the clustering and processability of the CFs, which is important for the transportation and storage of the product; usually, the sizing agent content is 0.5 to 1.5 wt.%. Using sizing agents improves the chemical activity of the CF surface, introduces more active functional groups, produces physicochemical bonding with the matrix resin, and improves the interfacial properties of the fiber composite. In contrast, as the CF develops cracks or defects on its surface during processing, stress concentration is easily formed, inducing fiber fracture; introducing the sizing agent protects the fiber and avoids brittle fracture. Fig.1-4 shows the preparation process of CNT/ CF multiscale reinforcement synthesized by sizing method [78].

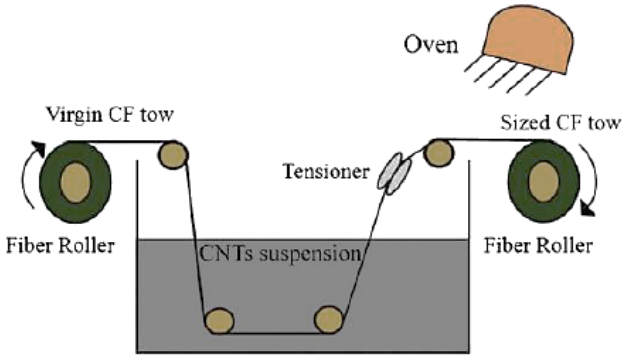

Fig. 1-4 CNT/CF multiscale reinforcement synthesized by sizing

Polymer coating is a modification method that improves the wettability and reactivity of CFs and substrates by coating the surface of the CFs with a polymer, thereby introducing active functional groups and increasing the surface energy of the

fibers. Polymer coating technologies mainly include interfacial polycondensation reactions, plasma polymerization, and electrochemical polymerization. Among them, electropolymerization is the most used. Hung et al [79]. subjected a monomer solution composed of phenol, acrylic acid, and m-phenylenediamine to an electrochemical reaction via electropolymerization, introduced active groups such as hydroxyl, carboxyl, and amino groups on the surface of CFs, and achieved good infiltration of matrix resin on the surface of the CFs. The interlaminar shear and tensile strengths of the composite were increased by 135% and 64%, respectively. However, this method has some disadvantages. A portion of the electrolyte monomer is unstable and prone to polymerization reaction. Thus, the process of electropolymerization requires continuous replenishment of monomer. If the conditions are not properly controlled, it causes uneven coating of polymer molecules on the surface of the CFs, which is not conducive to the improvement of the interfacial properties of the composite materials.

Coupling agent coating is a modification method that improves the interfacial properties of composite materials using two functional groups with different properties in the coupling agent to chemically react simultaneously with the CFs and matrix resin, firmly joining them through chemical bonding. Wen et al [80]. modified the surface of CFs by a two-step process (shown in Fig.1-5): first, the CF was sliced by electrochemical oxidation, and then a silane coupling agent KH550 was applied to the surface of the CF. The interface performance of the modified CF epoxy resin composite considerably improved, and the IFSS and ILSS of the composite increased by 73.1% and 61.2%, respectively.

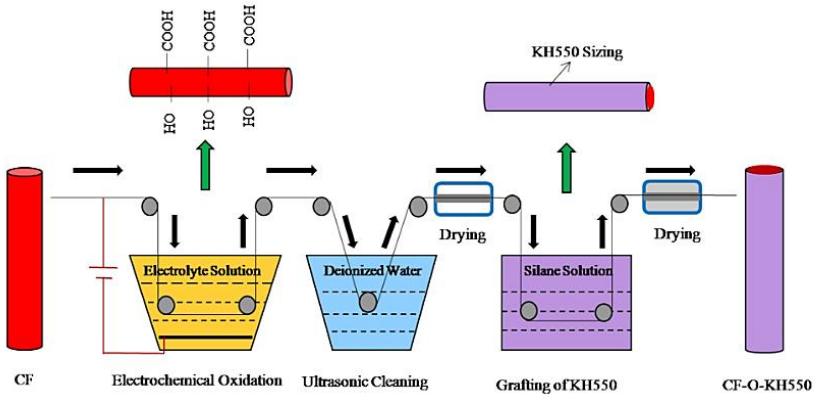

Fig. 1-5 The schematic illustration of two-step surface treatment

1.3.2.4 Multi-scale modification

In recent years, with the rise of nanomaterials, multi-scale modification of CF surface using nanoparticles combined with other small molecules or polymers has become a hot spot in the research of CF composite interface modification. Multi-scale interface modification of CFs increases the contact area between the CF and resin and improves the mechanical locking cooperation between interfaces. However, nanomaterials on CFs effectively disperse the stress load, produce crack deflection effect, avoid stress concentration, and effectively improve the toughness of composite materials.

Carbon nanotubes and graphene oxide are the first choices for multi-scale surface modification of CFs due to their excellent physical, mechanical, thermal, and optoelectronic properties. The introduction of carbon nanotubes and graphene oxide increases the interfacial bond strength and surface roughness of CFs, thus enhancing the mechanical locking cooperation between CFs and resin matrix. Moreover, the chemically modified carbon nanotubes contain reactive groups on their surface, which forms connections with the resin matrix through covalent bonds, thus improving the stress transfer capability. In addition, the excellent mechanical properties of carbon nanotubes and graphene oxide improve the toughness of CF composites (Fig. 1-6 shows the mechanism of carbon nanotube modified carbon fiber reinforced polymer matrix composite). At present, the main methods used to prepare carbon nanotubes/CFs and graphene oxide/CFs are vapor phase deposition, chemical grafting, sizing, surface adsorption, and electrophoretic deposition [81-84].

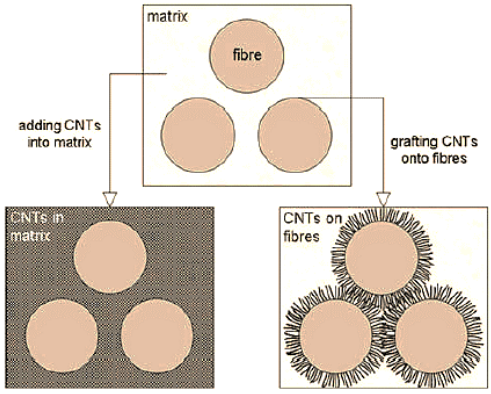

Fig1-6 Schematic diagram of CNTs modified carbon fiber reinforced polymer matrix composites

Chemical vapor deposition (CVD) is one of the most commonly used methods for preparing carbon nanotube/CF multi-scale reinforcement. CVD is usually the process technology used to deposit CNT on the fiber surface after one or several carbon-containing gas molecules are introduced into the reaction chamber at high temperature, with chemical reactions taking place in the gas phase under the action of a catalyst [85,86]. Thostenson et al [87]. first used vapor deposition to realize carbon nanotube growth on the surface of CFs. At present, several literature reports exist on the vapor deposition of carbon nanotubes/CFs. Sager et al [88]. first treated CFs with ethanol, magnesium sulfate, and xylene for 30 min, and passed a mixture of hydrogen and argon gas at 800 °C. Carbon nanotubes were grown directly on the surface of the CFs by a vapor deposition technique and were used as reinforcement to prepare CF epoxy resin-based composites; the interfacial strength of the modified carbon fiber composites increased by 71% compared with that of conventional carbon fiber composites. Although the CVD method clearly improves the interfacial strength, toughness, and even the performance of composite materials, there are also many unavoidable drawbacks. The ultra-high temperature growth environment required by the CVD method not only requires high technical equipment but also etches the surface of the CF, which degrades the bulk strength of the fiber. Simultaneously, the residual catalyst particles on the surface negatively impact the improvement of the interface performance of the composite; the deposited CNT with high hydrophobicity reduces the compatibility and wettability of the fiber to the matrix.

The chemical grafting method is usually used to chemically treat the surface of CFs and carbon nanotubes to produce several active functional groups such as carboxyl (-COOH), hydroxyl (-OH), amine (-NH2), etc. These new functional groups are used to perform chemical reactions, such as esterification, amidation, and anhydride, to prepare CNT/CF multiscale complexes through the mutual bonding between chemical bonds. Peng et al [89]. first acidified CFs to generate functional groups, such as carboxyl groups, on the fiber surface, and then used PAMAM, a dendritic macromolecule, to graft carbon nanotubes onto the CF surface (as shown in Fig. 1-7).

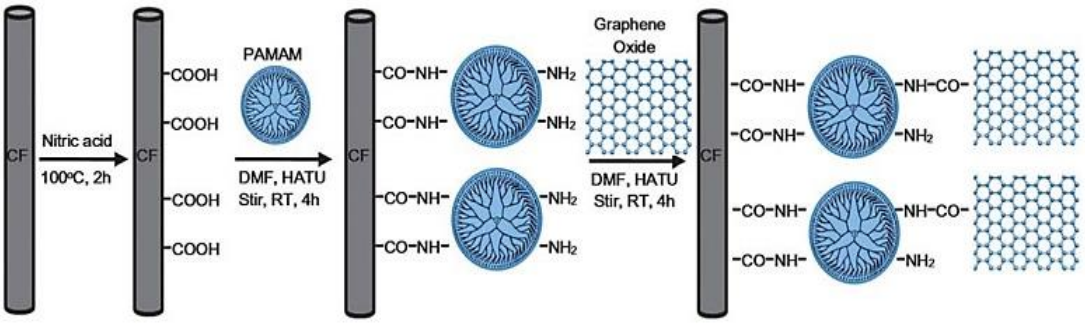

Fig. 1-7 Schematic diagram of grafting procedures

Based on the diazo reaction, Wu et al [90]. grafted carbon nanotubes with phenylamino groups and then modified the functionalized carbon nanotubes onto the surface of CFs to increase the surface roughness and wettability of the CFs and enhance the interface performance of the CFEP composites. Compared with the unmodified CF composites, the ILSS and IFSS of the modified CF-g-CNT0.5R MPSR composites increased by 73.36% and 66.91%, respectively. The connection diagram of functional carbon nanotubes on the surface of carbon fiber is shown in Fig. 1- 8.

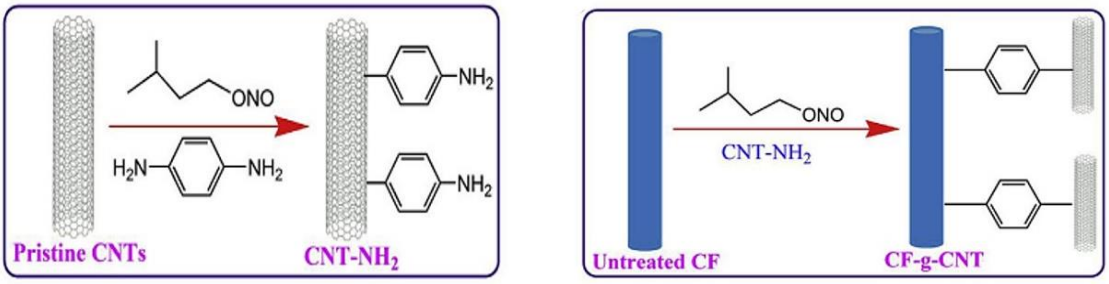

Fig. 1-8 Schematic diagram of connection technology of functional CNT on carbon fiber surface

Since its discovery in the early nineteenth century, electrophoretic deposition (EPD) has been used mainly as a colloid treatment method. The electrophoretic deposition method is based on the principle of electrophoresis to make carbon nanotubes move and deposit on the surface of the CF under the action of an electric field. After acidification modification, the surface of the acidified carbon nanotubes contains several carboxyl groups, which are electronegative in aqueous solutions. Under the electrophoretic effect, with the CFs as anodes, carbon nanotubes move directionally to the CFs and deposit on their surface. Wu et al [91]. deposited CNT uniformly on the surface of CF fabric by electrophoretic deposition process to produce

CNT/CF multi-scale reinforcement and then used solution pre-impregnation treatment to further improve the interfacial impregnation properties of CNT/CF fiber bundles and PC matrix, resulting in significant improvement in the mechanical properties of fiber composites. The tensile strength (344.8 MPa) and modulus (37.8 GPa) of the modified CF composites increased by 46.5% and 57.5%, respectively, and the impact strength (36.5 kJ/m2) and storage modulus (49.0 GPa) increased by 268.7% and 78.4%, respectively (as shown in the Fig.1-9). Moaseri et al [92]. uniformly deposited aminated carbon nanotubes on the surface of CFs in the aqueous phase by electrophoretic deposition and rapidly converted them into covalent grafting through a diazo reaction. The main principle is that, after multi-step treatment of carbon nanotubes, a relatively rich amine group is formed on the surface, allowing carbon nanotubes to be uniformly dispersed in water, and simultaneously, due to its negative electrokinetic potential in water, migrate to the cathode under the effect of an electric field. Finally, the diazo electrografting reaction is further performed using the amine group deposited on the fiber surface. Bekyarova et al [93]. used the EPD method to deposit CNT on the surface of CF fabrics to produce CNT/CF multiscale reinforcements, and the modification of CF by CNT allowed for improving the interlaminar shear strength of the composites and considerably enhancing the out-of-plane conductivity of the composites.

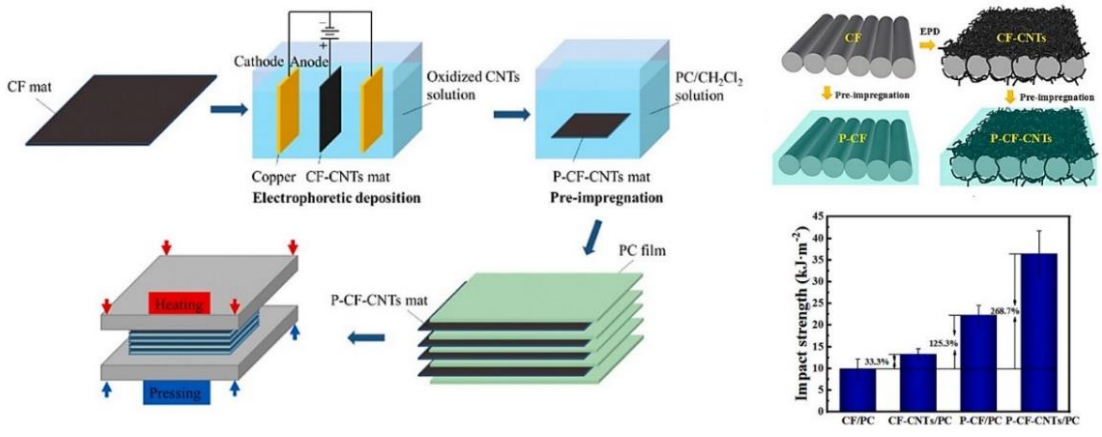

Fig. 1-9 Schematic diagram of the preparation routes of CFRP nanocomposites

As a mature industrial method, electrophoretic deposition, used to prepare CNT/CF multi-size materials, is characterized by its simple operation, short time, and strong controllability; however, it has certain disadvantages. First the process of

electrophoretic deposition is accompanied by water electrolysis, and the bubbles generated from hydropower are easily attached to the surface of the CFs; a large number of bubbles affect the deposition of carbon nanotubes. In addition, the adhesion between the carbon nanotubes and CFs is weak, and carbon nanotubes easily peel off.

1.4 Magnetron sputtering technology

1.4.1 Magnetron sputtering principle

Magnetron sputtering is a high-speed and low-temperature sputtering technology that uses an orthogonal electromagnetic field, which increases the dissociation rate by 5–6% and increases the sputtering rate by about 10 times compared to tertiary sputtering, with deposition rates of several hundred to 2000 nm per minute [94,95].

In magnetron sputtering, a DC voltage is added between the anode and cathode to form an electrostatic field, and a circular closed magnetic field (generated by the magnet inside the target) is established with a transverse magnetic field component parallel to the target surface placed on the surface of the cathode; the transverse magnetic field and the electric field perpendicular to the target surface form a confining orthogonal electromagnetic field for the trapping of secondary electrons (Fig. 1-10).

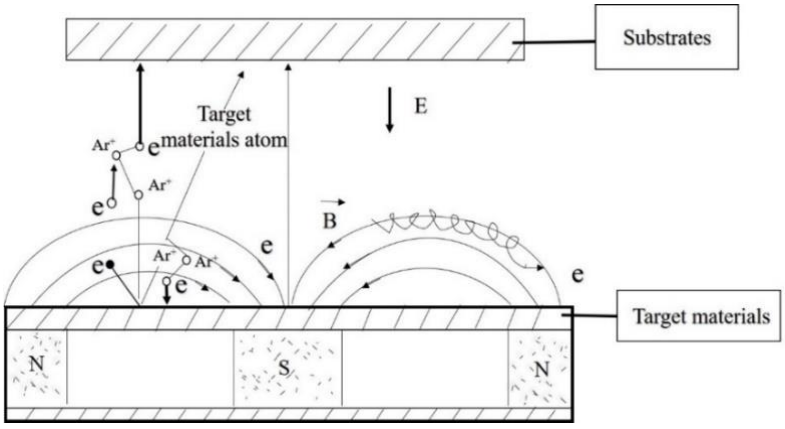

Fig. 1-10 Principle of magnetron sputtering

Compared with other sputtering technologies, magnetron sputtering has the outstanding advantages of high efficiency, low temperature, and little damage to the film layer.

Presently, magnetron sputtering has been used to prepare carbon-particle films. Diamond-like carbon (DLC) films treated by magnetron sputtering have excellent wear

resistance, high-temperature oxidation resistance, and improved optical and electrical properties of the material surface [96,97]. The early unbalanced magnetron sputtering technology is required to explore and understand the wear resistance of DLC film materials as well as the influence of magnetron sputtering technology on the morphology and structure of carbon films [98-101]. However, few researchers have applied magnetron sputtering to modify the interface of CFRP composites.

1.4.2 Film growth process by magnetron sputtering

Analyzing the growth law of magnetron-sputter deposited films from an atomic point of view, it can be seen that films generally consist of molecules, foreign atoms, and atomic clusters arriving at the surface of the substrate, accumulating thereon according to certain rules, and then forming through the process of coalescence. The growth is a non-equilibrium process. The formation of magnetron-sputter deposited thin films can generally be described as follows: The particles sputtered from the target surface move towards the substrate where they collide with the substrate surface or target particles that have already formed a thin film; some of these impinging atoms are directly bounced and re-enter the plasma or adsorb to the inner wall of the vacuum cavity, and most of them are deposited on the substrate or the surface of the growing thin film. As the particles deposited on the surface have their energy and substrate temperature, they diffuse, migrate, and do not move after occupying a proper location. Clearly, in this process, target atoms keep depositing on the substrate or the surface of the formed film. If the particles and surface are not firmly bonded, then, under the bombardment of other target particles, a back-sputtering phenomenon will occur, wherein film-forming particles are sputtered out; this process is called particle disassociation. The particles deposited on the surface migrate, expand, and condense into atomic clusters; the condensation process continues, leading to continued growth of atomic clusters to form stable nuclei. The deposited particles grow continuously in three-dimensional directions and spread in two-dimensional directions to form island-like structures, which are connected in a network to form a continuous film. In summary, the film growth process consists of deposition, diffusion, desorption, and condensation.

The films deposited by magnetron sputtering can be amorphous, polycrystalline (microcrystalline structure), or monocrystalline. The movement of the deposited atoms on the substrate surface, resulting in a regular state of atomic arrangement inside the film, is influenced by the interactions between the deposited and substrate surface atoms, resulting in different growth morphologies of the film. At present, it is generally accepted that film growth mode can be classified into three types: layer island, layered, and island growth modes, as shown in Fig. 1-11.

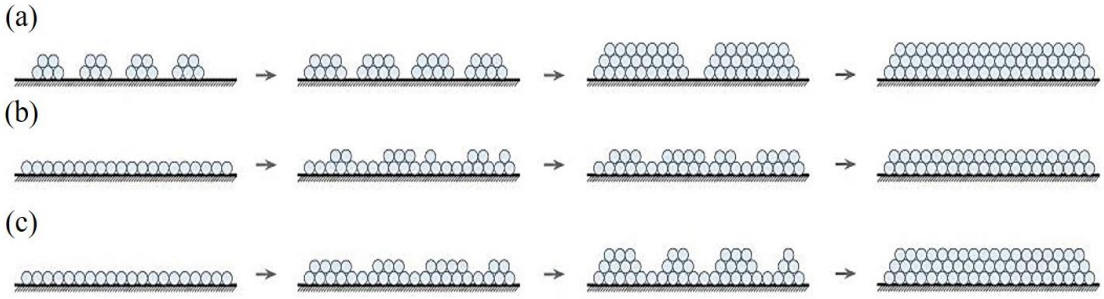

Fig. 1-11The growth models of film

(a) Island growth mode (b) Layered growth mode (c) Layer island growth mode

(1) Island growth mode: When the deposited atoms have poor wettability with the substrate atoms, they do not easily spread on the substrate surface but tend to combine with their own type. After the deposited atoms form the smallest stable nuclei on the surface of the substrate material, the nuclei grow into islands on a three-dimensional scale and form a continuous film when the islands are connected, while forming new nuclei that continue to grow into islands; the surface of this film is relatively high and low, and the film has many voids and relatively high roughness. Island growth mode is widely present when depositing metal films on insulators, graphite, mica, and halide crystal substrates.

(2) Layered growth mode: During the deposition of the film, if the bonding ability of the deposited atoms with the substrate atoms is greater than that of the deposited atoms with their own type, the deposited atoms are first nucleated on the surface of the substrate. The expansion of the smallest stable nucleus leads to the spreading of the deposited atoms in the two-dimensional plane; thereby, the plane layers are formed. The crystal nuclei grow and connect into a film of monatomic layers. When the first layer

is deposited, the second layer is deposited, and then the second layer is deposited. The second single-atom layer completely covers the first layer, and the layer growth continues as long as the binding energy of the substrate atoms to the atoms deposited onto the surface is greater than the binding energy of the deposited atoms themselves. The surface of the film grown in layers is smooth and flat with high quality, and the single crystal epitaxial growth of a semiconductor film follows this growth model.

(3) Layer island growth mode: The layer island model is an intermediate model between layered and island growth. After the first layer of the laminar growth mode covers the surface of the substrate, the remaining growth layers continue to grow in layers during the deposition process; simultaneously, the film-forming particles are gradually increased in three-dimensional directions, forming an island structure of the deposited material. This growth mode is generally used for depositing a metal film on a metal or semiconductor substrate.

1.5 Purpose and significances of research

This study aimed to provide a new method for improving the mechanical properties of CFs and CFRP composites. The surface modification of CFs using the nanostructure property of magnetron-sputter deposited films is expected to realize the purpose of repairing surface defects and improving the mechanical properties of CFs without changing their structure and composition using a characteristic target material that is homogeneous with the CF. The mechanism of the effect of magnetron sputtering on the mechanical properties of CFs is also discussed.

The research objective is to improve the mechanical properties of CFEP composites without sacrificing the mechanical properties of the CF. An easy-to-operate, non-polluting, and non-contaminating method of interface modification of the CFRP composites was developed by employing the surface modification of the CF using magnetron sputtering. The mechanical engagement between the CFs and resin matrix was improved by utilizing the surface characteristics of magnetron-sputter deposited films on the surface of the CF, thus improving the wettability of the resin matrix to the CFs owing to the nano-size characteristics of magnetron-sputter deposited films. Finally,

a composite interfacial layer is constructed by the magnetron-sputter deposited film, with the multi-size interfacial layer feature playing a role in transferring loads and cracks to the CF composites, ultimately improving the mechanical properties of the CFEP composites. The interface modification mechanism and damage mode of CF composites with carbon films deposited by magnetron sputtering were studied theoretically and experimentally to provide a new method for improving the mechanical properties of damage-free CFRP composites.

An in-depth analysis of magnetron-sputter deposited carbon films was conducted to accurately analyze the action of magnetron sputtering on CF modification. The effects of the magnetron sputtering process parameters and deposition substrate on the surface morphology and microstructure of the magnetron-sputter deposited carbon films, as well as the morphology, structure, and property changes of magnetron-sputter deposited carbon films modified by heat treatment, were discussed to provide a theoretical basis for constructing multilayer interfacial layer structures of CFRP composites at a later stage.

1.6 Outline of dissertation

The purpose of this paper is to analyze the effect of magnetron sputtering, as a means for the surface modification of CFs, on the mechanical properties of the CF and the interfacial and mechanical properties of CF resin-matrix composites.

In Chapter 1, the existing problems of CF composites, interfacial modification methods of CF composites, interfacial bonding mechanism, surface modification methods, and magnetron sputtering mechanism are outlined.

In Chapter 2, the macroscopic and microscopic structures of magnetron-sputter-deposited carbon films are characterized. Further, the effects of magnetron sputtering process parameters and different substrates on the morphology and structure of carbon films are analyzed, in addition to the changes in the structural properties of magnetron-sputtered carbon films under 800–1200 ℃ heat treatment conditions.

In Chapter 3, the influence of magnetron sputtering modification on the properties of CFs is described, and the influence of magnetron sputtering technology on the

mechanical and surface properties of CFs, as well as the adhesion strength between the carbon films and CFs under different magnetron sputtering conditions are analyzed.

In Chapter 4, the mechanical properties of CFRP composites are analyzed and the damage mechanisms are described based on understanding carbon film properties under different magnetron sputtering process conditions. The effects of magnetron sputtering modification means and process parameters on the interfacial and mechanical properties of CF composites are also discussed.

In Chapter 5, a summary of the research and conclusions are presented.

References

[1] L. Zhao, Q. Ge, J. Sun, J. Peng, X. Yin, L. Huang, J. Wang, H. Wang, L. Wang. Fabrication and characterization of polyphenylene sulfide composites with ultra-high content of carbon fiber fabrics. Advanced Composites and Hybrid Materials. 2019.2(3):481-491

[2] D. Aleksendric, P. Carlone. Introduction to composite materials. Soft computing in the design and manufacturing of composite materials.2015:1-5

[3] M. Sharma, S.L. Gao, E. Mader, H. Sharma, L.Y. Wei, J. Bijwe. Carbon fiber surface and composite interphases. Composites Science and Technology. 2014.102:35-50

[4] Z.Y. Yang, D. Zhang, C.H. Gu, R. X. Zhao, X.B. Zuo, L.Y. Tong, C.Y. Shang, H.J. Sun. Research and application of advanced resin matrix composites for aerospace shuttle vehicles abroad. Acta Materiae Compositae Sinica. 2022.(39)7:3029-3043

[5] Y. T. Fu, X. F. Yao. A review on manufacturing defects and their detection of fiber reinforced resin matrix composites. Composites Part C: Open Access. 2022.(8) :100276

[6] H. Ahmad, A. A. Markina, M. V. Porotnikov, F. Ahmad. A review of carbon fiber materials in automotive industry. IOP Conference Series: Materials Science and Engineering. 2020.971:032011

[7] F.P. Rita, D. Carpio, O. Torres, C. Oscar, F. Silva, H. Bruno, O. Mutlu, J.C.M.Souza. The influence of inorganic fillers on the light transmission through resin-matrix composites during the light-curing procedure: an integrative review. Clinical Oral Investigations. 2022. (26):5575-5594

[8] L.Y. Xing, Z.H. Feng, J.W. Bao, S.M. Li. Facing opportunity and challenge of carbon fiber and polymer matrix composites industry development. Acta Materiae Compositae Sinica. 2020.(37)11: 2700-2706

[9] S. Kangishwar, N. Radhika, A.A. Sheik, A. Chavali, S. Hariharan. A comprehensive review on polymer matrix composites: material selection, fabrication, and application. Polymer Bulletin. 2022.1:DOI:10.1007/s00289-002-04087-4

[10] S. Chand. Review carbon fibers for composites. Journal of Materials Science.2000. (35): 1303-1313

[11] S. S. Yao, F. L. Jin, K. Y. Rhee, D. Hui, S. J. Park. Recent advances in carbon-fiber-reinforced thermoplastic composites: A review. Composites Part B: Engineering. 2018. (142): 241-250

[12] BA Newcomb. Processing, structure, and properties of carbon fiber. Composites Part A: Applied Science and Manufacturing. 2016.91:262-282

[13] P.J. Yang, J.M. Yuan, L.P. He. Carbon fibers surface modification and effects on the interfaces between fibers and resin matrices: A review. Materials Reports. 2017. (31): 129-136

[14] L.M. Kong, X.B. Wang, W. Zheng, S.W. Tian, Y.Y. Qi, Y.J. Xue, B.C. Wang. Effects of plasma treatment on properties of carbon fiber and its reinforced resin composites. Materials Research Express, 2020,7(6):065304

[15] C. Zhang, Z.Z. Liu, M.J. Sun, X. Li. Surface treatment on carbon fiber by cold plasma. Materials Reports. 2018,31(5):294-296

[16] E. Hassan, T. Elagib, H. Memon, M. Yu, S. Zhu. Surface modification of carbon fibers by grafting PEEK-NH2 for improving interfacial adhesion with polyetheretherketone. Materials., 2019. (12):778-789

[17] S.B. Zhang, Q.L. Dai. The surface modification of carbon fiber for thermoplastic HDPE composites. Surface and Interface Analysis. 2018,51(2):184-189

[18] O. Zabihi, M. Ahmadi, Q.X. Li, S. Shafei, M. G. Huson, M. Naebe. Carbon fiber surface modification using functionalized nanoclay: A hierarchical interphase for fibre-reinforced polymer composites. Composite Science and Technology. 2017.(148)18: 49-58

[19] J. Li, W.C. Jiao, M.L. Yan, Z.X. Liu. Research progress on composited interface design of grafting carbon nanomaterials onto carbon fibers. Fiber Reinforce Plastics Composites. 2018.(1): 108-113

[20] Q.H. Wu, R.F. Zhao, W.J. Liu, X. Zhang, X. Shen, W.L. Li, G.W. Diao, M. Chen. In-depth nanocrystallization enhanced Li-ions batteries performance with nitrogen-doped carbon coated Fe_3O_4 yolk shell nanocapsules. Journal of Power Sources. 2017. 344(15): 74-84

[21] X.M. Yao, X.Y. Gao, J.J. Jiang, C.M. Xu, C. Deng, J.B. Wang. Comparison of carbon nanotubes and grapheme oxide coated carbon fiber for improving the interfacial

properties of carbon fiber/epoxy composites. Composites Part B. 2018.132:170-177
[22] S.Q. Hu, Q. Lu, Z.K. Wang, X.J. Ji, C.L. Li, S.Q. Sun. Advances in the interfacial bonding characteristics of carbon nanotube/ polymer composites. Acta Materiae Compositae Sinica. 2017. 34(1): 12-22
[23] H.L. Cao, Y.C. Shi, H. Shen, H.D. Zhan, J.R. Liu. The production of core-shell structure carboxylated carbon nanotubes/polypyrrole composite materials in different reaction media and further investigation on their core-shell structure. Key Engineering Materials. 2017,730:37-41
[24] M.Z. Sang, S.H. Wang, Z. Long, Z.Q. Li, S. Guo. Preparation and properties of carbon fiber-based composites Co-modified with graphene and carbon nanotubes. China Plastics. 2018. 32 (6)：124-130
[25] T.R. Pozegic，J.V. Anguita，I. Hamerton, K.D.G.I. Jayawardena, J.S. Chen, V. Stolojan, P. Ballocchi, R. Walsh, S.R.P.Silva. Multi-functional carbon fibre composites using carbon nanotubes as an alternative to polymer sizing. Scientific Reports. 2016. (11):1-11
[26] M. Chiara, E. Lertora, C. Gambaro. Cold plasma pretreatment of carbon fibre composite substrates to improve adhesive bonding performance. Advances in Aerospace Engineering. 2014.(11):325729
[27] W.M. Yang, Y.W. Liu, L.X. Xu, Y.X. Leng, Y.X. Huang. Review of film growth by sputtering technology. Journal of Vacuum Science and Technology.2005.25: 204-210
[28] Z.B. Zhao, K.Y. Teng, N. Li, X.J. Li, Z.W. Xu, L. Chen, J.R. Niu, H.J. Fu, L.H. Zhao, Y. Liu. Mechanical, thermal and interfacial performances of carbon fiber reinforced composites flavored by carbon nanotube in matrix/interface Composite Structures. 2017.159:761–72
[29] L. Liu, T. Wang, J.L. Huang, Z.B. He, Y. Yi, K. Du. Diamond-like carbon thin films with high density and low internal stress deposited by coupling DC/RF magnetron sputtering. Diamond and Related Materials. 2016.70:151-158
[31] Y.X. Gan. Effect of interface structure on mechanical properties of advanced composite materials. International Journal of Molecular Sciences. 2009.10:5115-5134
[32] L. Dobrzynski. Interface response theory of discrete composite systems. Surface science reports. 1986. 6:119-157

[33] C.Y. Fang, Y.H. Zhou, L.X. Jia, R.S. Yan. Interfacial properties of multicomponent plasma-modified high-performance fiber-reinforced composites: A review. Polymer composites. 2022: DOI.org/10.1002/pc.26870

[34] L.F. Song, C.Y. Yang. Research progress of composite interface theory and surface treatment of quartz fiber. Journal of Textile Science and Engineering. 2018. 35:171-176

[35] A. Valadez-Gonzalez, M.V. Moreno-Chulim, P.J. Herrera-Franco. Modification of the fibre surface for the optimization of mechanical properties in natural-fiber reinforced polymers. Materials and Product Technology. 2009.36:417-430

[36] K. Hirogaki, I. Tabata, K. Hisada, T. Hori. An investigation of the interaction of supercritical carbon dioxide with poly (ethylene terephthalate) and the effects of some additive modifiers on the interaction. The Journal of Supercritical Fluids. 2005.36:166-172

[37] A.K. Singh, R. Bedi, B.S. Kaith. Mechanical properties of composite materials based on waste plastic- A review. Materialstoday Proceedings. 2020.26:1293-1301

[38] I. Norio, P. Eleni, S. Yhihiro. Effect of coupling treatment of carbon fiber surface on mechanical properties of carbon fiber reinforced carbon composites. Composites Part A. 1998.29:965-972

[39] M.H. Choi, B.H. Jeon, I.J. Chung. The effect of coupling agent on electrical and mechanical properties of carbon fiber /phenolic resin composites. Polymer. 2000. 41:3243-3252

[40] M.S. Anbupalani, C.D. Venkatachalam, R.Rathanasamy. Influence of coupling agent on altering the reinforcing of natural fibre-incorporated polymers-A review. Journal of reinforced plastics and composites. 2020.39:520-544

[41] M. Aljnaid, R. Banat. Effect of coupling agents on the olive pomace-filled polypropylene composites. E-Polymers. 2021. 21:377-390

[42] R. Rothon. Particulate-filled polymer composites. 1995. Beijing: World Book Publishing Company

[43] M.J. Sun, B.F. Hu, Y.S. Wu, Y.X. Da, Y. Tang, W.Q. Huang. The surface of carbon fibers treated continuously by using cold plasma. Acta Materiae Composite Sinica.

1986.3:1-7

[44] J. Jang, H.J. Yang. The effect of surface treatment on the performance improvement of carbon fiber /polybenzoxazine composites. Journal of Materials Science. 2000.35. 2297-2303

[45] O. Zabihi, M. Ahmadi, Q.X. Li, S. Shafei, M.G. Huson, M. Naebe. Carbon fibre surface modification using functionalized nanoclay: A hierarchical interphase for fibre-reinforced polymer composites. Composites Science and Technology. 2017.148:49-58

[46] R. Han, X.R. Wang, M. Li, G. Chen, Z. Z. Wang, J.L. Zhang. Preparation of surface roughened basalt fiber and its effect on tensile properties of polypropylene matrix composites. China plastics industry.2021.49（12）:40-45

[47] S. Tiwari, J. Bijwe. Surface treatment of carbon fibers-A review. Procedia Technology. 2014. 14:505-512

[48] X. Ma, H.P. Qiu, Y.Y. Liang, S.H. Liu, X.M. Wang, Y.L. Zhao, M.W. Chen, W.J. Xie. Effects of CVD BN coatings on flexural properties of Si_3N_4/SiBN composites by precursor infiltration pyrolysis. Materials reports.2021.35:86-89

[49] T. Kamae, L.T. Drzal. Carbon fiber/ epoxy composite property enhancement through incorporation of carbon nanotubes at the fiber-matrix interphase-Part I: The development of carbon nanotube coated carbon fibers and the evaluation of their adhesion. Composites Part A.2012.43:1569-1577

[50] X. Fan. Application status and development trend of carbon fiber reinforced plastic. Chemical Industry.2019.37:12-16

[51] Y.Y. Yang, A.A. Ibrahim, J.L. Stockdill, P. Hashemi. A density-controlled scaffolding strategy for covalent functionalization of carbon-fiber microelectrodes. Analytical methods. 2015.7:7352-7357

[52] H.M. Lee, L.K. Kwac, K.H. An, S.J. Park, B.J. Kim. Electrochemical behavior of pitch-based activated carbon fibers for electrochemical capacitors. Energy Conversion and Management. 2016.125:347-352

[53] M. Smith. New developments in carbon fiber. Reinforced Plastics. 2018.62:266-269

[54] N.Raphael, K.Namratha, B.N. Chandrashekar, K.K.Sadasivuni, D. Pommanna, A.S. Sitha, S. Krishnaveni, C. Cheng, K. Byrappa. Surface modification and grafting of carbon fibers: A route to better interface. Progress in Crystal Growth and Characterization of Materials. 2018.64:75-101

[55] H.J. Song, Z.Z. Zhang, Z.Z. Luo. A study of tribological behaviors of the phenolic composite coating reinforced with carbon fibers. Materials Science and Engineering. 2007. 445:593-599

[56] J.B. Donnet, G. Guilpain. Surface treatments and properties of carbon fiber. Carbon. 1989.27:749-757

[57] H.G. Chae, B.A. Newcomb, P.V. Gulgunje, Y.D. Liu, K.K. Gupta, M.G. Kamath, K.M. Lyons, S. Ghoshal, C. Pramanik, L. Giannuzzi, K. Sahin, L. Chasiotis, S. Kumar. High strength and high modulus carbon fibers. Carbon. 2015.93:81-87

[58] S.L. Gao, E. Mader, S.F. Zhandarov. Carbon fibers and composites with epoxy resins: Topography, fractography and interphases. Carbon. 2004. 42:515-529

[59] H. Dvir, J. Jopp, M. Gottlieb. Estimation of polymer-surface interfacial interaction strength by a contact AFM technique. Journal of colloid and interface science. 2006.304:58-66

[60] W.X. Fan, Y.X. Wang, C.G. Wang, J.Q. Chen, Q.F. Wang, Y. Yuan, F.X. Niu. High efficient preparation of carbon nanotube-grafted carbon fibers with the improved tensile strength. Applied Surface Science. 2016. 364. 539-551

[61] M. Sharma, S.L. Gao, E. Mader. Carbon fiber surfaces and composite interphases. Composites science and technology,2014,102:35-50

[62] C.Q. Yu, L. Chen, Y.C. Pei. Effect of carbon fiber coating on thermal conductivity of carbon fiber reinforced lithium alumina silicate glass-ceramics composites. Journal of Materials Engineering，2018. 46: 101-105

[63] H. Fu, J.L. Chen, K. Wang, Y. Zhao. Effects of heat treatments on the interfacial crystallization and mechanical properties of carbon fiber/polyamide 6 composites. Acta Materiae Compositae Sinica. 2017.35：815-822

[64] O. Zabihi, M. Ahmadi, Q.X. Li, S. Shafei, M.G. Huson, M. Naebe. Carbon fiber surface modification using functionalized nanoclay: hierarchical interphase for fiber-

reinforced polymer composites. Composite Science and Technology. 2017. 148:49-58

[65] M.W. Judith, M. Bauer, F. Schubert, O.C. Jumaa, S. Horn. Anodic oxidation of carbon fiber surfaces: influence of static and dynamic process conditions. Key Engineering Materials. 2018. 742:440-446

[66] P.J. Yang, J.M. Yuan, L.P. He. Carbon fibers surface modification and effects on the interfaces between fibers and resin matrices: A revies. Materials Reports. 2017.31. 129-136

[67] C. Mandolfino, E. Lertora, C. Gambaro. Cold plasma pretreatment of carbon fibre composite substrates to improve adhesive bonding performance. Advances in Aerospace Engineering. 2014. 11:1-7

[68] E.A.M. Hassan, T.H.H. Elagib, H. Memon, M. Yu, S. Zhu. Surface modification of carbon fibers by grafting PEEK-NH2 for improving interfacial adhesion with polyetheretherketone. Materials. 2019. 12: 778-789

[69] X.S. Zhou, Y.D. Wang, P.D. Kuang, A.Y. Jiang, B.F. Zhang. Research progress of surface modification technology of carbon fiber. China Synthetic Fiber Industry. 2019.42: 72-75

[70] Y.B. Li, Q.Y. Peng, X.D. He, P.A. Hu, C. Wang, Y.Y. Shang, R.G. Wang, W.C. Jiao, H. Z. Lu. Synthesis and characterization of a new hierarchical reinforcement by chemically grafting graphene oxide onto carbon fibers. Journal of Materials Chemistry.2012,22:18748-18752

[71] J.L. Yu, L.H. Meng, D.P. Fan, C.H. Zhang, F. Yu, Y.D. Huang. The oxidation of carbon fibers through $K_2S_2O_8/AgNO_3$ system that preserves fiber tensile strength. Composites Part B: Engineering. 2014. 60: 261-267

[72] J.X. Hao, F. Du, W.H. Wang. Effect of surface treatment of short carbon fibers on the properties of wood flour/high density polyethylene composite. Acta Materiae Compositae Sinica. 2018. 35: 298-303

[73] J. Liu, Y.X. Guo, J.Y. Liang. Study on electrochemical oxidation of carbon fibers surface. Chemical Industry and Engineering Progress. 2004. 23:282-285

[74] F. Severini, L. Formaro, M. Pegoraro, L. Posca. Chemical modification of carbon fiber surfaces. Carbon. 2002.40:735-741

[75] X.D. He, F.H. Zhang, R.G. Wang, W.B. Liu. Preparation of a carbon nanotube/carbon fiber multi-scale reinforcement by grafting multi-walled carbon nanotubes onto the fiber. Carbon. 2007.45:2559-2563

[76] L. Jia, L.H. Zhou, Z.Y. Xue, H.M. Qi, F.Z. Hu. Surface of carbon fiber grafted by plasma technology and its influence on the C/PAA composite.2004.21: 45-49

[77] J.Q. Li, Y.D. Huang, W. Zhuo, Z.W. Xu. The effect on carbon fiber surface structure and tensile strength irradiated by γ-ray. Journal of Aeronautical Materials. 2005. 25: 52-56

[78] H.W. Yao, X.H. Sui, Z.B. Zhao, Z.W. Xu, L. Chen H. Deng, Y. Liu, X.M. Qian. Optimization of interfacial microstructure and mechanical properties of carbon fiber/epoxy composites Via carbon nanotube sizing. Applied Surface Science. 2015. 347:583-590

[79] K.B. Hung, J. Li, Q. Fan, Z.H. Chen. The enhancement of carbon fiber modified with electropolymer coating to the mechanical properties of epoxy resin composites. Composites Part A. 2008.39:1133-1140

[80] Z.P. Wen, C. Xu. X. Qian, Y.G. Zhang, X.F. Wang, S.L. Song, M.Z. Dai, C. Zhang. A two-step carbon fiber surface treatment and its effect on the interfacial properties of CF/EP composites: The electrochemical oxidation followed by grafting of silane coupling agent. Applied Surface Science. 2019.486:546-554

[81] J.K. Kocsis, H. Mahmood, A. Pegoretti. All-carbon multi-scale and hierarchical fibers and related structural composites: A review. Composites Science and Technology. 2020.186:107932

[82] J.Chevalier, P.P. Camanho, F. Lani, T. Pardoen. Multi-scale characterization and modelling of the transverse compression response of unidirectional carbon fiber reinforced epoxy. Composite Structures.2019.209:160-176

[83] M. Haghgoo. R. Ansari, M.K. Hassanzadeh-Aghdam, M. Nankali. Analytical formulation for electrical conductivity and percolation threshold of epoxy multiscale nanocomposites reinforced with chopped carbon fibers and wavy carbon nanotubes considering tunneling resistivity. Composites Part A: Applied Science and

Manufacturing. 2019.126:105616

[84] X.J. Zhang, W.C. Yang, J.Y. Zhang, X.Y. Ge, X.R. Liu, Y.Z. Zhan. Multiscale graphene/carbon fiber reinforced copper matrix hybrid composites: Microstructure and properties. Materials Science and Engineering: A. 2019.743:512-519

[85] R. Hawaldar, I. Bdikin. Large-area high-throughput synthesis of monolayer graphene sheet by hot filament thermal chemical vapor deposition. Scientific Reports. 2012. 682:1038-1047

[86] C.Zhang, B.Y. Man. Facile synthesis of graphene on single mode fiber via chemical vapor deposition. Applied Surface Science. 2014.307:327-332

[87] E.T. Thostenson, W.Z. Li, D.Z. Wang, Z.F. Ren, T.W. Chou. Carbon nanotube/carbon fiber hybrid multiscale composites. Journal of Applied Physics. 2002. 91:6034-6037

[88] R.J. Sager, P.J. Klein, D.C. Lagoudas, Q. Zhang, J. Liu, L. Dai, J.W. Baur. Effect of carbon nanotubes on the interfacial shear strength of T650 carbon fiber in an epoxy matrix. Composites Science and Technology. 2009.69:898-904

[89] Q.Y. Peng, X.D. He, Y.B. Li, C. Wang, R.G. Wang, P.A. Hu, Y.D. Yan, T. Sritharan. Chemically and uniformly grafting carbon nanotubes onto carbon fibers by Poly (Amidoamine) for enhancing interfacial strength in carbon fiber composites. Journal of Materials Chemistry. 2012.22:5928-5931

[90] G.S. Wu, L. Liu, Y.D. Huang. Grafting of active carbon nanotubes onto carbon fiber using one-pot aryl diazonium reaction for superior interfacial strength in silicone resin composites. Composites Commuications.2019(13):103-106

[91] Y.D. Wu, D. Dhamodharan, Z. Wang, R. Wang, L.X. Wu. Effect of electrophoretic deposition followed by solution pre-impregnated surface modified carbon fiber-carbon nanotubes on the mechanical properties of carbon fiber reinforced polycarbonate composites. Composites Part B. 2020(195):108093

[92] E. Moaseri, M. Karimi, M. Maghrebi, M. Baniadam. Two-Fold enhancement in tensile strength of carbon nanotube-carbon fiber hybrid epoxy composites through combination of electrophoretic deposition and alternation electric field. International

Journal of Solids and Structures. 2014. 51:774-785

[93] E. Bekyarova, E.T.Thostenson, A.Yu, H. Kim, J. Gao, J. Tang, H.T. Hahn, T.W. Chou, M.E. Itkis, R.C. Haddon. Multiscale carbon nanotube-carbon fiber reinforcement for advanced epoxy composites. Langmuir. 2007. 23:3970-3974

[94] G. Brauer, B. Szyszka, M. Vergohl, R. Banorf. Magnetron sputtering milestones of 30 years. Vacuum. 2010.84:1354-1359

[95] G.R. Harp, S.S. Parkin. Epitaxial growth of metals by sputter deposition. Thin Solid Films. 1996. 288: 315-324

[96] J.T. Gudmundsson. Physics and technology of magnetron sputtering discharges. Plasma Sources Sciences and Technology.2020.29:113001

[97] S. Meskinis, A. Ciegis, A. Vasiliauskas, K. Slapikas, T. Tamulevicius, A. Tamuleviciene, S. Tamulevicius. Optical properties of diamond like carbon films containing copper, grown by high power pulsed magnetron sputtering and direct current magnetron sputtering: structure and composition effects. Thin Solid Films. 2015. 581: 48-53

[98] S. Flege, R. Hatada, A. Hanauer, W. Ensinger, T. Morimura, K. Baba. Preparation of metal-containing diamond like carbon films by magnetron sputtering and plasma source ion implantation and their properties. Advances in Materials Science and Engineering. 2017:9082164

[99] S.I. Kim, B.B. Sahu, B.M. Weon, J.G. Han, J. Koskinen, s. Franssila. Making porous conductive carbon films with unbalanced magnetron sputtering. Japanese Journal of Applied Physics. 2015.54: 010304

[100] D.L.C.E Silva, L.R.P Kassab, J.R. Martinelli, A.D.D. Santos, S.J.L.Ribeiro, M.V.D. Santos, Characterization of thin carbon films produced by the magnetron sputtering technique. Material Research. 2016. 19. 669-72

[101] S. Meskinis, A. Ciegis, A. Vasiliauskas, k. Slapikas, T. Tamulevicius, S. Tamulevicius. Optical properties of diamond like carbon films containing copper grown by high power pulsed magnetron sputtering and direct current magnetron sputtering structure and composition effects. Thin Solid Films. 2015.581: 48-53

Chapter 2

Effect of magnetron sputtering process on the structural properties of deposited carbon films

Chapter 2: Effect of magnetron sputtering process on the structural properties of deposited carbon films

2.1 Introduction

Nanomaterials refer to materials with a scale between 1～100 nm and have nano properties. Nanomaterials have obvious surface effect, macroscopic quantum tunneling effect, quantum size effect and small size effect, and exhibit special chemical and physical properties, which can be widely used in construction, ceramics, textile, biomedical and other industries [1-3]. Nanofilms are a kind of two-dimensional nanomaterials, which are a kind of membrane material composed of grains or particles with sizes between 1～100 nm. Nanofilms can be prepared by chemical and physical methods, the common physical preparation methods include ion beam sputtering, direct current (DC) or radio frequency (RF) sputtering, etc., the common chemical preparation methods include sol-gel method, chemical vapor deposition and electrochemical method [4], etc. Sputtering is one of the most widely used processes for depositing nanofilms, while magnetron sputtering is one of the main methods for preparing nanofilms by physical vapor deposition. Magnetron sputtering is a method in which a gas discharge generates positive ions to bombard a target at high speed under the action of an electric field, causing atoms in the target to escape and deposit a thin film on the surface of the substrate, and is currently the main way to prepare carbon films.

The preparation methods of carbon films mainly include vacuum deposition and liquid deposition, such as cathodic arc deposition, pulsed laser deposition, ion beam deposition, plasma-enhanced chemical vapor deposition and other methods. Among them, magnetron sputtering technology is one of the main methods of carbon film preparation with the advantages of uniform film formation, fast deposition speed and no damage to the substrate material [5-7]. It is well known that carbon is a kind of complex carbon disorder structure, which combines three hybrid structures of SP^1, SP^2 and SP^3, and is a metastable amorphous carbon material. Because of the small content of SP^1 hybridized carbon atoms in them, carbon materials are usually considered to be composed of two hybridized forms, SP^2 and SP^3. Different magnetron sputtering

techniques and processing processes have great influence on the content of SP^2 and SP^3 and cluster morphology in the carbon film structure, forming carbon nanofilms with different morphological structures [8-12]. In order to better study the effects of magnetron sputtering process on the structure and properties of carbon films, this chapter analyzes the effects of magnetron sputtering process on the surface morphology and structure of carbon nanofilms by adjusting the magnetron sputtering time and sputtering power to prepare carbon films with silicon wafers and carbon fibers as substrates, respectively.

Carbon materials are produced via high temperature carbonization performed under an inert gas atmosphere. Different carbonization temperatures will affect the structure and final properties of the carbon material. It has also been shown that different magnetron sputtering substrate temperatures also have an important impact on the properties of the resulting carbon films. Therefore, researchers can change the structure and properties of carbon films by adjusting the substrate temperature or annealing process [13-16]. For example, the hardness and elastic modulus of a carbon film decreases upon increasing the substrate temperature during the condensation reaction [17]. This increase in condensation temperature is beneficial to the orderly formation of aromatic rings and graphite-like clusters in carbon films. At condensation temperatures T > 450 °C, the growth mechanism of the carbon films changes, and nuclei of the graphite phase form directly on the substrate. Annealing the carbon films in the 50–300 °C temperature range also facilitates the regularization of the aromatic ring structure. The majority of previous studies on heat treatment and annealing of carbon films are concerned with temperatures below 800 °C [18,19]; while there are also short-timescale annealing processes with an Fe catalyst in the temperature range 400–1000 °C [20], and carbon films deposited by chemical vapor deposition that are heat treated at temperatures between 800 and 1200 °C [21]. However, research on the structure of carbon films deposited by magnetron sputtering at temperatures between 800-1200 °C is rare [22]. In this study, in order to further analyze carbon films deposited by magnetron sputtering, carbon films deposited on silicon wafers were heat treated at

800–1200 °C, and the effects of the heat treatment temperature on the structure and performance of the resulting carbon films were analyzed, providing a theoretical basis for the structural modification and application of magnetron sputtered nanofilms.

2.2 Experimental part

2.2.1 Experimental materials

Commercially available 12K carbon fiber unidirectional cloth (Toray, Japan) with a single-fiber diameter of 7 μm was employed in this study and the specific performance indicators shown in Table 2-1. The carbon target (99.9% purity, Φ 60 mm, and thickness of 2 mm) was purchased from Beijing Ruifa Zhiyuan Technology Co., Ltd, China. Monocrystalline silicon wafer (2 inch) was purchased from Zhejiang Lijing Company, China. A desizing pretreatment of the carbon fiber was carried out prior to use.

Table 2-1 Carbon Fiber Performance Index

Fiber number (K)	Diameter (μm)	Density (g/cm3)	Tensile strength (GPa)	Tensile modulus (GPa)	Elongation (%)
12	7	1.8	4.9	2.35	2.1

2.2.2 Magnetron sputtering deposition treatment

(1) Substrate preparation

The carbon fiber unidirectional cloth and silicon wafer were first cleaned in an ultrasonic cleaner using ionic water, acetone, and absolute ethanol for 20 min, respectively in order to remove the impurities and oil stains adsorbed on their surface. Distilled water was then used to wash the materials several times until there was no odor. Finally, the washed materials were removed and dried in a vacuum drying oven heated at 100 ℃. The monocrystalline silicon substrate was polished.

(2) Carbon film deposition

The equipment used for depositing the carbon film in this thesis was a JGP-450A multifunctional high vacuum magnetron sputtering instrument, which was equipped with three target positions in the vacuum chamber, and the target head can be installed using a 60 mm diameter target material. The instrument was equipped with two DC power supplies and one RF power supply, with the RF power supply frequency being 13.56 MHz and the maximum output power being 500 W. The target head was installed

at the bottom of the vacuum chamber and the substrate was located on the cover of the vacuum chamber. It was convenient to install and replace the sample, and moreover, this bottom-up deposition mode can prevent impurities on the inner walls of the vacuum chamber from falling onto the surface of the substrate. A schematic diagram of the equipment is shown in Fig. 2-1.

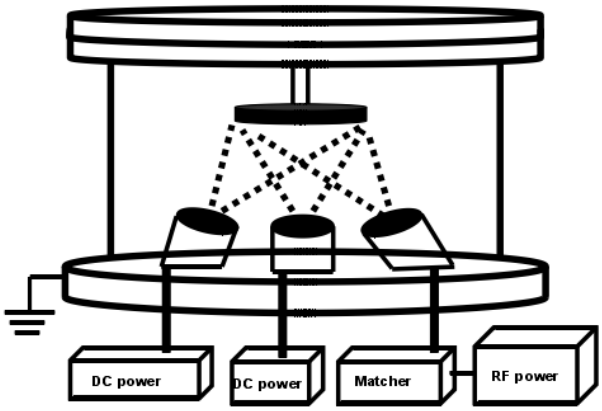

Fig. 2-1 Schematic diagram of magnetron sputtering equipment structure

The deposition of the carbon films on the silicon wafer and carbon fiber substrates was carried out using a magnetron sputtering deposition procedure. The carbon target was installed on a cathode plate. A single carbon fiber, multifilament carbon fiber, and silicon wafer were used as the substrate, which was placed under the substrate support and subjected to the magnetron sputtering process. For the surface modification of a single carbon fiber, the multifilament carbon fiber was first expanded for dispersion. The dispersed carbon fiber was fixed on polyester fabric with glue and then used as the base material for modification. The process is shown in Fig. 2-2.

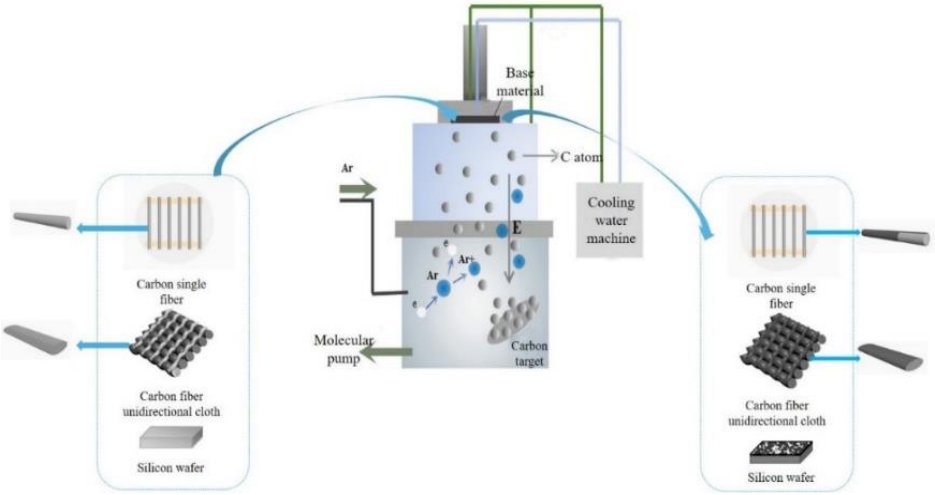

Fig. 2-2 Schematic of the magnetron sputtering modification process

The main sputtering process parameters were as follows: Sputtering pressure, 1.0 Pa; back vacuum, 2×10^{-3} Pa; target substrate distance, 4 cm; working gas, 80 mL/min high-purity argon (99.999%); substrate support rotating speed, 30 rpm. The sputtering time and power were used as the variable parameters. The specific sputtering process and sample numbers are shown in Table 2-2.

Table 2-2 Magnetron sputtering process parameters and sample number

Sample number	Sputtering power/W	Sputtering time/min
Si-C1/ F-SC1/F-MC1	0	0
Si-C2/ F-SC2/F-MC2	250	20
Si-C3/ F-SC3/F-MC3	250	30
Si-C4/ F-SC4/F-MC4	250	40
Si-C5/ F-SC5/F-MC5	250	50
Si-C6/ F-SC6/F-MC6	150	20
Si-C7/ F-SC7/F-MC7	350	20
Si-C8/ F-SC8/F-MC8	450	20

Note: Si-CN represents the carbon film specimen deposited on silicon wafer, F-SCN represents the specimen modified by spreading fiber, and F-MCN represents the specimen modified by bundle fiber, where N represents the specimen number.

2.2.3 Carbon film heat treatment

Using the magnetron sputtering method described above, the carbon films were deposited on silicon wafers with a sputtering power of 350 W and sputtering pressure of 1 Pa for 30 min, and the target-to-substrate distance was set at 40 mm. The silicon wafer with carbon film was then placed in a vacuum tube furnace for heat treatment. The heat treatment temperature was carried out in the range of 800–1200 °C. A vacuum treatment was conducted prior to heating to prevent oxidation of the a-C film. The time required for the vacuum pumping treatment was 3 min. When the barometer reached –0.1 MPa, nitrogen was injected. This vacuum pumping process was repeated 3 times with a duration of 5 min for each cycle. A continuous flow of nitrogen was maintained during the heat treatment. The specific process is shown in Fig. 2-3 and the specific heat treatment conditions and sample numbers are shown in Table 2-3.

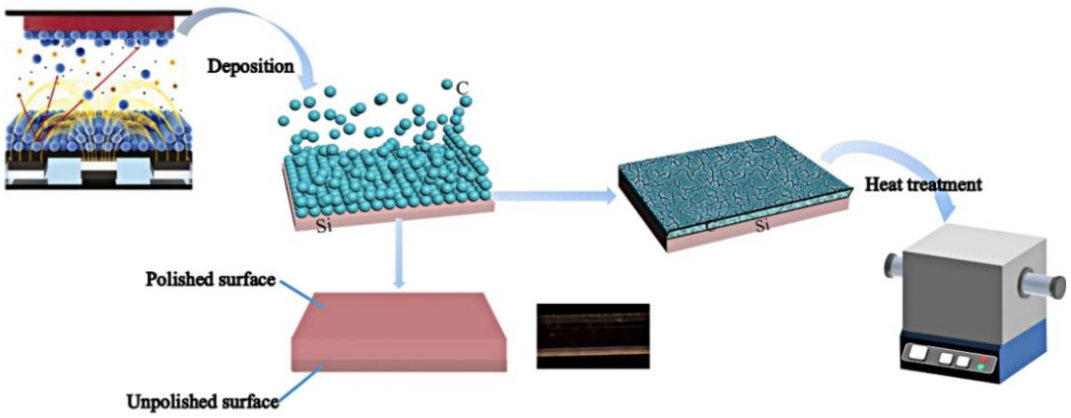

Fig.2-3 Diagrammatic of the Carbon film process

Table 2-3 Magnetron Sputtering Technology and Sample Number

Sample number	Sputtering pressure /Pa	Sputtering time/min	Sputtering power/w	Temperature of heat treatment/°C
1#	1	40	350	none
2#	1	40	350	800
3#	1	40	350	900
4#	1	40	350	1000
5#	1	40	350	1100
6#	1	40	350	1200

2.2.4 Performance testing and characterization

2.2.4.1 Scanning electron microscopy (SEM)

The surface and cross-sectional morphology of the carbon films on carbon fibers and silicon substrates were characterized using scanning electron microscopy (SEM) operated at an acceleration voltage of 5 kV in order to measure the thickness of the carbon films and diameter of the single carbon fiber. The back of the carbon fiber, silicon wafer, or composite fracture surface to be tested on the copper base material was fixed using conductive tape and a gold spraying treatment carried out. A cold field emission scanning electron microscope was then used to characterize the morphology of the sample.

2.2.4.2 Atomic force microscopy (AFM) analysis

The weak interactions formed between the atomic force microscope probe and sample were used to obtain information on the materials surface, which can effectively observe the surface morphology and reflect the state of the measured material surface.

In this paper, AFM was used to characterize the surface morphology and roughness of the carbon films formed on the silicon wafer and carbon fiber substrates before and after the modification process. The sample was fixed on the sample table using double-sided tape and the surface morphology of the sample analyzed in tapping mode over the scanning range of 3 μm × 3 μm and 1 μm × 1 μm, respectively. The surface roughness of the samples was calculated using the analysis software provided with the AFM instrument. In order to obtain reliable results, the specimens were scanned at 5 different points during the test.

2.2.4.3 X-ray diffractometer analysis (XRD)

XRD was used to investigate the phase composition of the materials and characterize the phase composition of carbon films deposited on the silicon wafer, carbon fiber, and heat-treated silicon wafer substrates using the different magnetron sputtering process parameters studied. The X-ray source was Cu-Kα, the scanning speed was 6°/min, and step-by-step value was 0.05°.

2.2.4.4 Raman spectroscopy (Raman)

Raman spectroscopy was used to analyze the vibrations of the C atoms in carbon films deposited on the silicon wafer and carbon fiber substrates before and after the magnetron sputtering modification process using an excitation wavelength of 532 nm and spectral range of 0-3200 cm^{-1}.

2.2.4.5 X-ray photoelectron spectroscopy (XPS)

The bonding characteristics of the films were analyzed using X-ray photoelectron spectroscopy (XPS, Thermo Scientific k-alpha) with a mono Al-Kα radiation source (1486.6 eV) and power of 160 W under a basic pressure of 5×10^{-7} Pa. The size of the analyzed area was 400 μm × 400 μm. The Lorentzian Gaussian fitting method was used to fit the composite peaks. Prior to the XPS analyses, the central areas of the samples were sputter-etched with Ar^{+} (15 keV) to remove the influence of surface adsorption and improve the accuracy of the test.

2.2.5 Carbon film mechanical property test

The hardness and elastic modulus of the carbon films were measured using a

nanoindentation instrument (TI980, Bruker, Hysitron, USA). The indenter used for the test was a standard diamond indenter. A displacement-controlled loading mode was adopted. The load function included a 5 s load time, 2 s hold time, and 5 s unload time. Six loading-hold-unloading hysteresis curves were obtained from different locations for each sample, which nearly overlap with each other indicating the homogeneous characteristics of the obtained films. The Oliver–Pharr [23] method was used to calculate the elastic modulus and hardness of the samples.

According to the ASTMD3359 [24] standard, the adhesion level of the carbon film and silicon wafer substrates was evaluated using a scratch test. Every 1 mm on the silicon wafer loaded with carbon film was scratched and then observed using an optical microscope. The bonding strength between the carbon film and silicon substrate was graded and evaluated according to the ASTMD3359 standard.

The linear reciprocating mode of a ball on disk micro-tribometer (UMT-2, Bruker, USA) was used to carry out friction measurements [25]. The dry friction tests (60% RH and 20 °C) were carried out at room temperature. In all of the measurements, the normal loads and sliding speeds were kept constant at 10 N and 75 mm/s, respectively. The grinding ball was a carbon steel ball with a diameter of 10 mm. The friction test was carried out using an amplitude of 5 mm and the action time was 30 min. Each tribology experiment was repeated five times and the trends observed for the friction curves were found to be nearly identical. The wear morphology of the carbon film was observed using laser confocal microscopy.

2.3 Experimental results and discussions

2.3.1 Surface morphology of carbon film

2.3.1.1 Surface morphology of carbon film on silicon wafer

Fig. 2-4 shows the surface morphology of the carbon films deposited on a silicon wafer substrate. The carbon film formed via magnetron sputtering was composed of fine carbon particles with nanometer size and microcracks on the surface of the carbon film. When the magnetron sputtering process was varied, the surface morphology of the resulting carbon film was different. The surface particle size of the carbon film

deposited using different magnetron sputtering increased with an increase in the magnetron sputtering power, and when the magnetron sputtering power was 150 and 250 W, the pores between the microcracks on the surface of the carbon film were obvious. With an increase in the magnetron sputtering power, the pores between the microcracks on the surface of the carbon film decrease, and the interparticles exhibit an obvious island structure. This is because when the sputtering power is 150 W, the energy of the incident ions is low, and the energy obtained by the carbon particles is also low, which cannot complete the diffusion and aggregation on the surface of the substrate. As the sputtering power increases, the degree of ionization of the discharge carrier increases, prompting the deposited atoms to move with higher energy, the island structure on the substrate surface is enhanced, and the particle size on the film surface increases. When the sputtering power continues to increase and reached 450 W, it makes the atoms originally deposited on the surface of the film sputter again and produce vacancy defects, which also makes the carbon particles overgrow, and the particle size on the surface of the carbon film further increases and exhibit a crack-like morphology.

The particle aggregation state on the surface of the carbon film deposited using different magnetron sputtering times increases upon increasing the sputtering time. The surface of the carbon film formed at a sputtering time of 20 min has obvious cracked pores, the cracked pores on the film surface gradually decrease with an increase in the magnetron sputtering time, and the carbon film deposited under these conditions was composed of particles without aggregation. Upon extending the magnetron sputtering time, particle aggregation appears on the surface of the carbon film, and the particle size on the surface increases. This is because the amount of deposited carbon film begins to increase with an increase in the sputtering time and the atomic islands grow until a continuous dense film is formed. At the same time, as the sputtering time is prolonged, the substrate temperature increases, diffusion was enhanced, the carbon atoms form aggregates on the substrate surface, and the surface particle size increases.

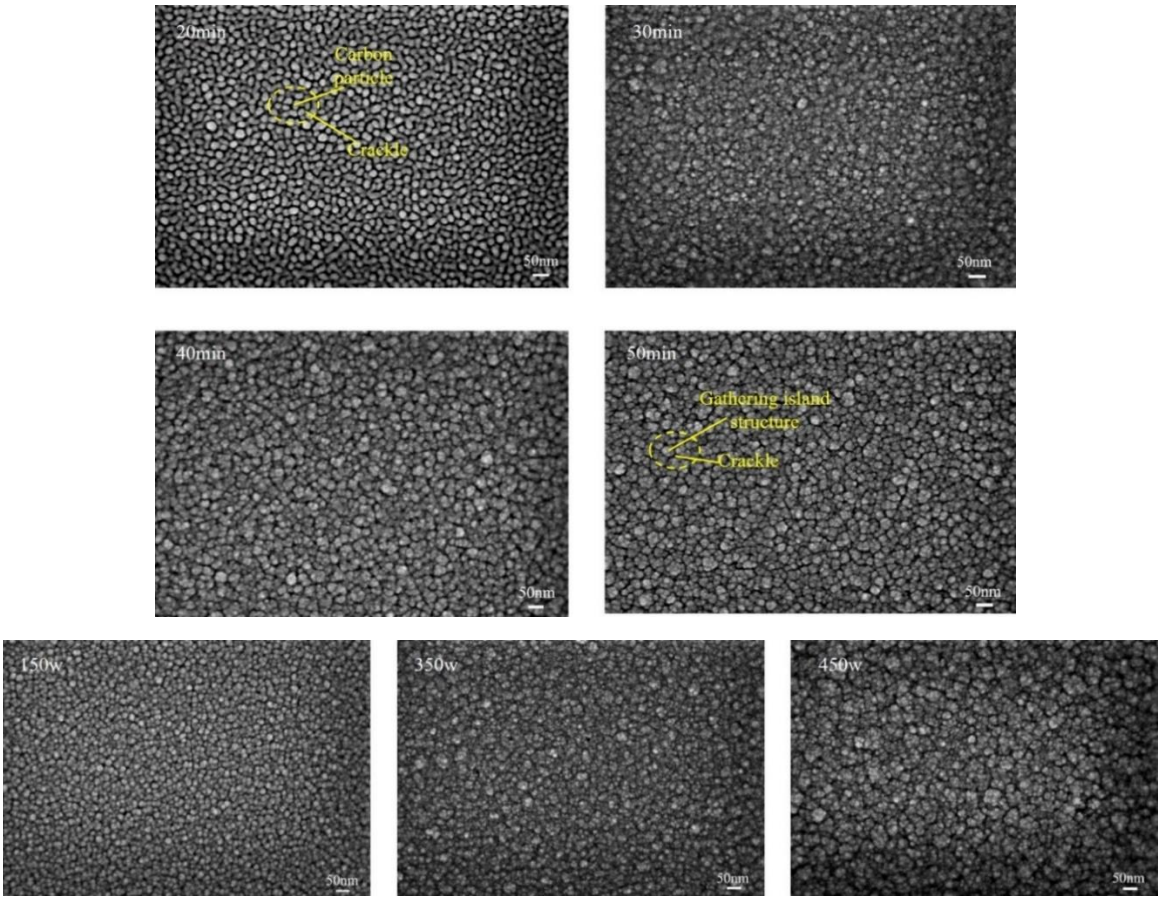

Fig.2-4 SEM images of surface of carbon films on silicon wafer

Fig. 2-5 shows the cross-sectional morphology and thickness of the carbon film deposited on a silicon wafer substrate under the different magnetron sputtering process conditions studied. The cross-section of the carbon films have a typical columnar structure. Due to the compacting effect of the magnetron sputtering power on the carbon film, the thickness of the carbon film increases upon increasing the sputtering power, and the columnar structure of the carbon film cross-section was enhanced. The increase in sputtering power was conducive to the enhancement of the diffusion and aggregation of the carbon particles, which improves the denseness of the carbon film produced. The cross-sectional thickness of the carbon film continuously increases with an increase in the magnetron sputtering time. This is because when the deposition time is short, the amount of carbon film deposited is small, and as the sputtering time increases, the amount of deposition increases, and the thickness of the resulting carbon film increases.

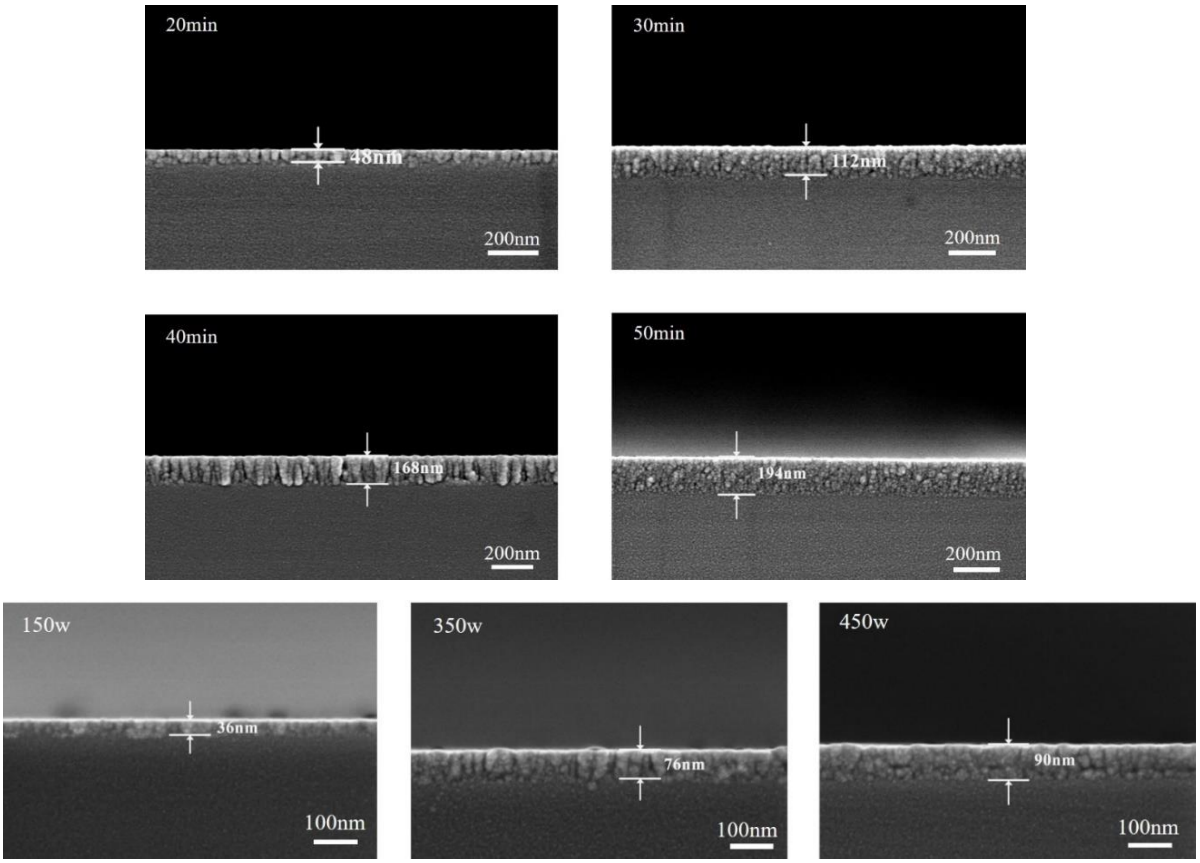

Fig. 2-5 The cross-sectional pattern and thickness of carbon film on silicon wafer

2.3.1.2 Surface morphology of carbon film on carbon fiber

Fig. 2-6 shows the surface morphology of the carbon fibers after modification using the magnetron sputtering process. After the magnetron sputtering treatment, the surface of the carbon fibers was covered by a carbon film. The carbon film deposited on the carbon fiber surface via magnetron sputtering also has microcracks and its morphology was similar to that of the carbon film deposited on the silicon wafer substrate.

When the magnetron sputtering power was the same, the microcracks on the surface of carbon fiber modified over 20 min were numerous and dense, and the density of the microcracks on the surface of the carbon fiber modified using a 30 min sputtering time was the best. The pores of the microcracks on the surface of the carbon fiber after a sputtering time of 40 and 50 min were slightly increased, and the surface aggregation on the carbon film deposited on the surface of carbon fiber was enhanced upon increasing the sputtering time. This is because the carbon fiber is curved and extending

the sputtering time increases the thickness of the carbon film, resulting in an increase in the radius of this curvature, which affects the connections in the lamellar structure of the carbon particles and the surface pore density of the carbon film. At a magnetron sputtering time of 20 min and sputtering power of 150 W, the carbon film deposited on the surface of carbon fiber exhibits obvious traces of inhomogeneity, but no obvious aggregation states were observed. When the magnetron sputtering power was 350 W, the microcrack pores on the surface of the carbon film significantly increase, and there are traces of carbon particles gathering to form sheets. When the sputtering power reached 450 W, the surface of the carbon film has some obvious carbon particle aggregation, the uniformity of the carbon film on the surface of the carbon fiber was enhanced at this time, and the stacking structure of the lamellae enhanced.

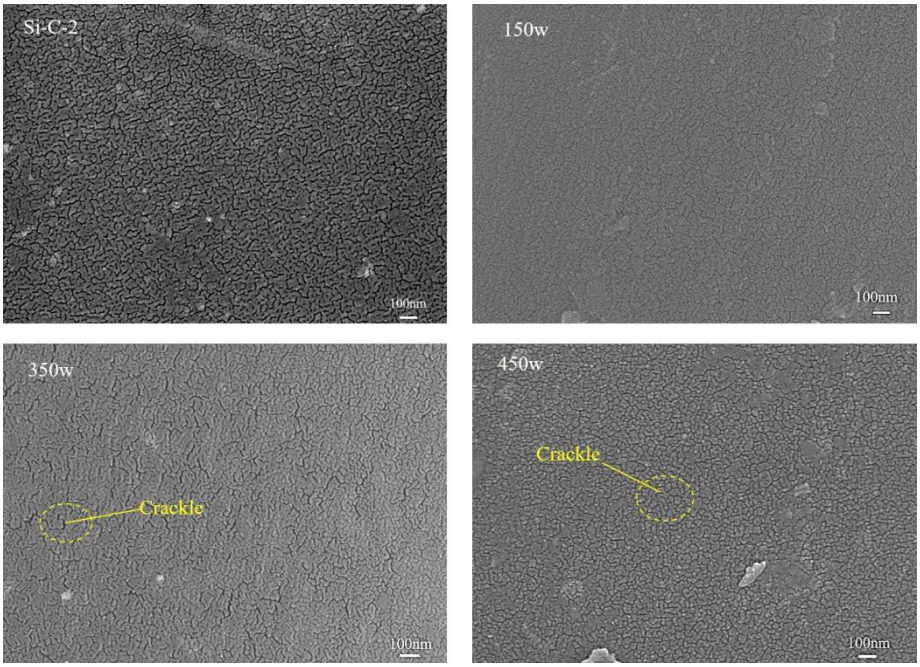

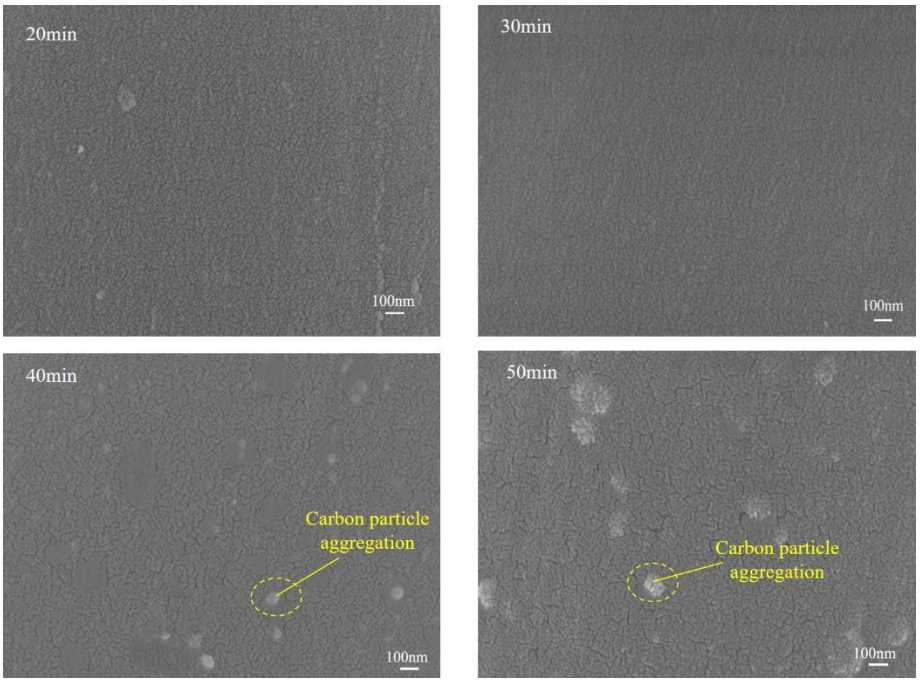

Fig. 2-6 Surface morphology of carbon fiber modified by magnetron sputtering

Fig. 2-7 shows the cross-sectional morphology of the carbon fiber treated using the 250 W and 30 min magnetron sputtering modification process. The carbon fiber surface was covered by a carbon film and the cross-section of carbon film deposited on the carbon fiber surface exhibits a typical columnar structure. The thickness of the carbon film observed in the carbon fiber cross-section was uniform and comparable to the thickness of the carbon film deposited on the silicon wafer under the same magnetron sputtering process conditions.

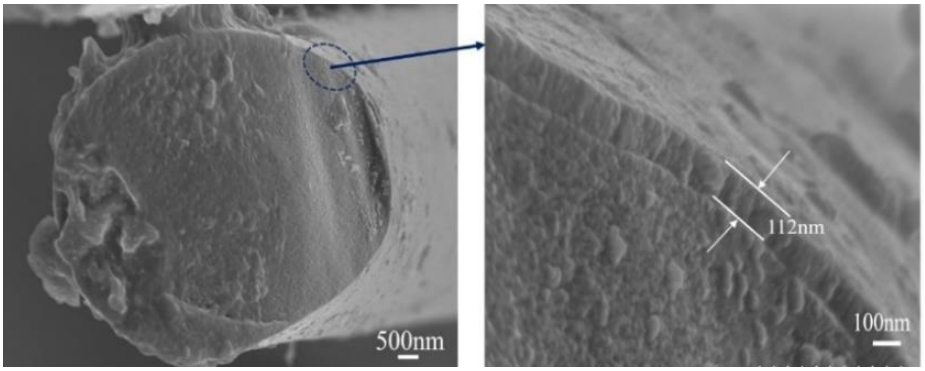

Fig. 2-7 Cross-sectional morphology of carbon fiber by 250w,20min modification

2.3.2 Surface roughness of carbon film

The carbon films deposited via magnetron sputtering have nanometer dimensions. In order to further characterize the effect of the variation in the magnetron sputtering

process parameters on the carbon film surface morphology on the nanometer scale, the carbon film morphology on the different substrates studied was characterized using AFM, and the carbon film surface roughness calculated using the roughness calculation software provided with the AFM instrument.

2.3.2.1 Surface roughness of carbon film on silicon wafer

Fig. 2-8 shows the morphological characterization of the carbon film deposited on the silicon wafer using AFM in the scanning range of 3 μm × 3 μm. The AFM results further demonstrate that the carbon film was composed of particles with nanoscale dimensions. The different roughness of the carbon film surface was observed with the different magnetron sputtering process parameters used. Under the same magnetron sputtering power conditions, the particle size of the carbon film was basically the same, but the aggregation pattern and uniformity of the carbon film surface were different under the different deposition time conditions studied. When the sputtering time was 20 min, there was a small amount of aggregated structures observed on the surface of the carbon film, but the size of these structures was small. Upon extending the sputtering time, the aggregated structure on the surface of the carbon film increases, and when the sputtering time reached 50 min, a larger-sized island structure was formed on the surface of the carbon film and the uniformity of the carbon film was reduced. Under the same magnetron sputtering time conditions, the particle sizes of the carbon films deposited using different magnetron sputtering power were significantly different, and the higher the sputtering power, the larger the particle size of the resulting carbon film. The carbon film deposited under 150 W conditions has obvious sputtering vacancies on its surface. The surface of the carbon film deposited under 350 W sputtering power conditions was dense with good uniformity and a small amount of the carbon particle aggregation state structures was observed. When the magnetron sputtering power reached 450 W, there was an obvious formation of the aggregation state on the surface of the deposited carbon film, the uniformity of the carbon film surface significantly decreased, and the roughness increased.

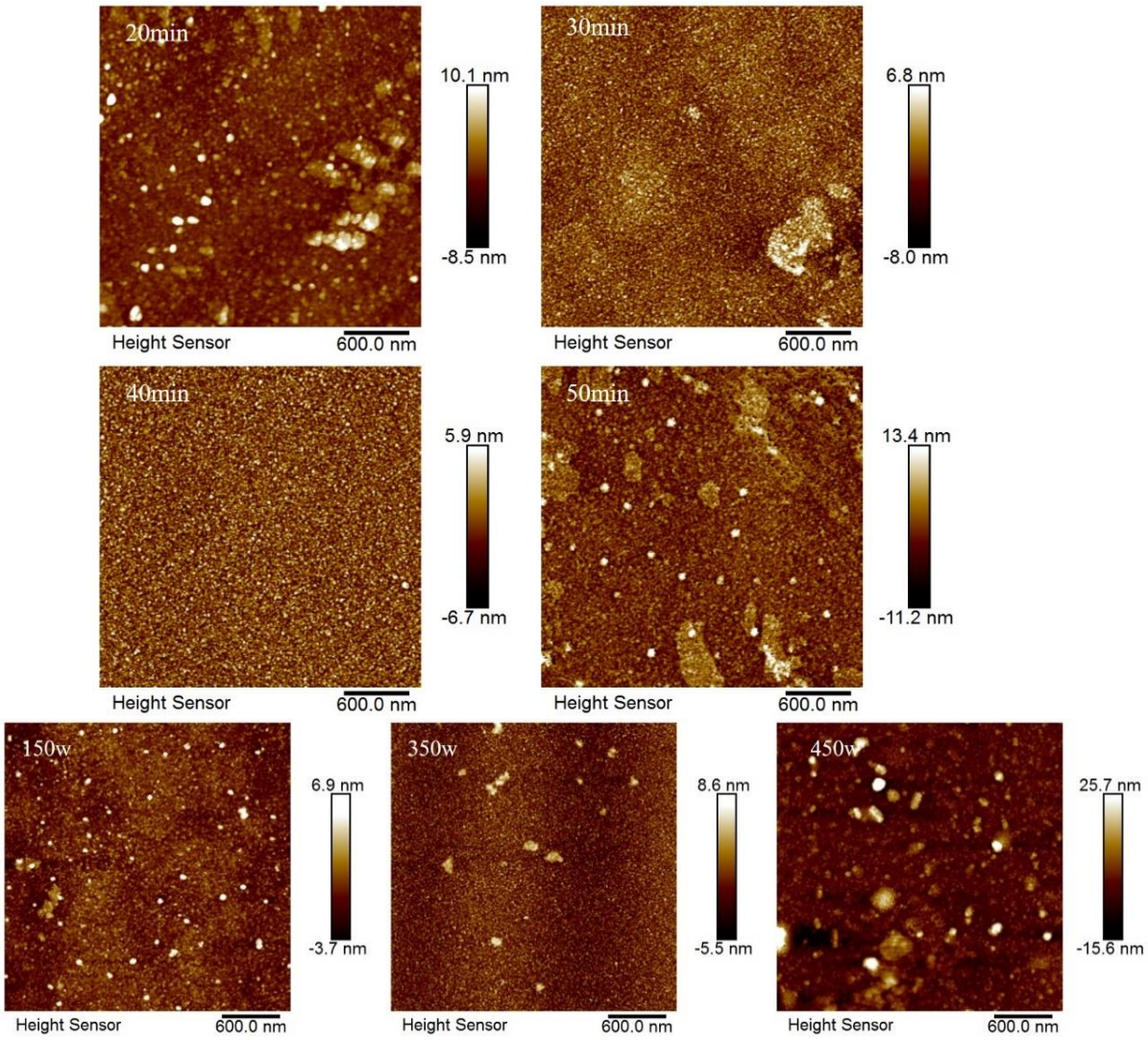

Fig. 2-8 AFM of carbon film on silicon wafer (3 μm × 3 μm)

Under the same magnetron sputtering power conditions and relatively short sputtering time, the amount of carbon particles deposited was low and the surface roughness was reduced. Upon extending the magnetron sputtering time, the amount of carbon particles deposited increases and the carbon film forms a more complete island structure. Further prolonging the sputtering time, the sputtered carbon atoms form aggregates, which increase the particle size and the surface roughness of the resulting carbon film. This can be further compared using the 3D scanning diagram of carbon film obtained using AFM (Fig. 2-9).

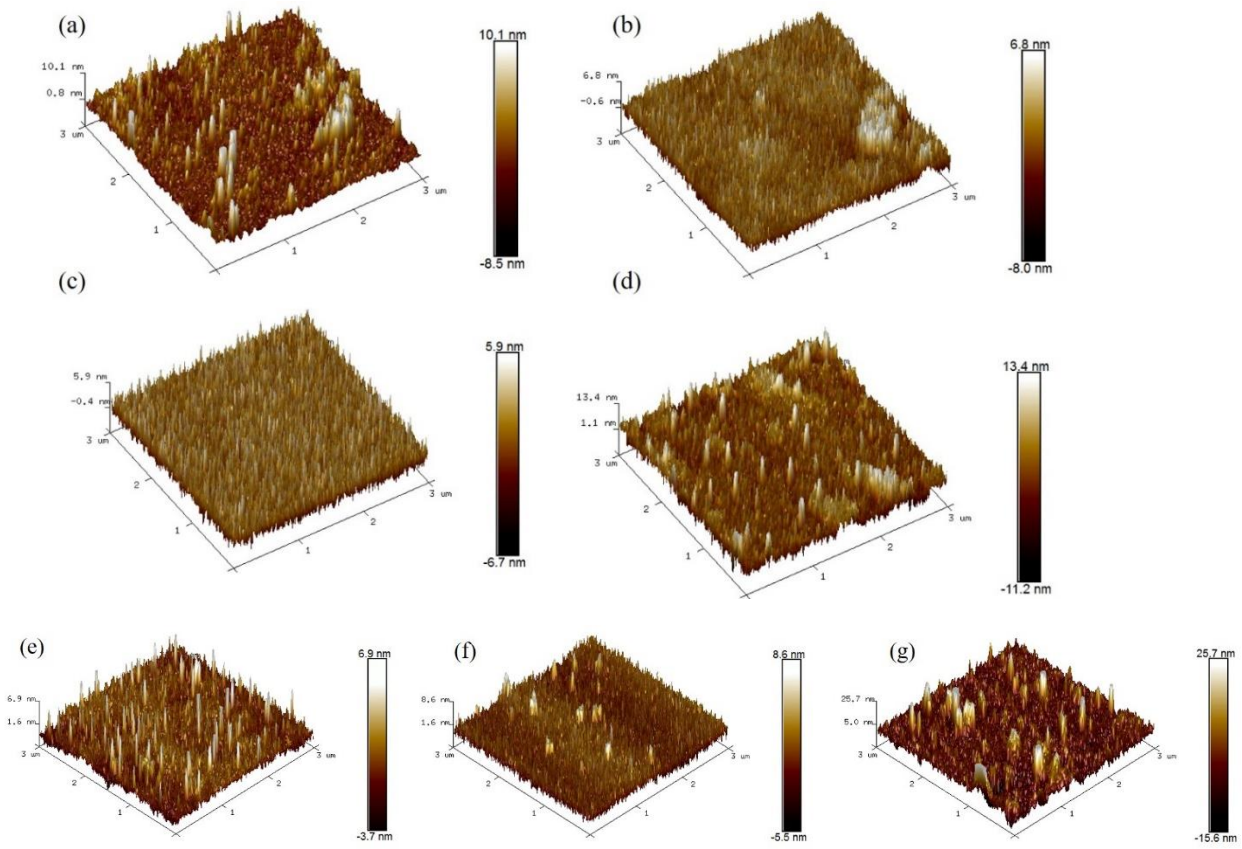

Fig. 2-9 3D AFM of carbon film on silicon wafer (3μm×3μm)

(a) 20min (b) 30min (c) 40min (d) 50min (e) 150w (f) 350w (g) 450w

Table 2-4 shows the surface roughness of the carbon films deposited on a silicon wafer substrate using different magnetron sputtering process conditions, which are consistent with the observed results, in which the surface roughness of the carbon films increases upon increasing the sputtering time and power.

Table 2-4 Surface roughness of carbon film on silicon wafer in different scanning ranges

Sample	3μm×3μm		1μm×1μm	
	Ra/nm	Rq/nm	Ra/nm	Rq/nm
Si-C-2	1.15	1.76	0.792	1.05
Si-C-3	1.35	1.73	1.28	1.62
Si-C-4	1.48	2.14	1.32	1.67
Si-C-5	1.94	2.61	1.85	2.45
Si-C-6	0.837	1.19	0.923	1.2
Si-C-7	1.22	1.57	1.26	1.57
Si-C-8	1.87	2.44	2.22	2.83

In addition, the surface roughness measured in the different scanning ranges of 3 μm × 3 μm and 1 μm × 1 μm show little difference.

2.3.2.2 Surface roughness of carbon fiber

Fig. 2-10 shows the changes in the carbon fibers on the nanoscale before and after modification via magnetron sputtering using AFM in the range of 3 μm × 3 μm. The surface of the unmodified carbon fibers was smooth and has a stripe structure, indicating that there are some defects on the surface of the unmodified carbon fibers. The surface of the carbon fibers modified using magnetron sputtering exhibits some obvious changes. There is an obvious granularity on the surface of the carbon fibers modified at 250 W and 20 min, but stripe structures still exist. Under the same magnetron sputtering power conditions, an increase in the magnetron sputtering time leads to the disappearance of the stripe structure on the surface of carbon fibers, the granular material on the surface of the carbon fiber increases, the particle size of the granular material increases, and the phenomenon of bumps and undulations appears. The surfaces of the carbon fibers modified using different sputtering power with the same magnetron sputtering time also have granular material, but no obvious undulation state larger granular material was observed. This is because the sputtering time of the carbon fibers modified using different magnetron sputtering powers was 20 min, and under this sputtering time condition, the carbon particles have not yet had enough time to aggregate and form island structures, so no larger granular material is formed. The existence of particulate matter on the surface of the modified carbon fibers can increase the specific surface area, increasing the contact area between resin matrix and carbon fibers, which is conducive to the mechanical meshing effect between the two phases of the composite interface.

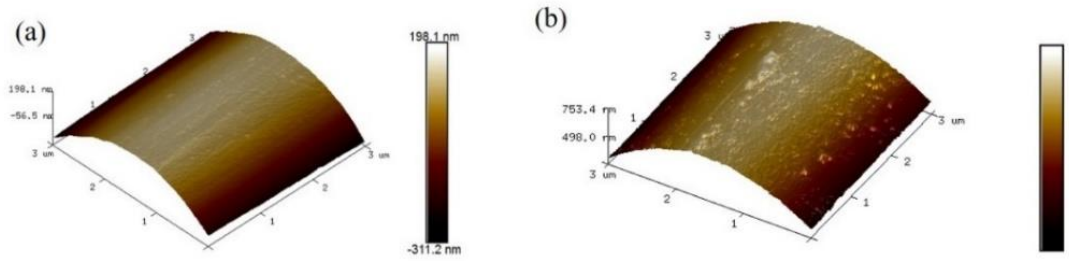

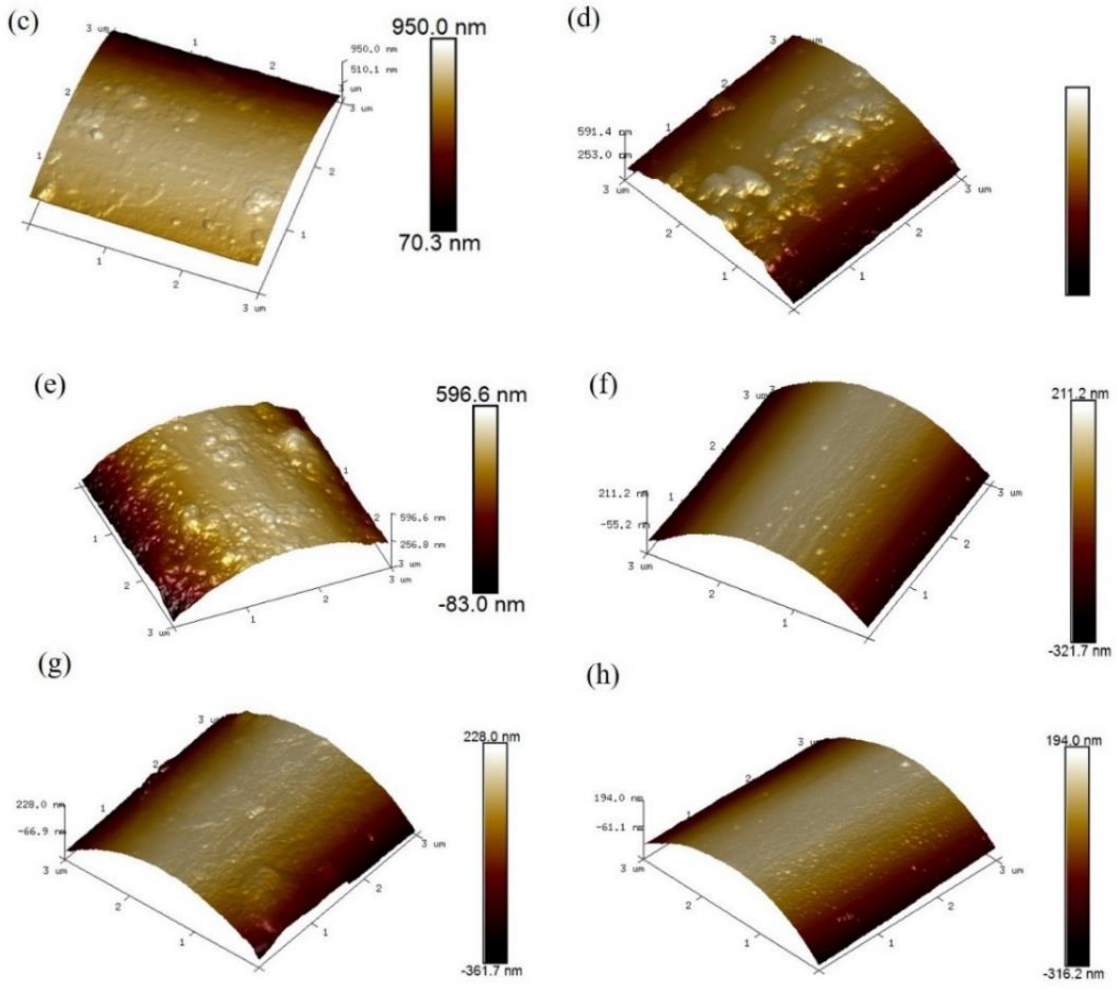

Fig. 2-10 Carbon fiber AFM (3μm×3μm)

(a) unmodified (b) 20min (c) 30min (d) 40min (e) 50min (f) 150w (g) 350w (h) 450w

Table 2-5 shows the surface roughness of the carbon fibers before and after the magnetron sputtering modification process. The arithmetic mean roughness (Ra) and root mean square roughness (Rq) of the unmodified carbon fiber surface were 84.8 and 98.9 nm, respectively under 3 μm × 3 μm scanning conditions. During the magnetron sputtering modification process used in this experiment, the surface roughness of the carbon fibers treated using the other modification conditions increases, but the increase was not significant with the exception of the surface roughness of the carbon fibers modified using 250 W and 20 min conditions, which decreased. The surface roughness of carbon fiber treated using the same magnetron sputtering power modification conditions increases with an increase in the magnetron sputtering time, but when the sputtering time was 50 min, the surface roughness of the carbon fibers slightly decreases.

The surface roughness of the carbon fibers modified over 40 min increased by 7.96%. Under the same sputtering time conditions, the surface roughness of carbon fiber also tends to increase with an increase in the sputtering power, and the surface roughness of the carbon fiber modified using 350 W and 20 min increased by 9.79%.

After the carbon fiber was modified via magnetron sputtering, the surface was covered by a carbon film composed of nanoscale carbon particles, and therefore, the surface roughness of the carbon fiber increases. However, under the 250 W and 20 min modification conditions, the carbon film could not completely cover the striped grooves on the original carbon fiber due to the short magnetron sputtering time and the low number of deposited carbon particles, but can still play a role in filling the stripes on the original carbon fibers. Therefore, the surface roughness of the carbon fibers slightly decreases.

Table 2-5 Surface roughness of carbon fiber in different scanning ranges

Sample	3μm×3μm		1μm×1μm		0.2μm×0.2μm	
	Ra/nm	Rq/nm	Ra/nm	Rq/nm	Ra/nm	Rq/nm
F-SC-1	84.8	98.9	10.7	12.9	1.29	1.63
F-SC-2	82.6	96.35	10.8	12.8	2.56	4.60
F-SC-3	85.27	100.68	11.3	13.1	1.89	2.47
F-SC-4	91.55	107	14.1	20.3	4.50	5.74
F-SC-5	90.2	106	17	20.5	5.75	7.16
F-SC-6	92.6	108	11.9	13.9	1.38	1.74
F-SC-7	93.1	110	12.8	15.5	2.54	1.45
F-SC-8	93.03	108.7	10.6	12.3	2.87	3.68

By comparing the surface roughness of the carbon film on silicon wafer prepared under the same magnetron sputtering process conditions, it was found that the surface roughness of the carbon fibers was much higher than that formed on the silicon wafer substrate. This is because there is a difference in the roughness of the substrate itself. The silicon wafer substrate was polished, so its surface roughness was small, so the difference in the roughness of the characterized carbon film can be judged to be caused entirely by the difference in the parameters used during the magnetron sputtering process. In contrast, the surface of the carbon fibers is curved and there are defects on

the surface of the carbon fibers with cross-stripe grooves. At the same time, because the carbon fibers were also applied to the slurry agent during processing, although most of it is removed by washing, there is still a small amount of residue. Therefore, the surface of the carbon fiber substrate was not smooth. In addition, the diameter of the single carbon fiber has an effect on the AFM scanning results. The single carbon fiber diameter was only ~7 μm, and the scanning range of AFM is 3 μm × 3 μm, which is approximately within the radius size of the carbon fiber itself, and can be influenced by its surface morphology. Therefore, we believe that this is the main reason why the surface roughness of the carbon fibers modified using magnetron sputtering does not change much from the surface roughness of unmodified carbon fibers. Meanwhile, when comparing the surface roughness of the carbon fibers in the different scanning ranges of 3 μm × 3 μm and 1 μm × 1 μm, it was found that surface roughness of the carbon fibers was significantly different under the two scanning conditions used.

Under 1 μm × 1 μm scanning conditions, the surface roughness of the unmodified carbon fiber was less than that observed for the carbon fibers after the magnetron sputtering modification process, but the surface roughness of carbon fiber measured under 1 μm × 1 μm scanning conditions was much smaller than that observed under 3 μm × 3 μm scanning conditions after the same magnetron sputtering process. The changing trend observed for the carbon fiber surface roughness due to the magnetron sputtering process was the same under the two different scanning range conditions, but the magnitude of these changes was different. The surface roughness of the carbon fiber measured under 1 μm × 1 μm scanning conditions was more obviously affected by the magnetron sputtering process. Under the same magnetron sputtering power conditions, when the sputtering time was increased from 20 to 40 min, the increase in the rate of the carbon fiber surface roughness was 3.66% and 1.59% for the 3 μm × 3 μm scanning conditions, and 33.14% and 68.67% for the 1 μm × 1 μm scanning conditions, respectively.

The surface of the unmodified carbon fibers has some undulations, but the fluctuation was small and the fluctuation range was uniform. The reason for the

roughness can be mainly attributed to the formation of carbon fiber surface grooves and residual slurry. The surface of carbon fiber modified via magnetron sputtering has obvious roughness with the exception for the carbon fiber surface modified under 150 W and 20 min conditions, which shows no obvious fluctuation. The carbon fiber surface modified via magnetron sputtering has an obvious island structure morphology. In addition, the surface fluctuation of the modified carbon fibers was no longer uniform. When the magnetron sputtering modification conditions were different, there is a difference in the size of the carbon fiber surface island structures. For example, the surface morphology of carbon fiber modified under 250 W and 20 min conditions has an obvious particle stacking structure and poor uniformity.

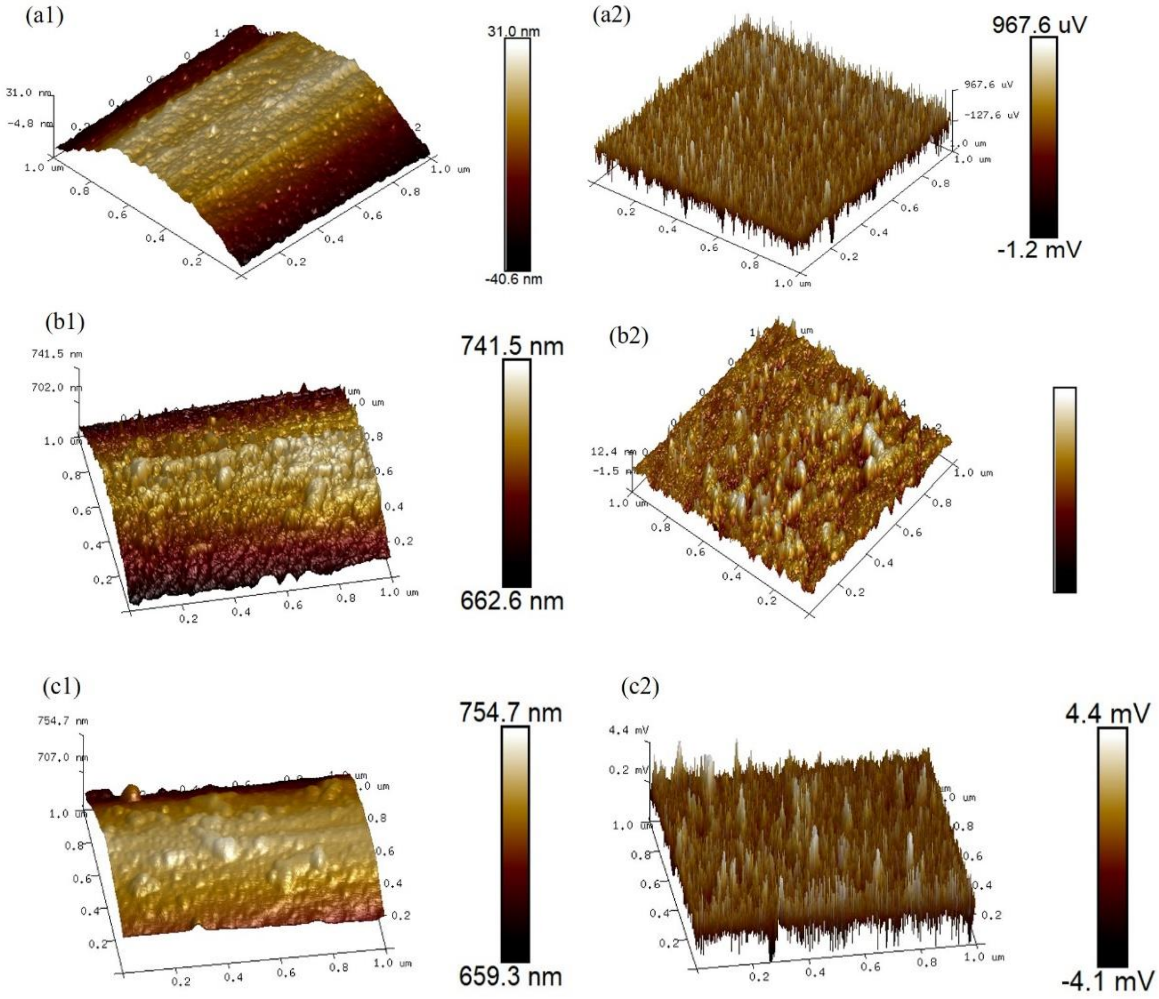

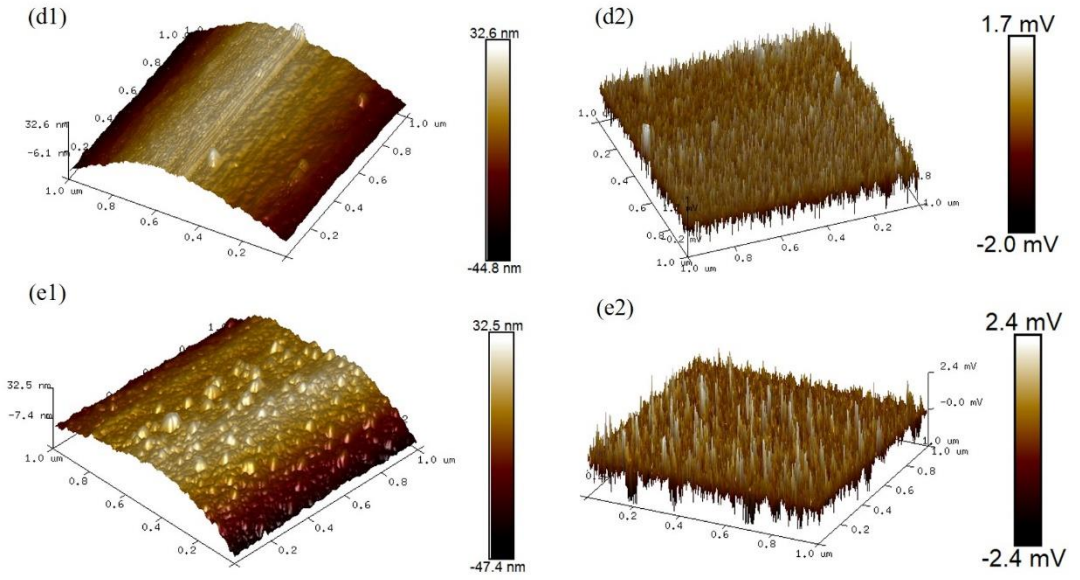

Fig. 2-11 AFM of carbon fiber (1μm×1μm)

(a1) (a2) unmodified, (b1) (b2) 20min, (c1) (c2) 30min, (d1) (d2) 150w, (e1) (e2) 350w

By comparing the surface roughness of a single carbon fiber in the different scanning ranges of 3 μm × 3 μm and 1 μm × 1 μm, and comparing the results with the surface roughness of a carbon film formed on the silicon wafer substrate, we believe that the effect of the magnetron sputtering process on the surface roughness of the carbon fibers was better reflected by the roughness calculation in a small scanning range. Therefore, the carbon fiber surface roughness in the range of 0.2 μm × 0.2 μm was calculated and it was found that the scale range of the carbon fiber surface roughness in this state was closer to the surface roughness of the carbon film formed on the silicon wafer substrate. The surface roughness of the modified carbon fibers in the range of 0.2 μm × 0.2 μm increased significantly when compared to that before the modification process with a maximum increase of 3.46 times.

The smoothness of the carbon fiber surface is one of the factors affecting whether the carbon fiber and resin matrix can exhibit good bonding performance. The increase in the surface roughness of the carbon fibers after the magnetron sputtering modification process is beneficial to the interfacial meshing between the carbon fibers and resin matrix during the preparation of carbon fiber composites.

2.3.3 Raman spectroscopy

Raman spectroscopy is one of the most important methods used to characterize the internal microstructure of carbon materials and is the most intuitive way to identify carbon species [28].

The Raman spectra of the carbon films are mainly composed of D peaks observed at ~1350 cm^{-1} and G peaks at ~1580 cm^{-1}. The D peaks represent carbon defects, which originate from the breathing vibrations of the six-membered carbon ring clusters, and are a sign of the disorder in the carbon structure. The G peaks originate from the in-plane stretching vibrations of all of the sp^2 orbitals (ring or chain) in the carbon material. In addition, the intensity ratio of the D to G peak (I_D/I_G) is often used to express the relative content of sp^2 and sp^3 hybridized carbon atoms in carbon materials [29]

2.3.3.1 Raman spectra of carbon films on silicon wafer

Fig. 2-12 shows the Raman spectra obtained for the carbon films formed on a silicon wafer substrate under the different magnetron sputtering process conditions studied. The carbon films deposited on silicon wafers using different magnetron sputtering conditions were found to have characteristic Raman peaks at ~1350 and 1580 cm^{-1}. All of the carbon films deposited by magnetron sputtering have a relatively sharp G peak at 1580 cm^{-1}, but the characteristic D peak near 1350 cm^{-1} varies with the magnetron sputtering process used. At a sputtering power of 250 W and magnetron sputtering time of up to 30 min, the carbon film on the wafer exhibits a small shoulder peak near 1350 cm^{-1}, which gradually decreases as the magnetron sputtering time increases. Similarly, when the sputtering time was 20 min, the carbon film deposited on the silicon wafer at different magnetron sputtering power also decreases with an increase in the sputtering power, and the characteristic peak near 1350 cm^{-1} gradually decreases. When the sputtering power was <250 W, the carbon film has obvious Raman characteristic peaks at ~1350 and ~1580 cm^{-1}, when the sputtering power was 350 W, the peak at ~1350 cm^{-1} was reduced to a small shoulder, and when the magnetron sputtering power reached 450 W, the peak at ~1350 cm^{-1} almost disappeared. However, upon fitting the Gaussian curve, the carbon film still has the corresponding D and G peaks at 1360 and 1580 cm^{-1}, respectively, which still shows the typical Raman

spectrum observed for carbon. The carbon structure on the surface of the carbon film formed on the silicon wafer substrate is the structure of the carbon target, which exhibits a strong graphitic structure, therefore the characteristic Raman peak near 1580 cm^{-1} was obvious. However, because the substrate is a silicon wafer, when the sputtering process was varied, it will cause the substrate temperature to change, which will affect the structural morphology of the carbon film formed on the silicon wafer. Ferrari has proposed a three-state model with increasing disorder in the carbon film structure: The first stage is the transformation process from intact graphite crystal to nano-graphite, the second stage is the transformation process from nano-graphite crystals to sp^2 bonded carbon, and the third stage is the transformation process from sp^2 carbon to sp^3 carbon. When the magnetron sputtering power was low and the sputtering time short, the carbon film was still in the first stage, so the Raman peaks show graphite-like characteristics. As the magnetron sputter-deposited carbon film is an unstructured mixture of sp^3 hybridized carbon in diamond and sp^2 hybridized carbon in graphite, when using visible light laser excitation, the π state resonates, whereas the σ state does not, resulting in a Raman spectrum being dominated by the sp^2 signal even if 10%–15% of the sp^3 structure was present in the carbon film structure, making the Raman spectrum of a-CF exhibit graphite-like carbon sp^2 peak positions. Therefore, when the sputtering time was prolonged and the sputtering power increased, it raises the temperature of the substrate and affects the microstructure of the carbon film deposited on the silicon wafer substrate. The G-peak position shifts to the high wavenumber region in the Raman spectrum.

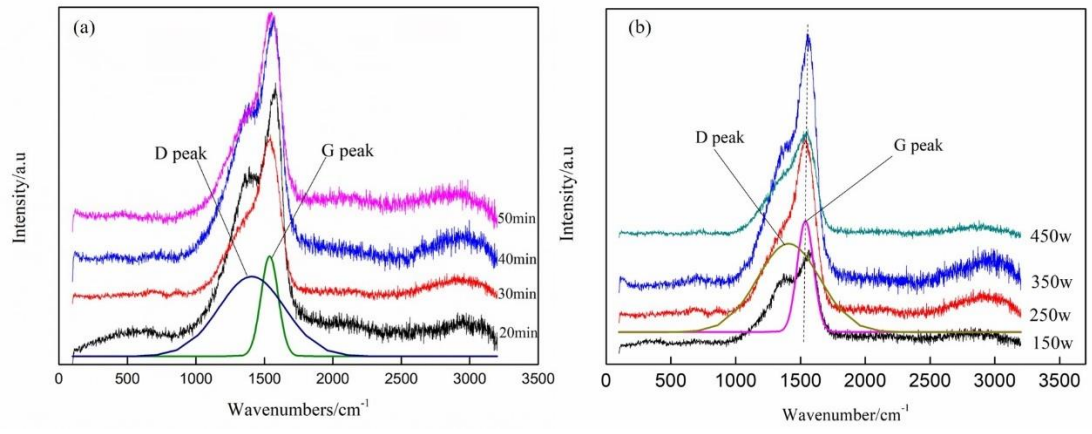

Fig. 2-12 Raman spectra of carbon films on silicon wafers

(a) Different sputtering time (b) Different sputtering power

2.3.3.2 Raman spectra of carbon fibers

Fig. 2-13 shows the Raman spectra obtained for the carbon fibers before and after the magnetron sputtering modification process. The carbon fibers before and after the modification process exhibit obvious Raman peaks at 1350 and 1580 cm^{-1}, in addition to the graphite secondary Raman peak at 2730 cm^{-1}. The magnetron sputtering modification treatment was found to have little effect on the hybridization structure of the carbon fibers. The effect of the different sputtering power conditions on the hybrid structure of the carbon fibers was greater than that of the sputtering time.

The Raman spectra obtained for the carbon fibers modified using the same sputtering power show regular changes with a gradual increase in the sputtering time, and the wavenumbers of the D and G peaks only fluctuated by ~10 cm^{-1}. When the sputtering power was the same and the sputtering time was <30 min, the D and G peaks show a tendency to move slightly to the high and low wavenumber region, respectively, upon extending the sputtering time. When the sputtering time was 20 min and the sputtering power was varied, the Raman spectra of the modified carbon fibers did not change regularly with the sputtering power.

This can be attributed to the carbon film content on the surface of the carbon fiber being reduced in the modified carbon fibers. This does not have a large impact on the structural composition, which are still dominated by the carbon fiber, so the Raman spectrum does not change significantly. However, the differences in the magnetron sputtering process can lead to differences in the morphology and stable structure of the deposited film on the surface of the carbon fibers, resulting in small differences in the Raman spectra obtained for the carbon fibers modified using the different magnetron sputtering processes studied. Due to the different sputtering power, the size of the carbon particles and stable state of the final carbon film formed by the sputtered carbon film are different, resulting in no regular changes in the Raman spectra being observed for the modified carbon fibers.

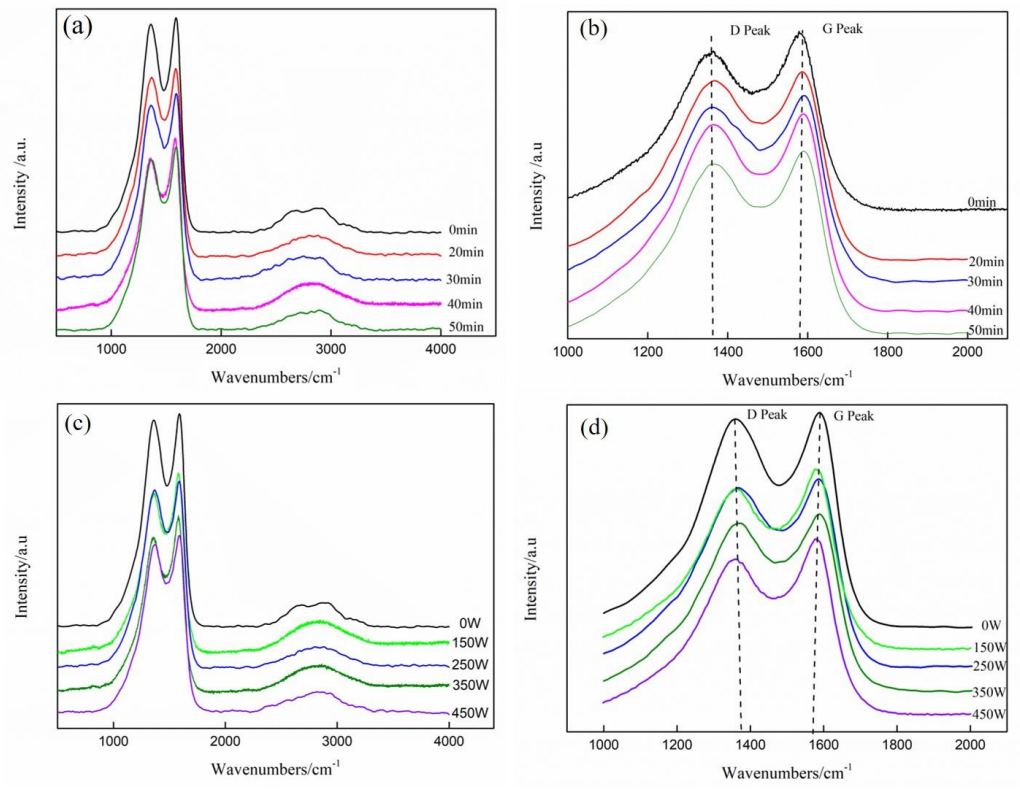

Fig. 2-13 Raman spectrum of carbon fiber modified by magnetron sputtering

(a) Treated at different sputtering time in the 500-4000cm^{-1} Raman shift range (b) Treated at different sputtering time in the 1000-2000cm^{-1} Raman shift range (c) Treated at different sputtering power in the 500-4000cm^{-1} Raman shift range (d) Treated at different sputtering power in the 1000-2000cm^{-1} Raman shift range

The I_D/I_G ratios observed at 1350 and 1580 cm^{-1} for the carbon fibers modified using magnetron sputtering are shown in Fig. 2-14.

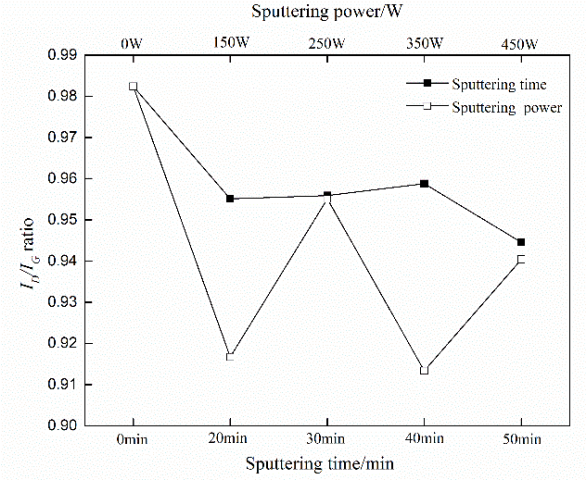

Fig. 2-14 I_D/I_G ratio of carbon fibers modified by magnetron sputtering

With the same sputtering power, the I_D/I_G ratios of the carbon fibers modified using different sputtering times were smaller than the unmodified carbon fibers, and the I_D/I_G ratio gradually decreases with an increase in the sputtering time, indicating that the degree of graphitization in the modified carbon fibers tends to increase. The I_D/I_G ratio of the carbon fibers modified using different magnetron sputtering power conditions was also smaller than that of the unmodified carbon fibers. Among them, the I_D/I_G ratios of the carbon fibers modified under 150 and 350 W conditions were relatively small, but the reasons for their smaller I_D/I_G ratios are different. For carbon fibers modified under 150 W sputtering conditions, the magnetron sputtering power was relatively low and the sputtering time relatively short, thus the particles deposited on the surface of the carbon fiber do not form a more complete layer structure, and the carbon particles do not gather into islands. Therefore, the performance of the carbon target structure on the carbon fiber was more obvious. The reason for the smaller I_D/I_G observed for the carbon fibers modified under a 350 W sputtering power can be attributed to the film structure formed by the carbon particles deposited on the surface of the carbon fibers having a more stable ordered structure, thus enhancing the ordered structure of the carbon fibers. When the sputtering power reached 450 W, the formation of the stable carbon film structure was affected by the large sputtering particles, which leads to the formation of an ordered graphite structure on the carbon fiber surface.

Although there is a significant difference between the Raman spectra obtained for the carbon films formed on the silicon wafer and modified carbon fiber substrates under the same magnetron sputtering process conditions, the Raman spectra of the carbon fibers before and after modification via magnetron sputtering do not change significantly, indicating that the modification process does not have a significant effect on the microstructure of the carbon fibers.

2.3.4 XRD analysis

2.3.4.1 XRD of carbon films on silicon wafers

Fig. 2-15 shows the XRD patterns obtained for the carbon film formed on the silicon wafer substrate and it was found that they show no obvious graphite crystal

diffraction peaks at 2θ = 25° with the exception for the carbon films prepared under 450 W and 20 min conditions, which show carbon (002) graphite crystal diffraction peaks at 2θ = 25°, and the XRD patterns show more of the characteristic diffraction peaks corresponding to the silicon wafer substrate. When the modification process uses a magnetron sputtering power of 250 W and sputtering time of 20 min, the carbon film does not show any obvious carbon diffraction peaks, and only the characteristic diffraction peaks corresponding to silicon (111) and silicon (220) at 2θ = 30 and 46° were observed, respectively. This can be attributed to the carbon film deposited on the silicon wafer not forming a dense carbon film due to the short sputtering time, and the deposited amount was small, so the characteristic diffraction peaks of carbon were obscured by the diffraction peaks of the silicon wafer substrate. Upon increasing the sputtering time, the steady-state of the carbon film layer deposited on the silicon wafer was enhanced and the amount of deposition increases, so that a sharp characteristic diffraction peak corresponding to carbon (111) was observed at 2θ = 42°. Similarly, when the modification conditions were 20 min sputtering time and 150 W sputtering power, the carbon film deposited on the silicon wafer exhibits no obvious characteristic carbon diffraction peak, only a weak silicon (311) peak, which indicates the existence of the carbon film on the silicon wafer and the carbon film exhibits a masking effect on the characteristic silicon peak. With an increase in the sputtering power, the XRD patterns of the carbon films on the silicon wafer substrate present a characteristic carbon (111) peak at 2θ = 42°, and when the sputtering power reached 450 W, the carbon film presents a characteristic diffraction peak for carbon (002) graphite crystals at 2θ = 25°.

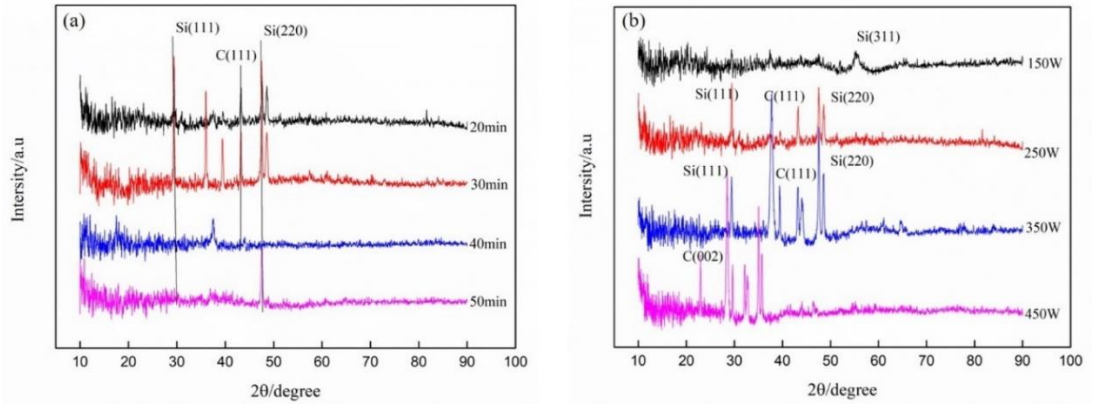

Fig. 2-15 XRD of carbon film on silicon wafer

(a) Different sputtering time (b) Different sputtering power

2.3.4.2 XRD of carbon fiber

Fig. 2-16 shows the XRD patterns of the carbon fibers before and after modification via magnetron sputtering. There are only two diffraction peaks exhibited in the XRD pattern of the carbon fibers both before and after the modification process: One is a sharp characteristic diffraction peak at $2\theta = 25°$, which corresponds to the carbon (103) plane of the typical graphite crystal structure of carbon fibers. The other peak is a weak diffraction peak corresponding to carbon (012) observed at $2\theta = 43°$; no other diffraction peaks were observed. This shows that the magnetron sputtering modification process has no effect on the physical phase structure of the carbon fibers. The d_{002} layer spacing of the carbon fibers modified via magnetron sputtering also exhibits a very small change with a tendency to decrease upon increasing the magnetron sputtering time and power. When the magnetron sputtering power was the same, the d_{002} layer spacing of the modified carbon fiber decreases gradually with an increase in the magnetron sputtering time. When the modified magnetron sputtering time was the same, the d_{002} layer spacing of the modified carbon fibers also decreases gradually with an increase in the magnetron sputtering power when the modified sputtering power was >250 W. The decrease in the modified carbon fiber d_{002} layer spacing indicates that the degree of graphitization in the modified carbon fibers after the magnetron sputtering process was slightly increased, which was consistent with the analysis of the Raman spectra obtained for the modified carbon fibers. The microstructure of the carbon targets used for the sputtering process differs from that of the carbon fibers due to the different processing methods used. The degree of graphitization in the carbon target was relatively high and well-ordered. Therefore, with an increase in the magnetron sputtering time, the thickness of the resulting carbon film formed on the surface of the carbon fibers increases, and carbon fiber exhibits an increase in the degree of graphitization. When the magnetron sputtering power was varied, the morphology of the layered structure of the carbon film deposited on the surface of the carbon fibers will be different, and the structure of the carbon film formed will have a weak effect on the microstructure of the carbon fibers.

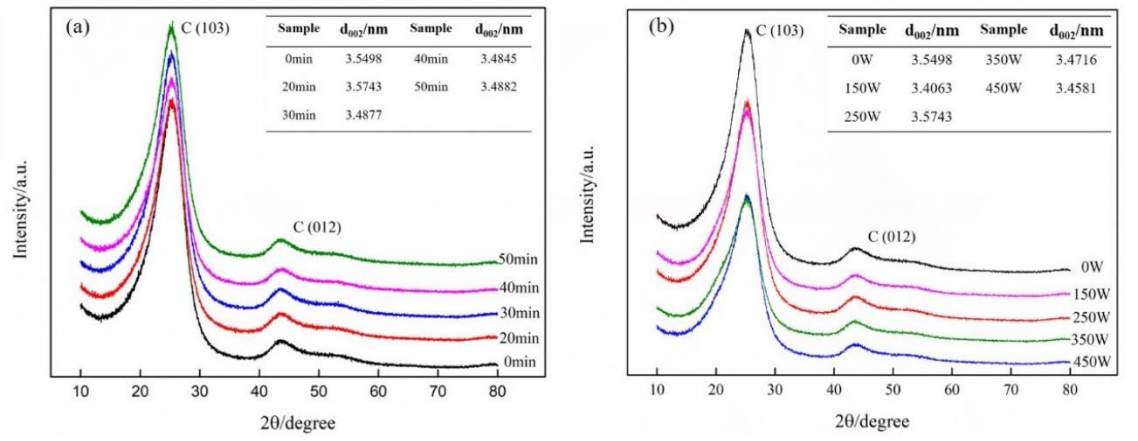

Fig. 2-16 XRD of carbon fiber

(a) Different sputtering time (b) Different sputtering power

2.3.5 Morphology and structure of carbon film after heat treatment

2.3.5.1 Raman spectroscopy

The Raman spectra of the carbon films before and after heat treatment are shown in Fig. 2-17. There are characteristic Raman peaks near 1360 cm^{-1} and 1580 cm^{-1} in the magnetron-sputtered carbon films, indicating that the magnetron-sputtered carbon films observed before and after heat treatment are a-C films. The intensity of the D and G peaks increased after heat treatment, and when the treatment temperature does not exceed 1100°C, the intensity of D and G peaks increases with increasing treatment temperature. This is due to an initially low degree of carbon atom aggregation in the a-C films. With increasing heat-treatment temperature, the carbon atoms in the a-C films move and diffuse, and the degree of carbon atom aggregation increases, which leads to the increased intensity of the D and G peaks. As shown in Fig. 2-17 (a), the D peak of the a-C films shifts to a lower wave number, while their G peak shifts to a higher wave number with increasing treatment temperature. However, at a treatment temperature of 1200°C, the wave number of the G peak is lower. It can be seen from the full width at half maximum (FWHM) shown in Fig. 2-17 (c) that the D peak gradually narrows with increasing treatment temperature. While treatment temperature does not exceed 1100°C, the G peak FWHM shows a narrowing with increasing treatment temperature, although when the treatment temperature reaches 1200°C, the G peak widens. The intensity ratio of the D peak to the G peak, I_D/I_G, decreases with increasing treatment temperature,

when the temperature does not exceed 1100°C, and increases when the treatment temperature reaches 1200°C.

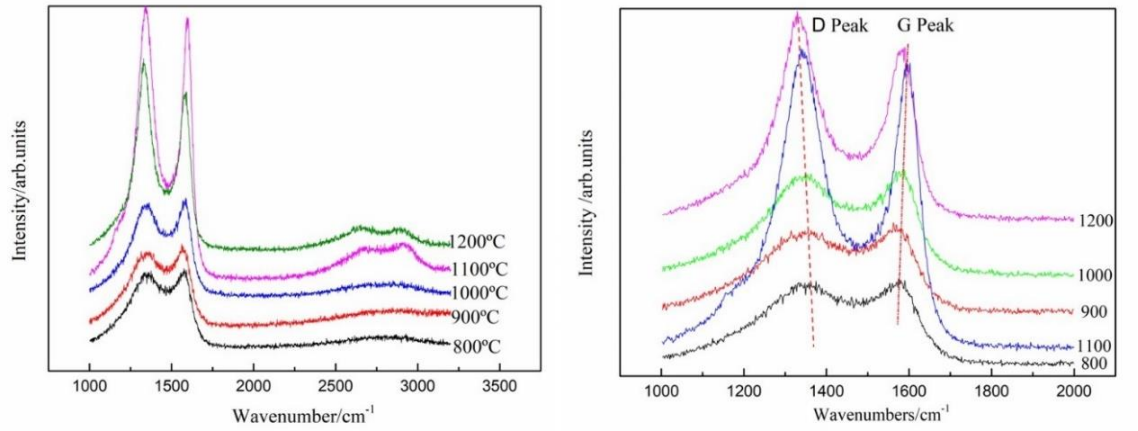

Fig.2-17 Raman spectra of carbon films after heat treatment

(a) Treated at different temperatures in the 1000-3000 cm^{-1} Raman shift range (b) Treated at different temperatures in the 1000-2000 cm^{-1} Raman shift range

These results show a reduction in the disordered structure, and an increased ordering of the a-C films with increasing heat-treatment temperature. This implies an increase in both sp^2-bonded carbon content and the degree of graphitization in the a-C films. However, crystals formed in a-C films belong to the carbon polycrystalline structure, which is composed of many small carbon single crystals with no specific orientation [16,19]. When the heat-treatment temperature reaches 1200°C, the crystals in the a-C films also aggregate, which restructures the carbon atoms and affects the formation of the ordered a-C film structure. The second-order Raman peaks of graphite are characterized by strong peaks near 2730 cm^{-1} and weak, sharp peaks near 3250 cm^{-1}. Compared with the first Raman peak, the second Raman peak is more sensitive to a small amount of disorder in the graphite lattice. The second-order Raman peak of graphite appears in the a-C film after heat treatment near 2730～3000 cm^{-1}[20]. With increasing heat-treatment temperature, the intensity of the second-order Raman peaks gradually increases, and the double-peak phenomenon becomes more apparent: the peaks narrow, which further explains the enhanced degree of graphitization in the a-C films.

2.3.5.2 XRD analysis

The XRD data for the magnetron-sputtered carbon film is shown in Fig.2-18.

There is no typical sharp characteristic diffraction peak of carbon in the untreated magnetron-sputtered carbon film near 2θ = 25°, only a wider diffraction packet, indicating that these carbon films deposited by magnetron sputtering belong to the a-C material group. However, there is a sharp characteristic peak at 2θ = 69°, which is the overlapping diffraction characteristic peak of the Si (400) of the substrate and C (103); according to an analysis of the crystallinity of these elements, the characteristic peaks of Si (400) diffraction are dominant. Only the magnetron-sputtered carbon film which was subject to heat treatment at 800°C has a weak diffraction peak package at 2θ = 25°, while the diffraction peaks of the other films disappear at this point. Fig. 2-18 show the results for films with a heat-treatment temperature beyond 900°C, with diffraction peaks characteristic of C (103) and Si (400) that are clearly separated at 2θ=69º, which indicates an enhancement of the microcrystalline structure of the a-C films. The diffraction peaks of lonsdaleite (102) and C (109) appear near 2θ = 61.8° and 2θ = 66.7° after heat treatment. Lonsdaleite, a type of diamond crystal structure, is considered to play an important role in the transformation of graphite to diamond [28]. It is shown that after heat treatment, new carbon crystals are formed in addition to the original carbon microcrystals, but these are not graphite crystals.

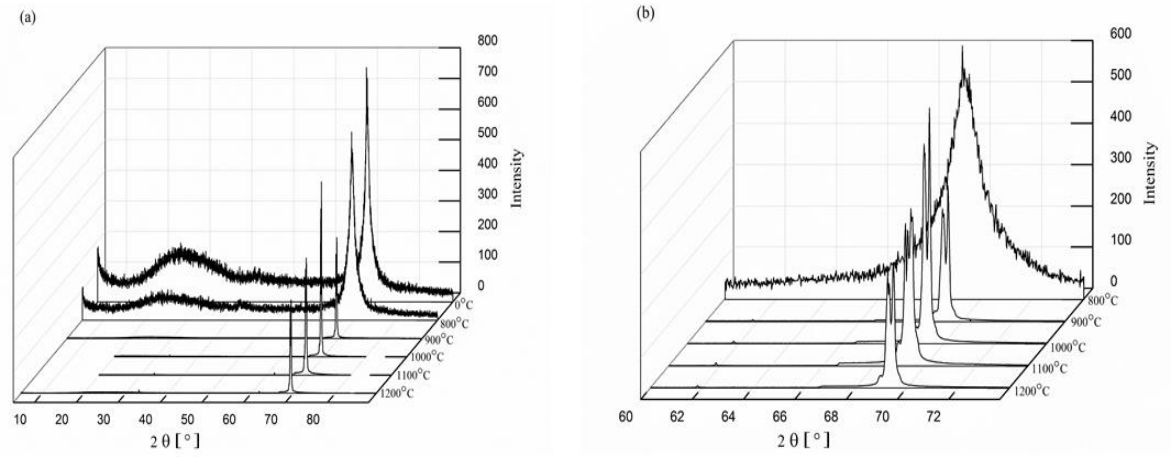

Fig. 2-18 XRD of the carbon films after heat treatment

(a) Full spectrogram (b) 2θ = 60-74°

2.3.5.3 XPS analysis

In order to further prove the effect of heat treatment on the microstructure of a-C

films, the a-C films under different heat treatment conditions were characterized by XPS. Fig.2-19 presents the XPS profiles of a-C films at various temperatures.

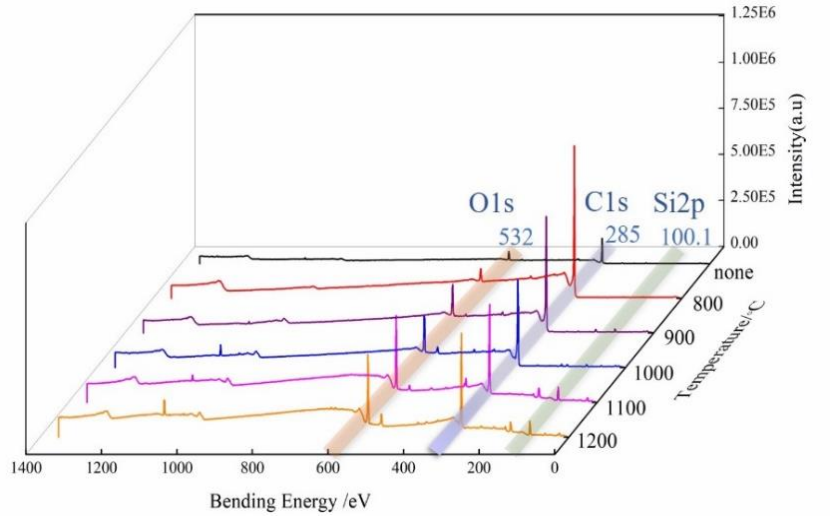

Fig. 2-19 XPS spectra of a-C films

For a-C films without heat treatment, the full XPS profile shows no other spectral peaks except for the main spectral lines of C1s and O1s. In addition to the C1s and O1s main spectral lines, heat treated a-C films exhibit Si2p and N1s spectral lines in the full spectrum. N1s spectral lines are near 1107 eV in the a-C films after heat treatment at 1100 °C and 1200 °C, which indicates the presence of residual air in the heating furnace chamber. The relative strengths of C1s and O1s after heat treatment were significantly greater than those of a-C films without heat treatment. The relative strength of C1s decreased and of O1s increased with an increase in the heat treatment temperature.

Fig.2-20 presents the changes in the contents of C and O in the a-C film correlated with changes to the heat treatment temperature. At 800–1200 ℃, the carbon content of the a-C film after heat treatment gradually decreased with an increase in temperature. Only temperatures at or below 1000 °C yielded a heat-treated carbon content that exceeded that of the a-C film without heat treatment. The change in the oxygen content of the a-C film after heat treatment is the opposite: at temperatures at or below 1100 ℃, the oxygen content of the treated a-C film increases with the increase in treatment temperature; at temperatures at or below 1000 °C, the oxygen content in the a-C film was less than that in the unheated a-C film.

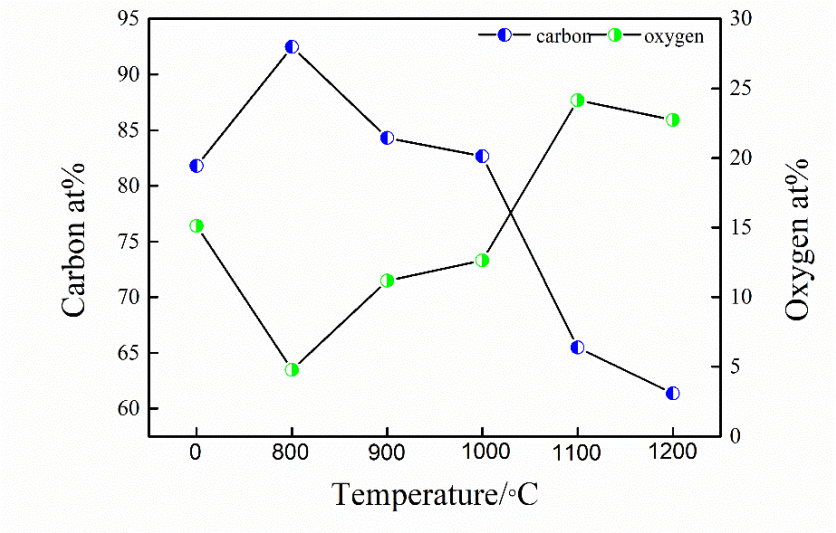

Fig. 2-20 The curve of carbon and oxygen content in a-C films

This is attributed to the many cracks present on the surface of the a-C film without heat treatment and the manner that oxygen is attached to the surface of the carbon film.

Fig.2-21 shows XPS of a-C films under different treatment conditions. The C 1s spectrum was composed of SP^2 and SP^3 peaks at around 284.6 eV and 285.5 eV, respectively, whereas the weaker peaks at 286.6 eV and 288.9 eV appeared from C-O and C=O/O-C=O bonds, respectively. The relative intensity of the C1s peak of the a-C film after heat treatment was significantly enhanced. By fitting the C1s peak, it was found that the SP2c content of the a-C film after heat treatment was significantly higher than that of the a-C film without heat treatment and that the SP2c content increased with an increase in the treatment temperature, which is consistent with the Raman analysis. Simultaneously, C-O and C=O bonds were present in the C1s peak spectrum of samples treated at temperatures between 800 and 1000 ℃, while no C=O bonds were present in a-C films without heat treatment and those treated at 1100 °C and 1200 °C.

No notable C-Si bond was observed near 283.4 eV of the C1s peak spectrum. This is because the content of the c-Si bond was low due to carbon oxygen adsorption and surface oxidation on the film surface and because the strength of the corresponding peak was weak and obscured by other peaks.

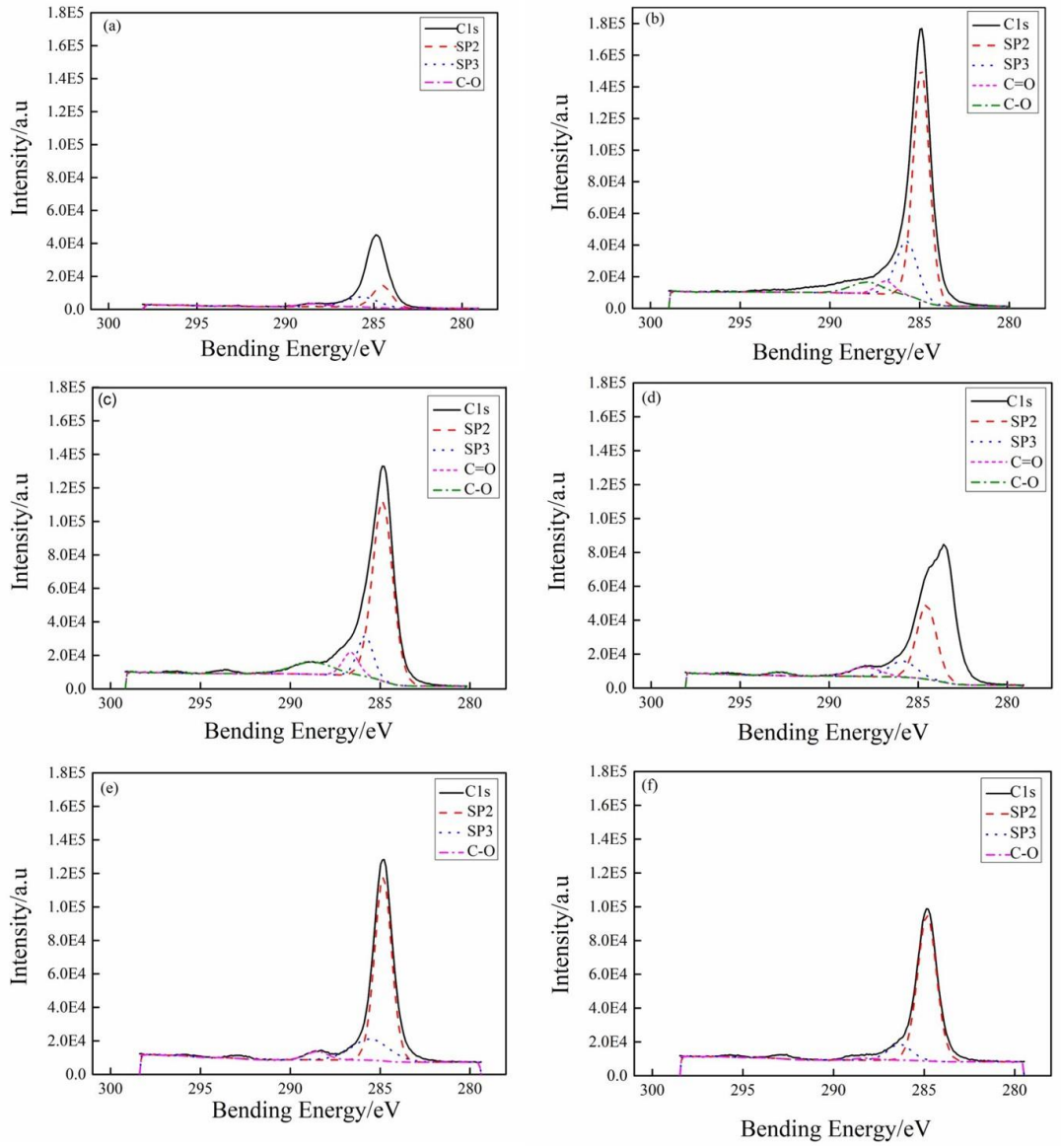

Fig.2-21 XPS spectra of C1s in a-C films

(a)none (b) 800℃ (c)900℃ (d) 1000℃ (e) 1100℃ (f) 1200℃

Fig. 2-22 presents the O1s spectrum showed C=O and C–O peaks at ~531.1 eV and 532.3 eV, respectively. Through fitting, the C=O concentration in the a-C film decreased after heat treatment, while the C–O concentration increased, which was also consistent with the fitting analysis of C1s.

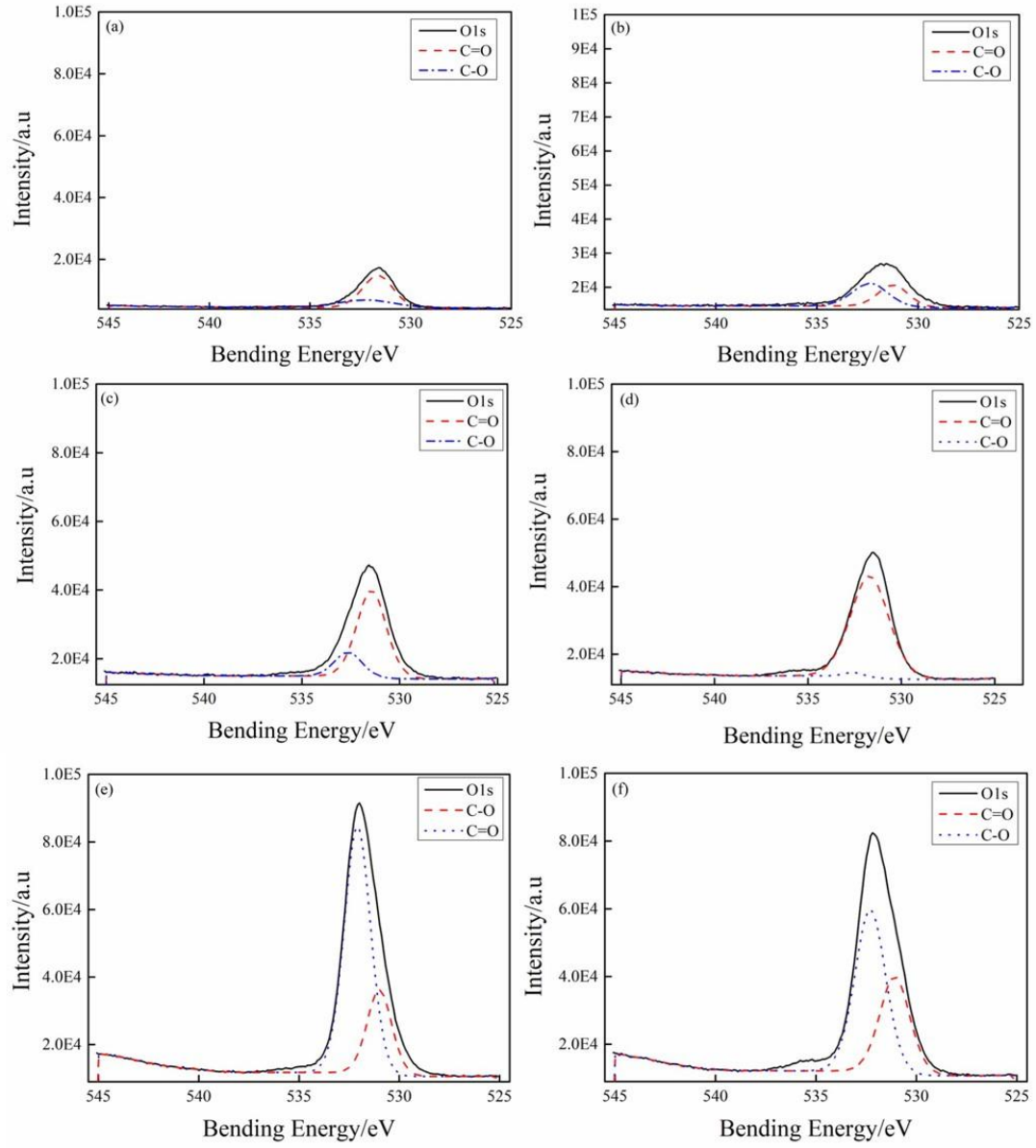

Fig. 2-22 XPS spectra of O1s in a-C films

(a) none (b) 800℃ (c) 900℃ (d) 1000℃ (e) 1100℃ (f) 1200℃

2.3.5.4 Surface morphology

The Fig. 2-23 and fig.2-24 shows the surface and cross-section morphologies of the carbon film before and after the heat treatment. The heat treatment significantly changed the apparent morphology of the carbon films. The surface of the untreated a-C film consisted of numerous cracks. After the heat treatment, the surface cracks disappeared along with the typical columnar structure of the cross section, forming a dense layered structure. For a heat-treatment temperature of 800°C, granular carbon

aggregates of uniform size appear on the surface of the carbon film, and there are cracks on the surface of the film. With increasing heat-treatment temperature, carbon aggregation with a lamellar structure appears on the surface of the a-C film, the number of flakes first increases and then decreases, the aggregated particle size of granular carbon first increases and then decreases, and there are fewer cracks on the a-C film surface. When the heat-treatment temperature reaches 1000°C, carbon accumulation occurs on the film surfaces. Heating to 1100°C prompts an enhancement of the stacking morphology on the film surfaces, while the number of flake aggregates decreases. At a heat-treatment temperature of 1200°C, the flake aggregates on the surface of the carbon film almost disappear, and a quicksand-like accumulation shape is formed on the surface of the carbon film, and no obvious cracks exists. The XRD analyses indicate that the crystalline structure appeared on the carbon film surfaces after heat treatment, the granular carbon aggregates are microcrystalline carbon, and the flake aggregates are lonsdaleite and new carbon crystal.

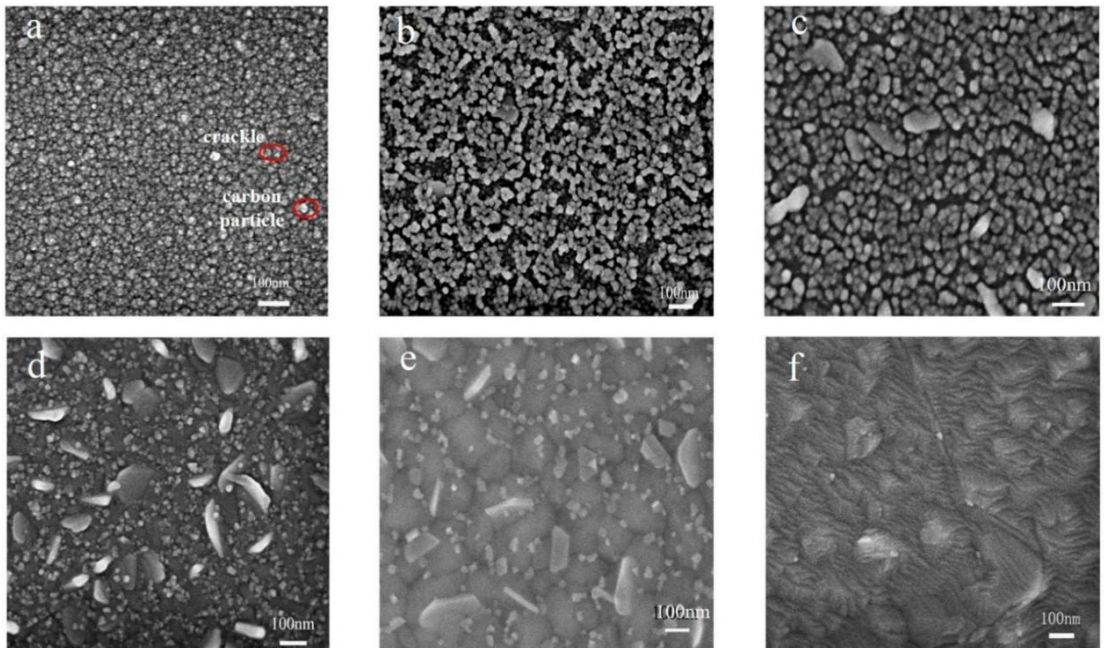

Fig.2-23 SEM images of surface of carbon films after heat treatment

(a)none (b) 800℃ (c)900℃ (d) 1000℃ (e) 1100℃ (f) 1200℃

After heat treatment, the columnar structure of the original magnetron-sputtered carbon film cross section disappears, and the surface layer of the film has a grain structure when treatment temperatures do not exceed 1000°C. With the further increase

in the heat-treatment temperature, the grain morphology of the surface layer cross section becomes less and less apparent, though the compactness of carbon film is enhanced. Carbon atoms in magnetron-sputtered carbon films are present in the form, but a-C, unlike other non-metals, is not composed of completely disordered atomic condensation groups.

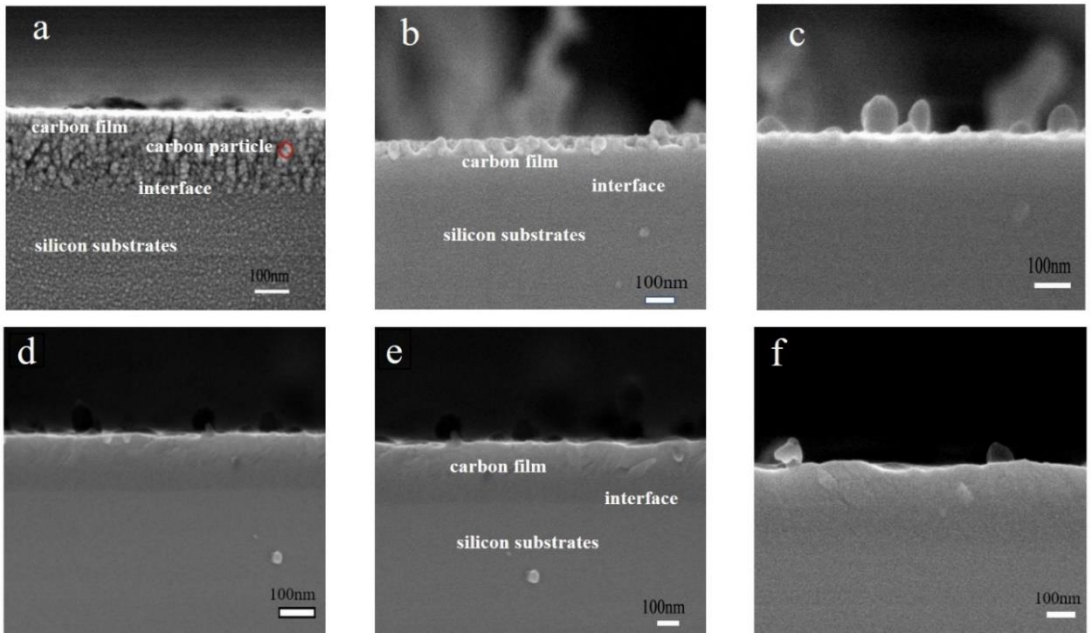

Fig.2-24 SEM images of cross-sectional of carbon films after heat treatment

(a)none (b) 800℃ (c)900℃ (d) 1000℃ (e) 1100℃ (f) 1200℃

The a-C structure contains a carbon micro-crystalline structure with a very small diameter, and a large number of irregular bonds exist at the edges of micro-crystalline regions [22]. After heat treatment, carbon micro-crystals aggregate and recombine to form a crystalline structure. As the same time, because the magnetron-sputtered a-C film is a carbon-atom accumulation film, the carbon particles diffuse, move, and fuse during heat treatment, which leads to the disappearance of the columnar cross-sectional structure of the magnetron-sputtered carbon film. When the heat-treatment temperature is relatively low, because of the slow diffusion of carbon atoms that only move within a small range, the carbon atoms on the surface of the a-C film first move and diffuse during heat treatment, which leads to grain structure formation on the a-C film surface. With increasing heat-treatment temperature, the diffusion speed and bonding ability of carbon particles increases, which results in an enlargement of the carbon crystals and

the aggregation morphology of the microcrystalline carbon. The continuous accumulation of carbon particles enhances the compactness of the a-C films.

2.3.5.5 AFM measurements of surface roughness

AFM images describing the surface morphology of magnetron-sputtered a-C films, before and after heat treatment, are shown in Fig. 2-25. There are carbon particles on the surface of the untreated magnetron-sputtered carbon films. The existence of lamellar crystals on the surface of a-C films after heat treatment at 800°C that were observed by AFM are shown in Fig. 2-25 (b). With increasing heat-treatment temperature, the lamellar crystals grow in the a-C film. The a-C film forms a continuous film structure when the treatment temperature reaches 1100°C, though there are still crystal particles on the surface of the film. When the treatment temperature reaches 1200°C, concave and convex surface structures form on the a-C films.

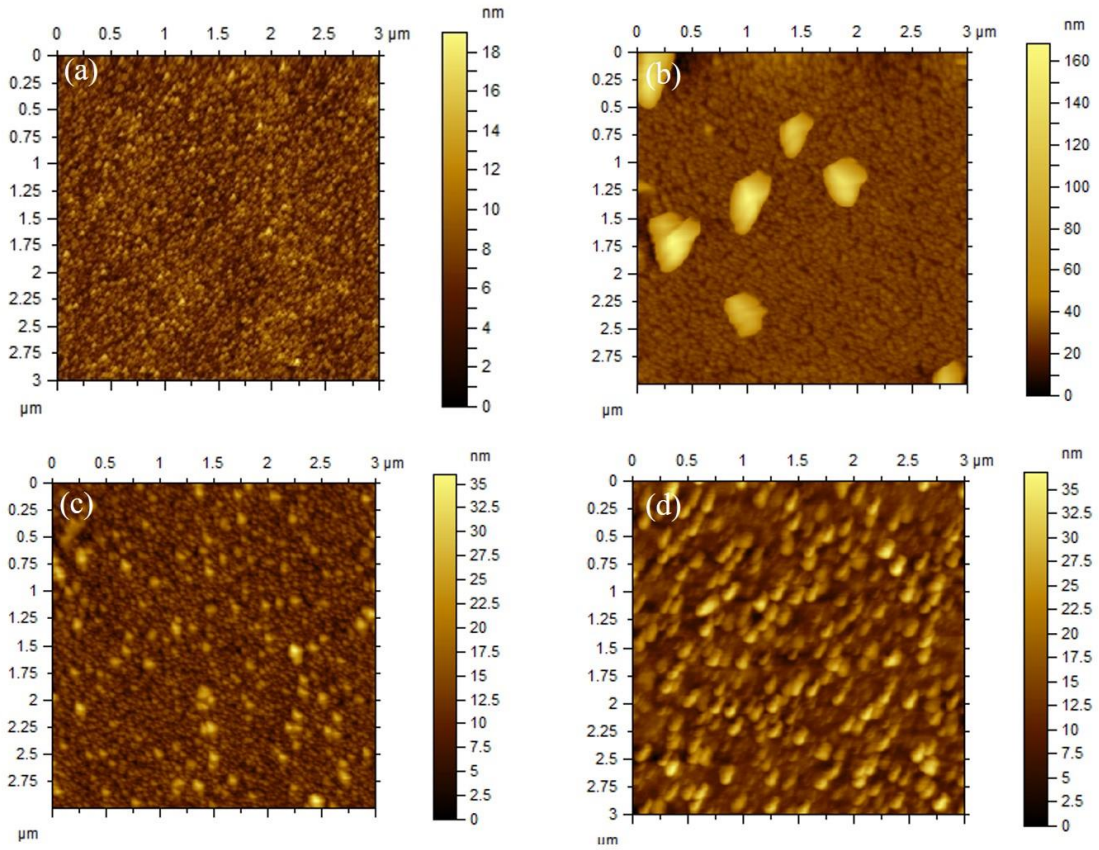

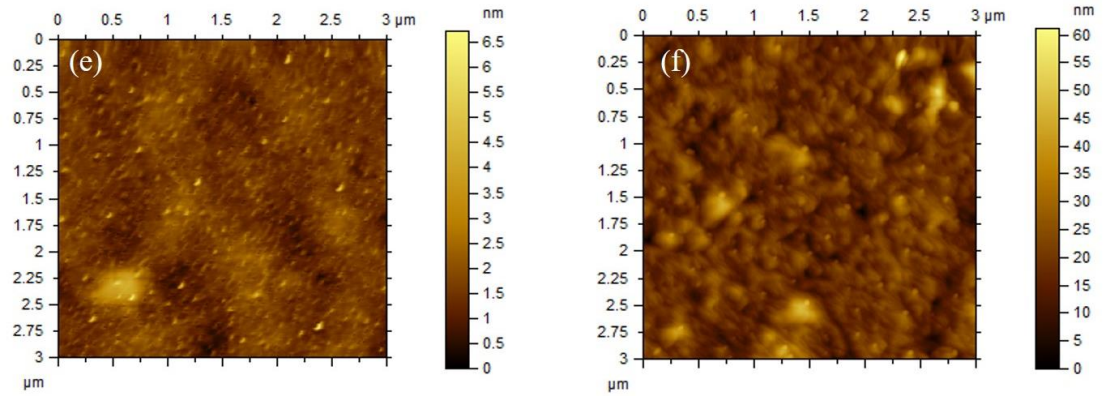

Fig. 2-25. AFM images of the carbon films after heat treatment

(a) None (b) 800 °C (c) 900 °C (d) 1000 °C (e) 1100 °C (f) 1200 °C

Fig.2-26 shows a simulation image of the effect of heat treatment conditions on the structure of carbon films.

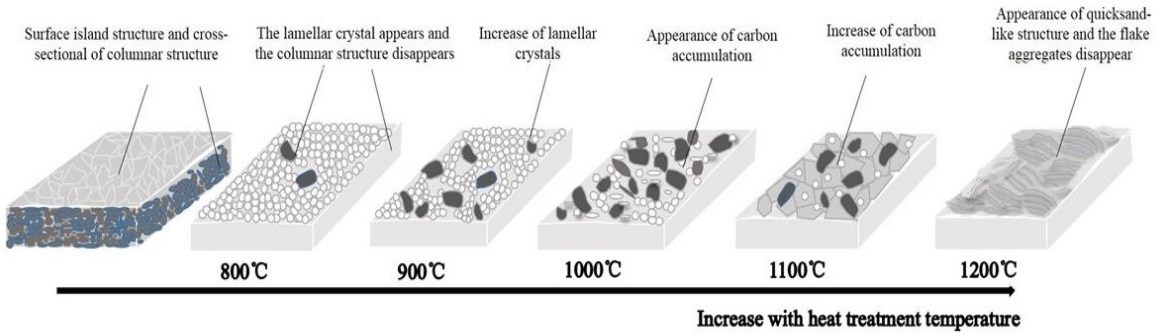

Fig. 2-26. Simulated image of the effect of heat treatment conditions on structure of carbon films

Fig.2-27 shows the effect of heat treatment on the surface roughness of magnetron-sputtered a-C films. Except for the decreased surface roughness of the a-C film that was subject to a treatment temperature of 1100°C, the surface roughness of heat-treated a-C films are higher than that of the untreated film. This is because at the initial stage of heat treatment, the treatment temperature is low, and the carbon particles have not obtained enough energy to complete diffusion and fusion. Although the aggregation of crystalline particles occurs on the a-C film surface, the lamellar crystals have not been fully formed and cracks exist, which affects the smoothness of the a-C film surface. With increased heat-treatment temperature, the carbon particles obtain enough energy for new crystal fusion, and the crystal structure is again aggregated, which reduces both the number of crystal particles and surface roughness of an a-C film. At a heat-treatment

temperature of 1200°C, flowing quicksand-like aggregates form on the carbon film surface, which increases the roughness. Prolonging the heat treatment enhances the degree of aggregation of carbon particles, and results in increased grain size and roughness on the film surfaces, which is consistent with our analysis of the influence of heat treatment on a-C film morphology.

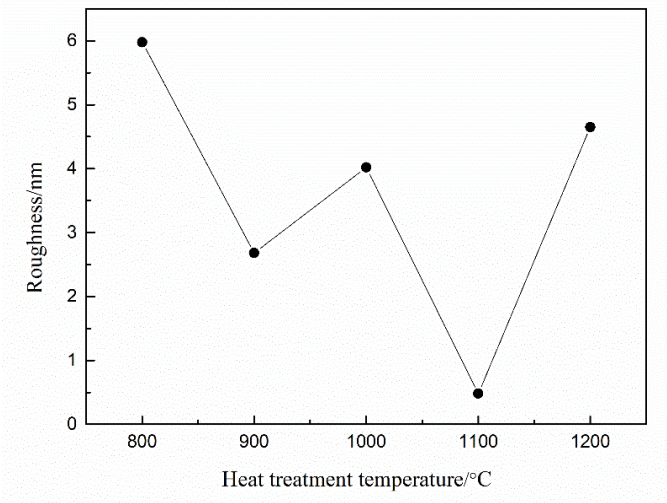

Fig. 2-27. Curve of influence of heat treatment process on surface roughness of a-C films.

2.3.6 Mechanical Properties of carbon film by heat treated

Fig. 2-28 shows the load-displacement curves of the a-C films before and after heat treatment. When the a-C films were pressed into the same depth after heat treatment at 900–1100 ℃, the load required for the treated a-C film was slightly higher than that for the untreated film. When the a-C films treated at 800 ℃ and 1200 ℃ were pressed into the same depth, the required load was the same as that of the untreated film. It is seen that total indentation depth is high in 1200℃ at a peak load of 10N. After unloading, the treated films at 800 ℃～1000 ℃ showed good elastic recovery and the least residual indentation depth.

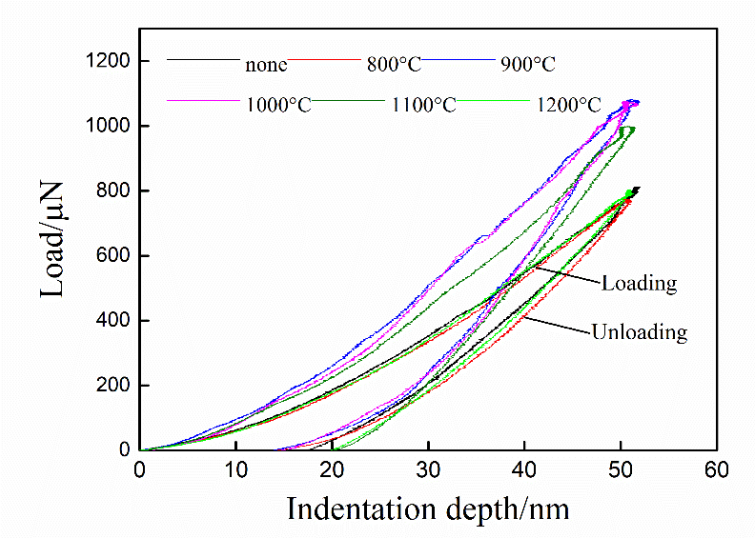

Fig.2-28 Load-displacement curves of a-C films

The hardness and Young's modulus were calculated using the Oliver-Pharr methods, the data are shown in Fig.2-29. For temperatures above 800 °C, the hardness of the a-C film after heat treatment increases compared to the untreated film. At 800 °C, hardness decreased slightly compared to the a-C film without heat treatment. The hardness peaked at 900 °C and then decreased gradually with the increase in heat treatment temperature. The Young's modulus of a-C films increased after heat treatment, the minimum increased by 4.7% and the maximum increased by 39.15%. From 800℃ To 1200℃, the Young's modulus increases, peaking at 900 °C, and then decreases as the heat treatment temperature rises. However, the analysis of the mechanical properties of the a-C film before and after heating shows that the effect of heat treatment temperature is not completely consistent with the trend of I_D/I_G change in the Raman spectrum analysis. Thus, the enhancement of the ordered structure of the a-C film is conducive to hardness improvement, but the change in the microstructure of the carbon film does not completely affect the hardness. Hardness is the ability of a material to resist local pressing onto its surface.

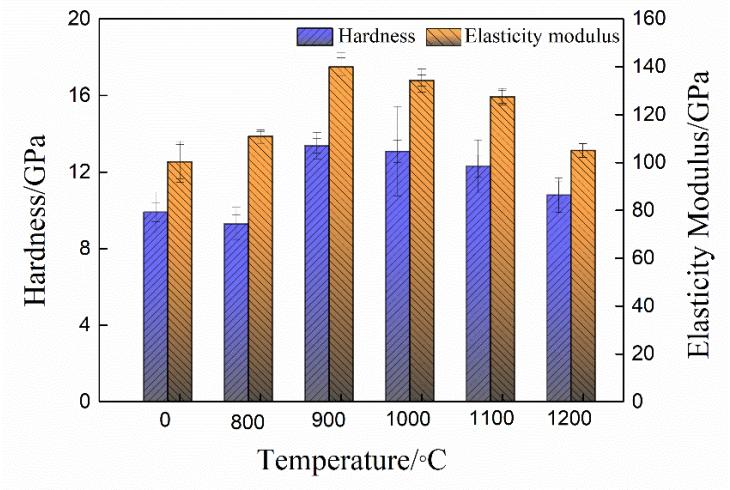

Fig. 2-29 Hardness and elastic modulus of a-C films

Because the a-C film without heat treatment is composed of carbon particles, the particles are displaced when a local hard object is pressed onto its surface. This is not conducive to the enhancement of the a-C film hardness. After heat treatment, the continuous layer structure effectively hindered the void movement during the pressing, which improved the hardness of the a-C film. Therefore, the surface structure of the a-C film also influenced the improvement in the carbon film hardness. The micro carbon crystals in the carbon film aggregated and recombined as the heat treatment temperature reached 1200 °C, which affected the continuous formation of the ordered structure of the a-C film.

Fig. 2-30 shows the change trend of hardness to Young's modulus ratio H/E and H^3/E^2. In essence, the values of H/E and H^3/E^2 are considered to reflect the resistance to elastic strain and plastic deformation of a material [30]. The H/E and H^3/E^2 are referred to as "elastic strain to failure" and "the resistance of materials to plastic deformation", respectively [31]. Furthermore, H^3/E^2 is reported to be proportional to the plastic deformation resistance of the coating. In general, the smaller the ratio of hardness to modulus, the smaller is the local elastic recovery of the indentation, and the deeper is the residual indentation after unloading. However, in this experiment, the H/E of the a-C film after the 800-1000 ℃ heat treatment is significantly less than that of the untreated a-C film, but its elastic recovery performance is better than that of the a-C film without the heat treatment. The residual indentation depth after unloading is

significantly less than that of the untreated a-C film. This is because the a-C film without the heat treatment is composed of carbon particles. When the carbon particles are subject to external force, void occurs between them. After the external force is unloaded, the carbon particles can easily return to their original relative positions. After the 800℃ heat treatment, the ordered structure in the microstructure of the a-C film is not enhanced, so its hardness is not increased, but the heat treatment improves the modulus of the a-C film, so the ratio of H/E and H^3/E^2 decreases significantly. This further shows that the mechanical properties of a-C films are not only affected by their microstructure, but also by their surface structure. After the heat treatment, the H^3/E^2 values of a-C films were higher than those of the untreated a-C film; however, after the 800℃ heat treatment, H^3/E^2 of a-C films decreased to a large extent.

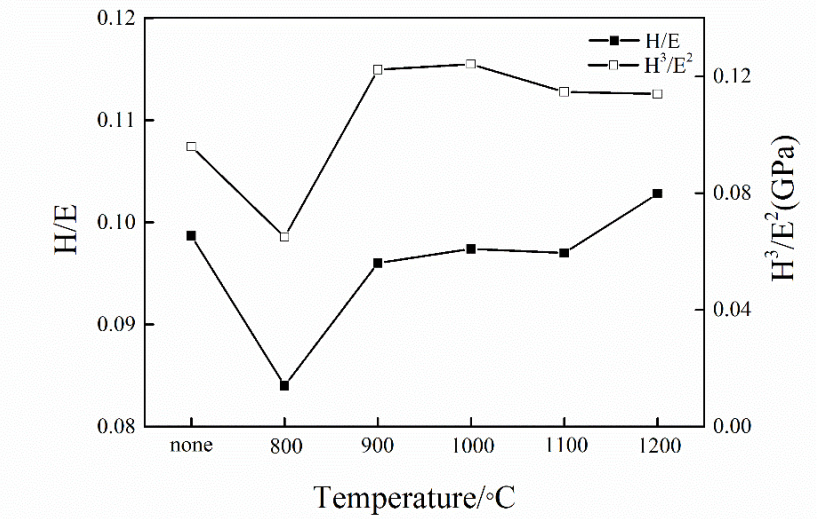

Fig. 2-30 The value of H/E and H^3/E^2

2.3.7 Adhesion performance

Scratch test is carried out to investigate the adhesion strength between the a-C films and silicon wafer. Table 2-6 shows the test results of adhesion performance.

Table 2-6 Adhesion between a-C film and silicon wafer

Sample number	Test level	Sample number	Test level
1#	0B	4#	5B
2#	3B	5#	5B
3#	3B	6#	5B

According to ASTMD3359 standard, the adhesion between the film and the substrate can be divided into 0-5 and 6 grades, among which, grade 5 is the best [32,33].

By comparing the peeling off of the carbon film on the surface of silicon wafer after scratch treatment (Fig.2-31), the adhesion between carbon film and silicon wafer was found to enhance continuously with the increase in the heat treatment temperature. For the carbon film without the heat treatment, the carbon film layer fell off along the cutting point after scratching, and the falling off area is greater than 80%. After the heat treatment, the adhesion between the carbon film and silicon substrate was found to be improved. When the heat treatment temperature reached 900 ℃, the falling off area was significantly reduced, and the falling off area was between 5% and 15%, although a large number of carbon films fell off at the notch after the scratch treatment. When the heat treatment temperature reached 1100 ℃, no evident carbon film was observed on the surface of the scratch treated silicon wafer.

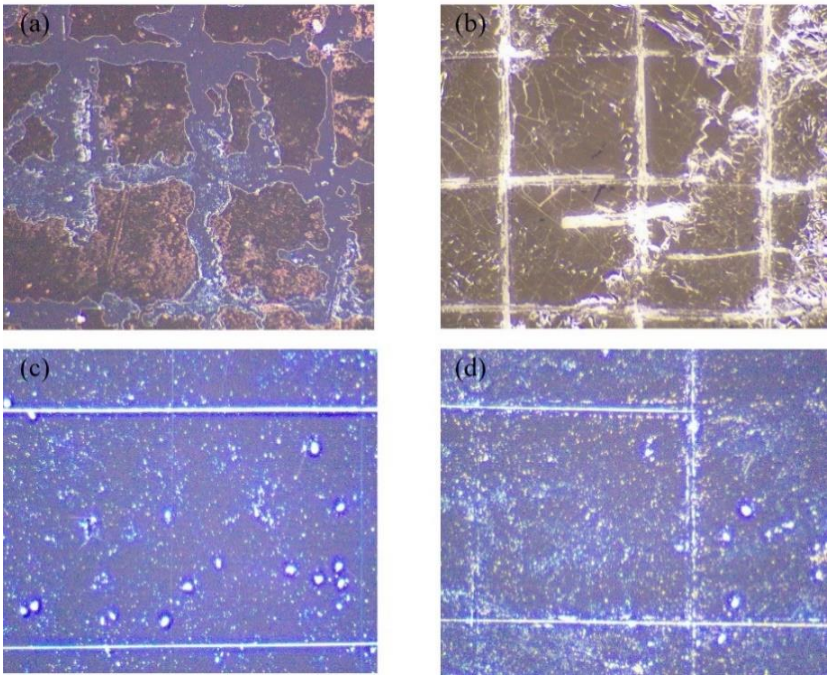

Fig.2-31 Surface morphology of a-C film after scratch treatment

(a)none (b) 800℃ (c)1100℃ (d) 1200℃

2.3.8 Tribological performance

Fig.2-32 shows the friction coefficient of the a-C film in the atmospheric environment before and after heat treatment. It can be seen from the figure that the friction coefficient of the a-C film increased slightly after heat treatment, increasing from 800 to 1000 ℃ and decreasing from 1000 to 1200℃. This is similar to the

variation seen in a-C film roughness with the heat treatment process; that is, the friction coefficient of the a-C film increased as its surface roughness increased.

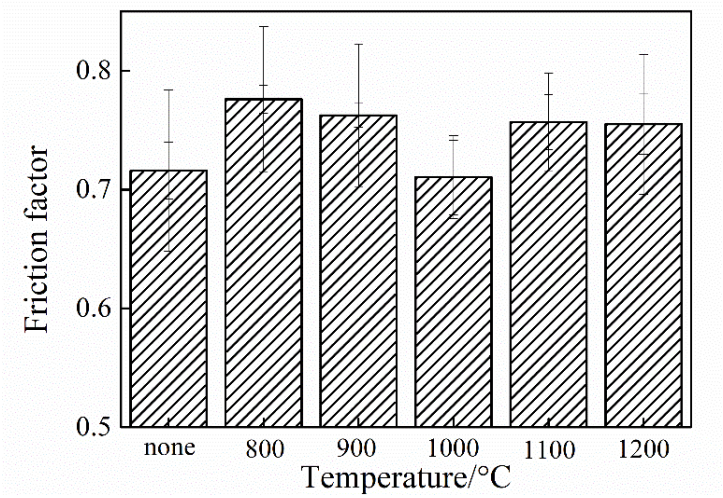

Fig.2-32 Friction coefficient of a-C films

The fluctuation region of the a-C film friction coefficient curve is different before and after heat treatment (Fig. 2-33). For the untreated a-C film, the friction coefficient fluctuation region fluctuates notably in the early stage of friction, at approximately 600 s after the friction begins. After heat treatment, the friction curve of the a-C film fluctuates after 1200 s of friction and decreases with the increase in heat treatment temperature. Of the heat-treated a-C films, the friction coefficient curve of those higher than 1000 °C show the smallest fluctuation. This shows that the friction damage mechanism of the a-C film is different before and after heat treatment.

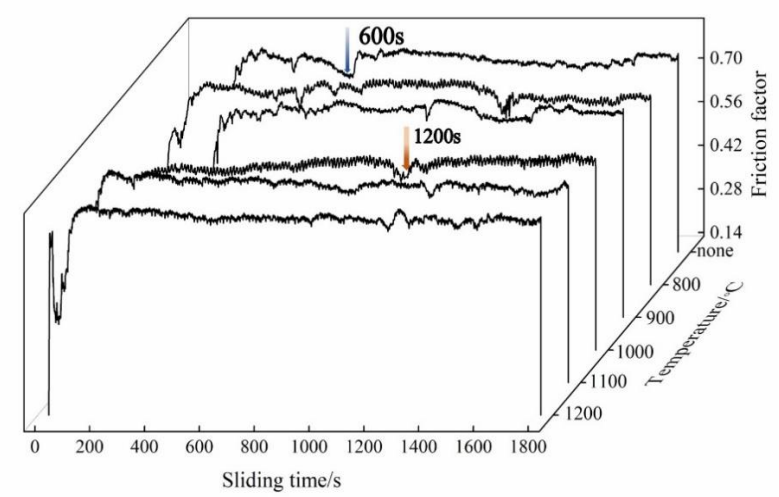

Fig.2-33 Friction coefficient curve of a-C films

Fig. 2-34 shows the wear rate of the a-C film. When the heat treatment temperature

did not reach 1200 °C, the wear rate of the a-C film after heat treatment was improved, and the wear rate of the a-C film decreased significantly. The wear resistance effect of the a-C mill after heat treatment at 1000 °C is the best, and the wear rate is 2.658×10^{-17}mm/N•mm, which is 28% lower than that before treatment. However, when the heat treatment temperature exceeded 1000 °C, the wear rate of the a-C film increased with the increase in treatment temperature. This is because, first, the a-C film structure from the particle accumulation state to the continuous layer structure, which reduces the transfer damage of carbon particles. The wear scar morphology of the a-C film before and after the heat treatment also shows this. Second, the hardness and modulus of the a-C film are improved by the heating treatment, which is conducive to the improvement of the wear resistance of the a-C film [34]. Moreover, the strengthening of adhesion between the a-C film and silicon wafer after the heat treatment also plays a positive role in improving the wear resistance of the a-C film after the heat treatment. Finally, the surface morphology of the a-C film also has a certain impact on its wear resistance. For example, although the hardness and modulus of the a-C film subjected to 900 °C heat treatment are higher than those of the 1000 °C treatment, the wear mark damage cross-sectional area of the a-C film after 1000 °C heat treatment is the smallest. This is because the surface friction coefficient decreases and plays a positive role [35].

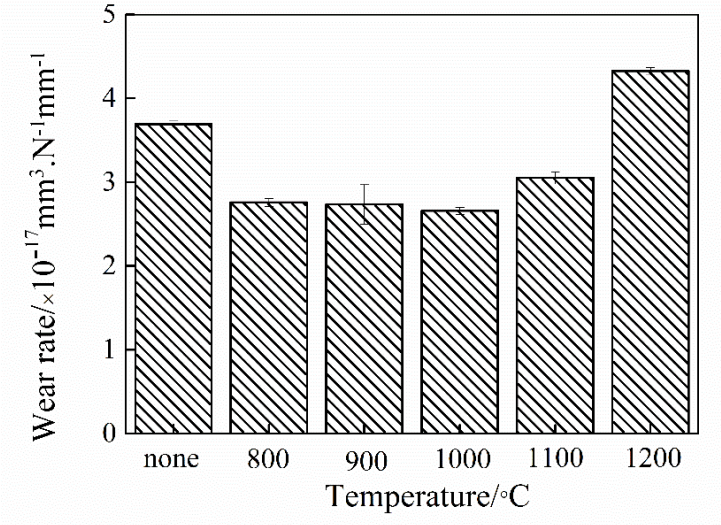

Fig.2-34 Wear rate of a-C films

As shown in the Fig. 2-35(a), during the grinding of the untreated a-C film, there

are distinct scratch marks on both sides of the wear mark, and serious damage occurs in the center of the wear mark. This shows that there were serious abrasive wear and adhesive wear mechanisms in the friction process of the a-C films. The a-C carbon film after 800 °C heat treatment still showed notable friction damage on both sides of the carbon film, but the damage at the center of the wear mark was significantly improved, and there was only a small amount of abrasive and adhesion damage due to the change in the surface structure of the film. At heat treatment temperatures of 900 °C and 1000 °C, there was only slight scratch damage on both sides of the carbon film with no evident abrasive wear and adhesive wear marks in the center of the wear mark. However, through the three-dimensional wear mark morphology of a-C film (Fig. 2-35(b)), it is found that there were gullies on the surface of a-C film after heat treatment at above 900℃. It shows that the wear mechanism changed from the mixed mechanism of abrasive damage to adhesive wear. When the a-C film was not heated, the film structure was formed through the accumulation of uniform carbon particles. Under the action of an external friction force, the carbon particles of the unheated a-C film are damaged and displaced, and some particles adhere to the friction ball. After the heat treatment, the surface structure of the a-C film changed from the accumulated form of carbon particles to a continuous layer structure and the adhesion between the a-C film and silicon wafer was strengthened. Under the action of an external friction force, the heat-treated a-C film's ability to resist damage was enhanced, and the surface damage of the carbon film was classified as scratch damage. However, with the increase in the friction coefficient of the a-C carbon film surface and the change in the SP^2 and SP^3 ordered structures in the microstructure, the friction damage on the film surface increased significantly. When the heat treatment temperature reached 1200℃, the wear marks on the carbon film surface were not sufficiently smooth, and distinct gullies and abrasive wear were observed. The specific damage mechanism is shown in the Fig. 2-36

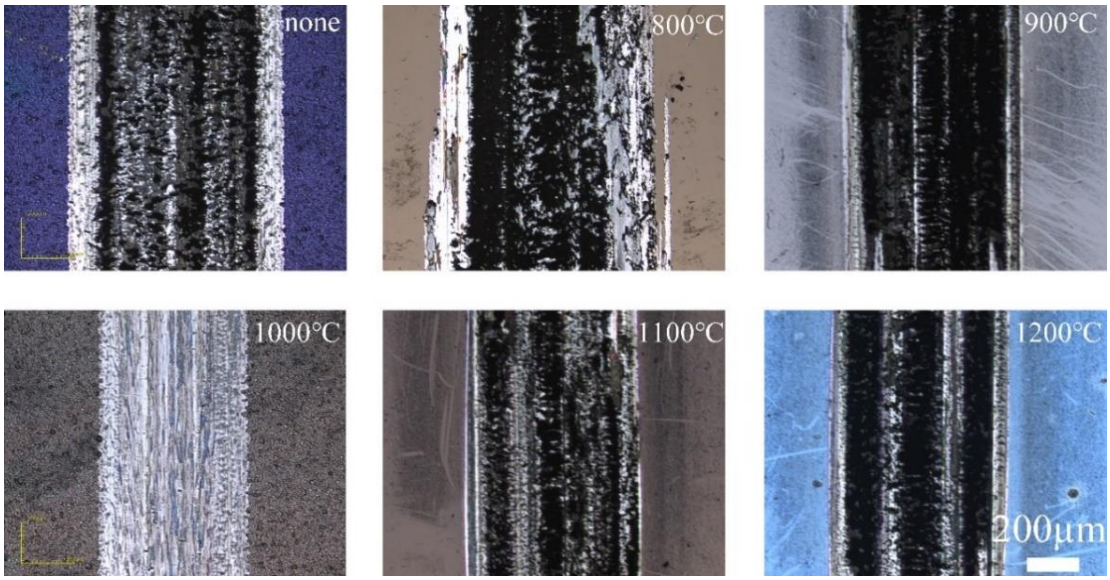

(a)

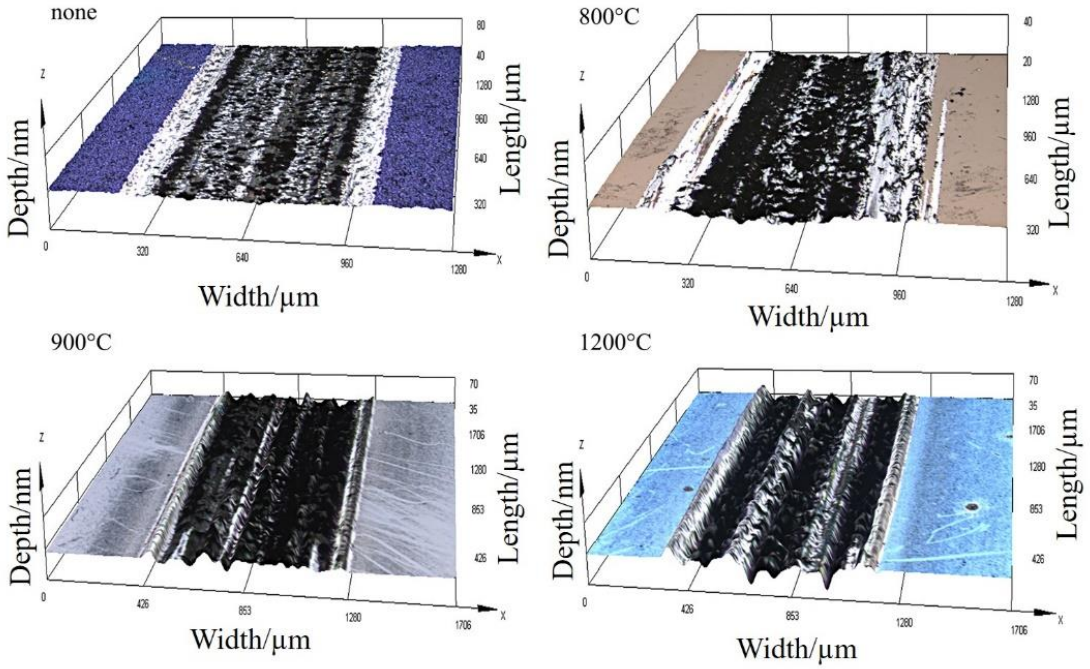

(b)

Fig.2-35 Wear mark morphology of a-C films

(a)plane wear mark morphology(b) three dimensional wear mark morphology

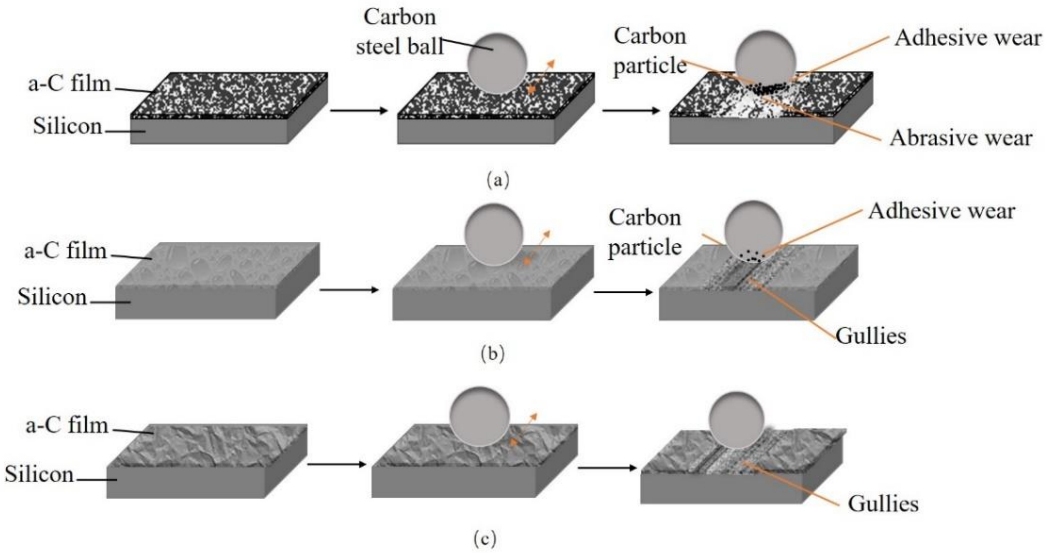

Fig.2-36 Diagrammatic of friction damage mechanism of a-C films(a) Friction process of untreated a-C film (b) Friction process of a-C film after 800℃ to 1000°C heat treatment (c) Friction process of a-C film after 1200℃ heat treatment

According to the previous analysis, the structure of the a-C film after heat treatment changes from the columnar structure of particle accumulation to that of a dense layer. This dense layer structure effectively improves the fracture and collapse of the a-C film caused by the columnar looseness of the film under an external force; as a result, its hardness and bearing capacity are improved. Moreover, the hybrid ratio of SP^2 and SP^3 in a-C films is not the only factor affecting the mechanical properties of a-C films. The XPS analysis of a-C shows that the oxygen content in a-C films vary at different heat treatment temperatures and that carbon and oxygen have different bonding structures.

When the a-C film was not heat-treated, oxygen existed on the surface of the carbon film in the form of adsorption owing to the numerous cracks on the surface of the carbon film. After heat treatment, the particles on the surface of the a-C film aggregated, the surface cracks disappeared, and the oxygen attached to the film surface escaped. At this time, the oxygen adsorption type on the a-C film surface transformed from physical to chemical adsorption, which lowered the oxygen content in the a-C film. Under the heat treatment condition of 800℃, the change in the a-C film structure mainly includes the movement of carbon particles. However, the change in the bonding

structure of the a-C film and stress release are insignificant, thus, it must be noted that the hardness and modulus of the a-C film are not significantly changed. With an increase in the treatment temperature, the reaction temperatures of carbon and oxygen were also reached. The oxygen within the carbon film escaped while the residual oxygen in the heating furnace reacted with the carbon film and silicon substrate and increased the oxygen content in the carbon film. When the a-C film was heat-treated, the oxygen underwent adsorption on the a-C film surface, and the escaped oxygen was chemisorbed and converted into adsorbed C=O. Thereafter, CO_2 formed and left the carbon film surface. When the heat treatment temperature exceeded 1000 °C, in the case of excess carbon, carbon reacted with carbon dioxide to form carbon monoxide and other bonds such as –C–CO, –C–OC, and C–O. Meanwhile, in a low oxygen environment, the carbon film reacts with silicon wafer to form silicon carbide. When the temperature reached 1200 °C, the ketone group desorbed and the C=O bond disappeared [36-38]. The reaction process is illustrated in Fig. 18. During this reaction, the bond structure in the a-C film changes significantly [39,40], which is accompanied with a massive release of internal stress. Owing to the change in stress in a-C film, the modulus of surface a-C film is different from that of an inner a-C film. The release of stress from the surface a-C film decreases its modulus. However, the change of mechanical properties is different from those reported in the heat treatment of other a-C films [41]. Owing to the reaction between a-C films and oxygen, a-C films with different oxygen contents and moduli are formed on the longitudinal structural layer on the surface of the silicon wafer. When under load, the movement of dislocation from the monolayer with a low shear modulus to that with a high shear modulus is prevented and the hardness of a-C film is improved by the difference in the dislocation line energy in each layer [42]. Heat treatment not only alters the bonding structure of a-C film but also changes the interface bonding morphology between the a-C film and carrier silicon wafer from the initial physical deposition bonding to chemical bonding. These changes in the microstructure and surface morphology facilitate the improvement of mechanical properties of a-C films.

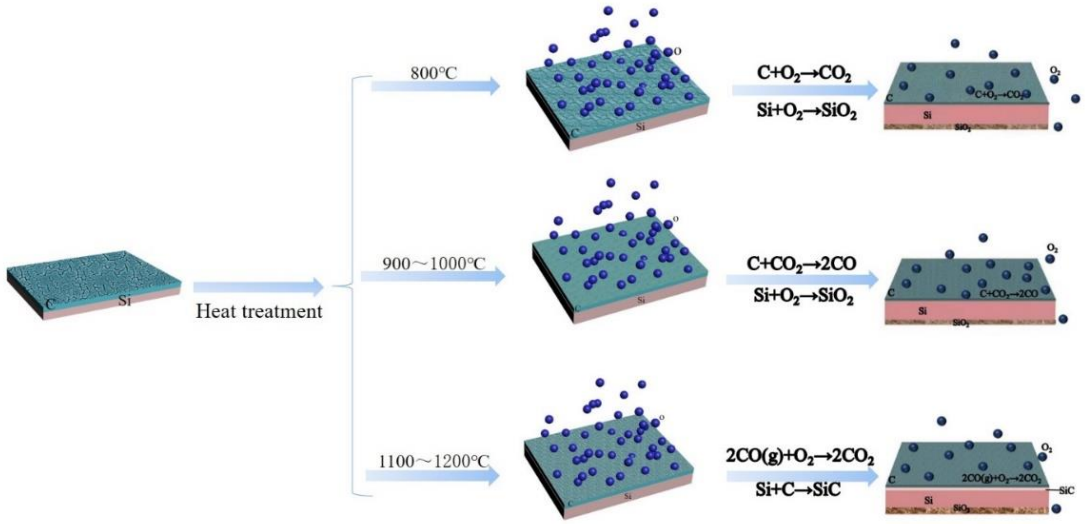

Fig.2-37 Diagrammatic of reaction process

2.4 Conclusion

(1) The surface morphologies of carbon films deposited on the surface of silicon wafers and carbon fibers using a magnetron sputtering process are similar, both consist of fine carbon particles and the surface of the formed carbon film has micro-cracks. When the magnetron sputtering process was varied, the carbon film surface morphology was different due to the effects of the carbon film forming process. Although the surface morphology of the carbon film deposited on the carbon fiber surface differs slightly from that of the carbon film deposited on the silicon wafer substrate due to the curved morphology of the carbon fibers, the cross-sections of the carbon film deposited on both substrates have a typical columnar structure, and the thickness of the carbon film formed under the same sputtering conditions is comparable. The roughness of the carbon film deposited on the silicon wafer gradually increased with an increase in the sputtering time and sputtering power, and the surface roughness measured in different scanning ranges of 3 μm × 3 μm and 1 μm × 1 μm did not change significantly. The surface roughness of the carbon fibers modified via magnetron sputtering also increased, but the surface roughness of the modified carbon fibers varied under the different scanning ranges used. Under the scanning conditions of 3 μm × 3 μm, the surface roughness of the carbon fibers before and after modification did not change significantly, and the maximum surface roughness only increased by 9.79%. Under 1 μm × 1 μm scanning conditions, the modified carbon fiber surface roughness

is further increased, when the modified conditions used a sputtering power of 250 W and sputtering time of 50 min, the modified carbon fiber surface roughness increased by 58.87%. When the surface roughness of the carbon fibers was calculated at 0.2 μm × 0.2 μm, the maximum increase in the surface roughness of the carbon fibers after modification was 3.46 times. According to the Raman spectra and XRD analysis of the modified carbon fibers, modification via the magnetron sputtering process had no significant effect on the hybridization and phase structure of the carbon fibers. Although the carbon target used differs from the carbon fiber in terms of the carbon structure due to the deposition amount being small, it does not affect the microstructure and phase composition of the carbon fibers.

(2) The microstructure and surface morphology of magnetron sputtered deposited carbon films are significantly changed after heat treatment. Heat treatment enhances the ordered structure of the carbon films and the cross-sectional structure is changed from carbon particle accumulation to a continuous layer structure. In addition, the surface is also changed from an aggregated state of carbon particles to lamellar structured crystals. As the heat treatment temperature increases, the number of lamellar structure crystals first increases and then decreases, and carbon build-up occurs on the surface of the carbon film. When the heat treatment temperature reached 1200 °C, the lamellar structure crystals disappear and a quicksand-like build-up structure is formed on the surface of the carbon film. Heat treatment causes the disappearance of the columnar cross-sectional structure of the magnetron sputter-deposited carbon films and enhances their density. With the exception of the surface roughness of the carbon film after heat treatment at 1100 °C being decreased, the surface roughness of the carbon films after heat treatment at the other temperatures studied increased, and the surface roughness of carbon film decreased with an increase in the heat treatment temperature. The intensity of the D and G peaks of the magnetron sputtered carbon films after heat treatment are enhanced. When the heat treatment temperature is <1100 °C, the ordered structure of the carbon films is enhanced with an increase in the heat treatment temperature and the degree of graphitization increases, but when the heat treatment temperature reached

1200 ℃, the enhancement in the aggregated state of the carbon microcrystals in the carbon film affects the further generation of the ordered structure of the carbon film. With an increase in the heat treatment temperature, the intensity of the secondary Raman peak of the carbon film gradually increased, and the double-peak phenomenon also becomes obvious. Upon extending the heat treatment process, the crystallization phenomenon in the carbon film is enhanced and new crystal structures are created, but not graphite crystals. The diffraction characteristic peaks of hexagonal carbon (102) and carbon (109) appeared at $2\theta = 61.8$ and 66.7°, and carbon microcrystal aggregates and lamellar structure crystals also appeared on the surface of the carbon film.

References

[1] Q. Wu, W.S. Miao, Y.D. Zhang, H.J. Gao, D. Hui. Mechanical properties of nanomaterials: A review. Nanotechnology Reviews. 2020. 9: 259-273

[2] K. Brainina, N. Stozhko, M. Bukharinova, E. Vikulova. Nanomaterials: electrochemical properties and application in sensors. Physical Sciences Reviews. 2018: 20188050

[3] H.L. Zhang, H.H. Duan, C.Z. Zhu, Z,H. Chen, H. Luo. Mini-review on the application of nanomaterials in improving anti-aging properties of asphalt. Energy and Fuels. 2021. 35. 11017-11036

[4] S. Mitra, A. Mandal, S. Banerjee, A. Datta, S. Bhattacharya, A. Bose, D. Chakravorty. Template based growth of nanoscaled films: a brief review. Indian Journal of Physics. 2011. 85: 649-666

[5] N. Savvies, B. Window. Diamondlike amorphous carbon films prepared by magnetron sputtering of graphite. Journal of Vacuum Science and Technology A. 1985. 3:2386

[6] L. Marcinauskas, V. Dovydaitis, A. Illjinas, M. Andrulevicius. Structural and optical properties of doped amorphous carbon films deposited by magnetron sputtering. Thin Solid Films. 2019. 681:15-22

[7] M. Nakamura, Y. Takagawa, K.I. Miura, J. Kobata, W. Zhu, N. Nishiike, K. Arao, E. Marin, G. Pezzotti. Structural alteration induced by substrate bias voltage variation in diamond-like carbon films fabricated by unbalanced magnetron sputtering. Diamond and Related Materials. 2018. 90: 214-220

[8] P. Kumar, M. Gupta, U.P. Deshpande, D.M. Phase, V. Ganesan, J. Stahn, Density and microstructure of a-C thin films, Diamond & Related Materials. 2018. 84: 71-76.

[9] I. Alexandrou, H.-J. Scheibe, C. J. Kiely, A. J. Papworth, G. A. J. Amaratunga, B. Schultrich. Carbon films with an SP^2 network structure, Physical Review B. 1999.60:10903.

[10] M. Rouhani, F. C. N. Hong, Y. R. Jeng. In-situ thermal stability analysis of amorphous carbon films with different SP^3 content, Carbon. 2018.130: 401-409

[11] Z.Y. Xu, H. Sun, Y. X. Leng X.Y. Li, W.M. Yang, N. Huang. Effect of modulation

periods on the microstructure and mechanical properties of DLC/TiC multilayer films deposited by filtered cathodic vacuum arc method, Applied Surface Science. 2015.328:319-324.

[12] T. F. Zhang, Z.X. Wan, J.C. Ding, S.H. Zhang, Q.M. Wang, K.H. Kim. Microstructure and high-temperature tribological properties of Si-doped hydrogenated diamond-like carbon films, Applied Surface Science. 2018. 435: 963-973.

[13] L.R Shaginyan, A.A Onoprienko, V.F Britun, V.P Smirnov, Influence of different physical factors on microstructure and properties of magnetron sputtered amorphous carbon films, Thin Solid Films 397(1) (2001) 288-295.

[14] W. Tillmann, N.F.L. Dias, D. Stangier, M. Bayer, H. Moldenhauer, J. Debus, M. Schmitz, U. Berges, C. Westphal. Interaction effects of cathode power, bias voltage, and midfrequency on the structural and mechanical properties of sputtered amorphous carbon films. Applied Surface Science. 2019.487:857-867

[15] S.P. Yong, H.K. Kim, The effects of annealing temperature on the characteristics of carbon counter electrodes for dye-sensitized solar cells, Curr. Appl. Phys. 11(4) (2011) 989-994.

[16] J Feng, H Jiang, Y.P Ma, Z.H Zhang, C Na, Influence of Processing Parameters on Structure and Transmittance of Diamond-Like Carbon Films, J. Mater. Sci. Eng.37(1)(2019)40-46

[17] A.A. Onoprienko, I.B. Yanchuk, Temperature dependence of the mechanical properties of amorphous carbon films deposited by magnetron sputtering, Powder Metallurgy and Metal Ceramics 45(3-4) (2006) 190-195.

[18] C.A. Taylor, M.F. Wayne, W.K.S. Chiu, Heat treatment of thin carbon films and the effect on residual stress, modulus, thermal expansion and microstructure, Carbon 41(10) (2003) 1867-1875.

[19] M. Rusop, A.M.M. Omer, S. Adhikari, S. Adhikary, H. Uchida, T. Soga, T. Jimbo, M. Umeno, Effects of annealing temperature on the optical, bonding, structural and electrical properties of nitrogenated amorphous carbon thin films grown by surface wave microwave plasma chemical vapor deposition, J. Mater. Sci. 41(2) (2006) 537-

547.

[20]Y. Tanaka, K.K.P. Ahmet, A. Nishiyama, N. Sugii, K.Tsutsui, K.Natori, T. Hattori, H. Iwai, Impact of annealing on structural change in amorphous carbon: Effect of Fe catalyst

[21] J. Kakinoki, K. Katada, T. Hanawa, Heat treatment of evaporated carbon films, Acta Crystallographica 13(5) (2010) 448-449.

[22] J.S Chen, Z. Sun, S.P Lau, B.K Tay, Structural and tribological properties of hard carbon film synthesized by heat-treatment of a polymer on graphite substrate, Thin Solid Films, (389)(2001)161-166.

[23] W.C. Oliver, G.M. Pharr. An improved technique for determining hardness and elastic modulus using load and displacement sensing indentation experiments. Journal of Materials Research. 1992. 7: 1564-1583.

[24] ASTMD3359-08 Standard test methods for measuring adhesion by tape test

[25] N.Kumar, G. Natarajan, R. Dumpala, R. Pandian, A. Bahuguna, S.K. Srivastava, T.R. Ravindran, S. Rajagopalan, S. Dash, A.K. Tyagi, M.S.R. Rao. Microstructure and phase composition dependent tribological properties of TiC/a-C nanocomposite thin films, Surface and Coatings Technol. 2014.258: 557-565.

[26] H. Okuda, R.J. Young, D. Wolverson, F. Tanaka, G. Yamamoto, T. Okabe, Investigating nanostructures in carbon fibres using raman spectroscopy, Carbon 130 (2017) 178-184.

[27] Y.J Wang, H.X Li, L.Ji, X.H Liu, Y.X Wu, H.D Zhou,Preparation and properties of graphite-like carbon films fabricated by unbalanced magnetron sputtering,Acta Physica Sinnica 61(5)(2012) 0561031-7

[28] Y.J, Wang, H.X., Li, L. Ji, X.H, Liu, Y.X. Wu, H.D. Zhou, J.M. Chen. Preparation and properties of graphite-like carbon films fabricated by unbalanced magnetron sputtering. Acta Physica Sinnica. 2012. 61:0561031–0561037

[29] M.M. Shi, D. Bao, S.J. Li, B.R. Wulan, J.M. Yan, Q. Jiang. Anchoring PdCu amorphous nanocluster on graphene for electrochemical reduction of N_2 to NH_3 under ambient conditions in aqueous solution. Advanced Energy Materials. 2018. 21:1800124

[30] H. Chen, K.H. Chen, Y.C. Xu, C.X. Pan, J.Y. Yi, C.J. Zhu. Microstructure, mechanical properties, and milling performance of arc-PVD AlTiN-Cu and AlTiN/ AlTiN-Cu coating. Journal of Central South University. 2018. 25:506-515

[31] J. Musil. Hard and superhard nanocomposite coatings. Surface and Coatings Technology. 2000, 125: 322-330.

[32] ASTMD3359-02 Standard test methods for measuring adhesion by tape test[1]

[33] Y. Xiao, J. Xiong, Z.X. Guo, J.B. Liu, L.M. Zhou, J.L. Ye, W. Zhao. Microsturctures and properties of PVD TiAlN coating deposited on cermets with different Ti (C,N) grain size, Journal of Central South University. 2020. 27: 721-735

[34] Y.Y. Lin, Z.F. Zhou, K.Y. Li. Improved wear resistance at high contact stresses of hydrogen-free diamond-like carbon coating by carbon/carbon multilayer architecture. Applied Surface Science. 2019. 477: 137-146

[35] L. Wang, L.H. Li, X.C. Kuang. Effect of substrate bias on microstructures and mechanical properties of WG-DLC coatings deposited by HiPIMS. Surface and Coatings Technology. 2018.352:33-41.

[36] L.R. Kong, S.Y. Zhang. Theoretical explanation of the special temperature dependaence of rate constant for oxidation of carbon. University Chemistry. 2016. 31:84-88

[37] L.X. Rao, H. Liu, W. Shao, H.L. Liu, X.L. Xing, Y.F. Zhou, Z.J. Shi, Q.X. Yang. Tailoring the mechanical properties of diamond-like carbon film by doping of trace nonmetal elements: A first -principles study. Journal of Alloys and Compounds. 2021. 868: 159151.

[38] L. Huang, D. Zhou, J.T. Yuan, C. Li, D.B. Hong. Influences of different temperatures on the mechanical properties and wear resistance against Ti_6Al_4V of Ti doped diamond-like carbon deposited on cemented carbide. Vacuum. 2021. 189: 110279.

[39] W. Zhang, A. Tanaka, K. Wazumi, Y. Koga, B.S. Xu. The effect of annealing on mechanical and tribological properties of diamond-like carbon multilayer films. Diamond and Related Materials. 2004. 13:2166-2169.

[40] J.S. Koehler. Attempt to design a strong solid, Physical Review B. 1970. 15: 547-551.

[41] Y.X. Wu, H.X. Li, L, Ji, Y.P. Ye, J.M. Chen, H.D. Zhou. A long-lifetime MoS_2/a-C:H nanoscale multilayer film with extremely low internal stress. Surface and Coatings Technology. 2013. 236: 438-443.

[42] G. Abadias, A. Michel, C. Tromas, C. Jaouen, S.N. Dub. Stress, interfacial effects and mechanical properties of nanoscale multilayered coatings. Surface and Coatings Technology. 2007. 202: 844-853.

Chapter 3

Effects of magnetron sputtering modification on properties of carbon fiber

Chapter 3: Effects of magnetron sputtering modification on properties of carbon fiber

3.1 Introduction

The characterization of the morphology and microstructure of the carbon film deposited via magnetron sputtering presented in Chapter 2 revealed that the carbon film layer can be constructed on the surface of the carbon fibers using magnetron sputtering technology and that the surface morphology of the carbon fibers can be significantly improved. Moreover, the microstructure of the carbon fibers was not significantly changed by the magnetron sputtering process. However, as a means of carbon fiber modification, its effects on the mechanical properties and surface properties of the carbon fibers are important.

The carbon fiber precursor has defects, and the production process forms internal holes, surface holes, internal cracks, surface cracks, and other defects in carbon fibers that affect their mechanical properties [1,2]. According to Gilaman's solid theoretical strength formula, the theoretical tensile strength limit of carbon fibers is 180 GPa [3]. However, the actual breaking strength of carbon fibers cannot reach this limit. In particular, although carbon fibers have excellent mechanical properties in the axial direction, their toughness is poor, resulting in asymptomatic damage to carbon fibers and their composites. The surface defects of carbon fibers are the main factor limiting their tensile strength. According to Yokotaka and other researchers, 6% of the fracture of brittle materials starts from internal defects, and 94% starts from surface defects [4]. At present, research on improving the mechanical properties of carbon fibers is focused on improving the properties of the carbon fiber precursors, e.g., improving the purity and reducing the influence of impurities in carbon fiber precursors. One method for this is the spinning process. The random distribution of defects in carbon fibers can be reduced by increasing the fineness of the precursor [5-9]. In recent years, with the development of nanotechnology, researchers have added carbon nanotubes or aramid nanofibers and other raw materials to carbon fiber precursors to improve the tensile properties of carbon fibers [10-12]. Although these modification methods can

effectively modify the defects of carbon fibers and improve their tensile properties, they increase the production cost, reduce the production efficiency, and restrict the application of carbon fibers.

At present, few studies have focused on the surface modification of carbon fibers, such as the preparation of a pyrolytic carbon layer on the carbon fiber surface by chemical vapor deposition, and the treatment of carbon fiber bundles in combination with heat treatment. These methods gradually change the tensile fracture mode of carbon fiber from brittle to ductile fracture, thereby improving their mechanical properties. Moreover, the current methods for carbon fiber surface modification have focused on the entire carbon fiber composite for investigating the influence of the modification methods on the interfacial bonding properties between the carbon fiber and matrix resin in the composite [13-16]. Among these, magnetron sputtering is a physical vapor deposition, whereby inert gas is ionized by direct current or high-frequency electric field to produce plasma. The ionized positive ions and electrons bombard the target at high speed. The target atoms or molecules are then sputtered and deposited on the substrate to form a thin film. Compared with the chemical vapor deposition technology, which is complex and unsuitable for material film deposition, magnetron sputtering has the advantages of high sputtering speed, dense film formation, good adhesion, availability of a wide range of target materials, variety of sputtering methods, high film-formation accuracy, and applicability to chemical or metal-organic chemical vapor deposition, which is difficult to grow and unsuitable for material film deposition [17,18]. Therefore, in this study, magnetron sputtering was conducted to modify the surface of the carbon fiber. Subsequently, the homogeneity of the carbon target material and carbon fiber was used to modify the physical defects on the surface of the carbon fiber, thereby improving its mechanical properties and surface energy. By adjusting the magnetron sputtering process parameters, the effects of magnetron sputtering modification on the tensile properties and surface energy of the carbon fiber were analyzed. Thus, this work is a prerequisite for improving the interface between the carbon fiber and matrix resin.

The wettability between the carbon fibers and resin matrix significantly affects the interfacial bonding properties of the composite. If the wettability is good, the resin can exhibit molecular-level spreading on the fiber surface, so that the surface molecules and functional groups of the carbon fibers and resin matrix are within the effective range of the mutual stress field, providing sufficient reaction opportunities for interfacial bonding. Good infiltration makes the resin matrix fully penetrate the defects or voids on the surface of the carbon fibers, increasing the mechanical locking ability between the fibers and the resin, which improves the overall interfacial properties of the composite. Conversely, if the wettability between the two is poor, the contact area between the resin matrix and the carbon fibers is limited, and defects and holes are easily formed in the interface area of the composite material, resulting in a low interfacial strength. Therefore, Consider using "good wettability between the fibers and the resin matrix is necessary for the composite material to have excellent interfacial properties [19-22]. However, the preparation process of carbon fibers results in the formation of a smooth, inert, messy layer graphite structure with low polarity and surface energy. An analysis of the surface roughness of magnetron sputtering-modified carbon fibers was presented in Chapter 2, which indicated that the magnetron sputtering increased the surface roughness of the carbon fibers and that can affect their surface wettability. Therefore, the multifilament carbon fibers and single carbon fibers after the modification treatment described in Chapter 2 were taken as the research objects. We evaluated their mechanical and surface properties, as well as the adhesion between the carbon film and carbon fibers, and analyzed the effects of different magnetron sputtering modification methods and process parameters on the properties of the carbon fibers.

3.2 Experiments part

3.2.1 Tensile test

In accordance with the ASTMD3379-75 standards [23], the tensile properties of the single carbon fibers were tested using a single-fiber strength meter (YG003E, Wenzhou Fang Yuan Instrument Co., Ltd., China) at a relative humidity of 65% ± 3%

and temperature of 20 ± 2 ℃. The single carbon fibers were fixed on the paper mold with an epoxy resin adhesive, as shown in Fig. 3-1. The sample card was then placed with the carbon fibers between the two collets of the tensile tester to cut the fibers according to the position shown in the middle of the paper mold to start stretching. The clamping distance was set as 20 mm, and the tensile loading speed was 10 mm/min. There were no less than 30 valid samples and invalid samples. The tensile breaking strength of the carbon fibers was calculated using Equations (3-1) and (3-2) [24,25].

$$\sigma_1 = \frac{F}{A_F} \tag{3-1}$$

$$A_F = \pi\gamma^2 \tag{3-2}$$

Here, σ_1 represents the tensile breaking strength of the single carbon fibers, GPa, F represents the tensile breaking force of the single carbon fibers, N, A_F represents the cross-sectional area of the single carbon fibers, mm^2, and γ represents the carbon fiber radius, μm.

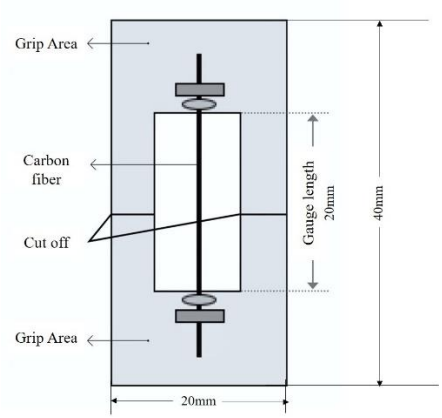

Fig. 3-1 Dimensions of a single carbon fiber tensile test specimen

An electronic universal strength machine (CSS-881, Changchun Research Institute for Mechanical Science Co., Ltd, China) was used to test the tensile properties of the multifilament carbon fibers. As the surface morphology of the carbon fibers treated under different modification conditions affected the properties of interface between the carbon fibers and resin and consequently the tensile performance of the multifilament carbon fibers, the test method ASTMD 4018 [26] was not applicable to the tensile performance test of the multifilament carbon fibers in this experiment. Therefore, the tensile properties of the multifilament carbon fibers were directly tested according to

the JISR 7608-2007 standard [27]. Two ends of the multifilament carbon fibers were fixed with reinforcing sheets. The tensile speed was set as 2 mm/min, and the upper and lower clamping distance was 200 mm. Each treatment process was tested 10 times, and the average values were taken. The tensile breaking strength of the multifilament carbon fiber was calculated using Equations (3-3) and (3-4):

$$\sigma = \frac{F}{A_F} \tag{3-3}$$

$$A_F = \frac{T}{\rho} \tag{3-4}$$

Where σ represents the tensile breaking strength of the multifilament carbon fibers, GPa, F represents the tensile breaking force of the carbon fibers, N, A_F represents the cross-sectional area of the carbon fibers, T represents the linear density of the multifilament carbon fibers, dtex, and ρ represents the density of the multifilament carbon fibers (g/m^3).

A large strength dispersion indicates uneven material quality and poor material reliability. To investigate the effects of the modification methods on the tensile properties of the carbon fibers, a Weibull analysis was performed on the tensile strength of the carbon fibers [28–32]. The Weibull distribution is a mature characterization tool for fiber strength. It based on the weakest-link theory and has been widely used in the study of the tensile strength of carbon fibers.

The strength distribution σ in this study was expressed by a two-parameter Weibull distribution, as follows:

$$P = 1 - \exp\{-(\frac{\sigma}{\sigma_0})^m\},\ \sigma > 0,\ \sigma_0 > 0,\ m > 0 \tag{3-5}$$

Where P represents the cumulative probability of the breaking strength of the fiber at the stress of σ, σ_0 is the scale parameter, and m represents the Weibull modulus.

The logarithms on both sides of Equation (3-5) were calculated to obtain Equation (3-6):

$$\ln(1 - \ln(1 - p)) = m ln\sigma - m ln\sigma_0 \tag{3-6}$$

Where $ln\sigma$ is the independent variable, and $\ln(-\ln(1-p))$ is the dependent variable. The Weibull modulus and scale parameters can be obtained via linear fitting,

where the slope is the Weibull modulus m, which can characterize the uniformity and reliability of materials. A larger m value indicates a smaller dispersion of the material.

3.2.2 Dynamic contact angle and surface energy analysis

In this experiment, the dynamic contact angle was used to evaluate the changes in the dynamic contact angle and surface energy of the carbon fibers before and after treatment, which provided a reference for assessing their wettability with the epoxy resin matrix. The non-polar liquid ethylene glycol and polar liquid deionized water were selected as the test solutions, and the polar and dispersion components of the surface energy for the two test liquids are presented in Table 3-1. A DCAT21 surface/interfacial tension analyzer and an OCA20 contact-angle meter (DataPhysics Instruments, Germany) were used to test a series of carbon fibers, and the testing principle is shown in Fig. 3-2. During the test, a rectangular cardboard fixture of 50 mm × 10 mm was used to fix the carbon fibers, and four carbon fiber monofilament samples were pasted on each test specimen at a parallel interval of 2 mm. The fiber length outside the fixture was kept at 6mm, the threshold value of carbon fiber insertion depth into the liquid was set as 4 mm, the fiber infiltration speed was 0.1 mm/s, the threshold value of the testing quality was set as 0.08 mg, and the test angles of forward and backward were set to velocity were set as 0.08 mm/s. The contact angle of the carbon fibers in the liquid was determined by calculating the mass change generated during the insertion of the carbon fiber sample into the test liquid according to Wilhelmy's equation:

$$\cos\theta = \frac{mg}{\pi d\gamma} \tag{3-7}$$

Where θ represents the contact angle of the carbon fiber as it advances in the test liquid, D represents the carbon fiber monofilament diameter, γ represents the surface tension of the test liquid (mJ/m^2), and g = 9.8 m/s represents the gravitational acceleration. The polar and dispersive components of the surface energy of the carbon fibers was calculated from the advancing contact angles of the fibers in the two different polar test liquids, as follows:

$$\gamma_1(1+\cos\theta) = 2\left(\gamma_f^d\gamma_1^d\right)^{1/2} + 2\left(\gamma_f^p\gamma_1^p\right)^{1/2} \tag{3-8}$$

Where γ_1^d is the dispersive component of the surface energy of the test liquid

(mJ/m^2), γ_1^p is the polar component of the surface energy of the test liquid (mJ/m^2), γ_1 represents the total surface energy of the test liquid (mJ/m^2), γ_f^d is the dispersive component of the surface energy of the carbon fibers (mJ/m^2), γ_f^p is the polar component of the surface energy of the carbon fibers (mJ/m^2), and γ_f represents the total surface energy of the carbon fibers (mJ/m^2).

Table 3-1 Surface tension of test liquids used

Test fluid	temperature （℃）	Surface tension（mJ/m^2）		
		γ_1^d	γ_1^p	γ_1
Deionized water	20	21.8	51	72.8
Glycol	20	29.0	19.0	48.0

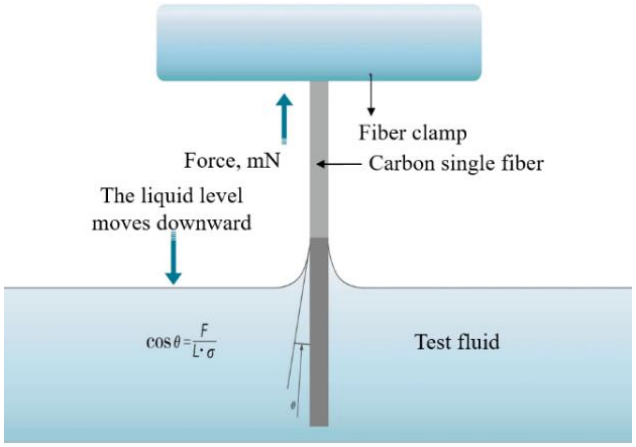

Fig. 3-2 Sketch of dynamic contact angle for single carbon fiber

3.2.3 Adhesion-strength test

The adhesion strength between the carbon film deposited on the carbon fiber surface and the fiber is the key factor affecting the mechanical properties of carbon fibers and the interface properties of carbon fiber composites. At present, there is no clear standard for evaluating the adhesive strength between the film and fabric. Therefore, with reference to the ASTMD3330 standard [33], the bonding properties between the deposited carbon film and carbon fibers under different magnetron sputtering conditions were evaluated using peeling experimental methods.

The adhesion strength between the carbon film and carbon fibers was tested using an electronic stripper (Y090A, YG003E, Wenzhou Fang Yuan Instrument Co., Ltd., China). First, 3M600 special test tape was cut into 110 mm × 19 mm pieces, which were

stuck to the carbon fiber surface during carbon plating. The carbon fiber specimen length was 60 mm, of which 10 mm was the peel test length, and 50 mm was the effective tear length. The clamping distance for stretching was approximately 50 mm. A 500-g weight was used to evenly press the tape and carbon fiber paste for 1 h. After the film and tape were fully laminated, the weight was removed, and the specimen was placed onto the tape for 24 h to ensure that the specimen and tape were also fully laminated. Finally, the test was conducted using a peel strength machine with a tensile speed of 200 mm/min, as shown in Fig. 3-3. The peel strength required to separate the carbon fibers from the carbon film was measured as the adhesion strength between the two.

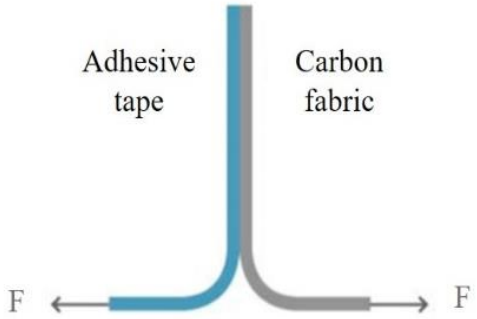

Fig. 3-3 Schematic of the adhesion strength test apparatus

3.3 Experimental result and discussions

3.3.1 Tensile properties of carbon fibers

3.3.1.1 Tensile properties of single carbon fibers

Fig. 3-4 shows the surface morphology of the carbon fibers after magnetron sputtering treatment. The carbon fiber diameter was examined using scanning electron microscopy. It was found that the diameter of the single carbon fiber were not significantly changed after the magnetron sputtering treatment. The characterization of the carbon-film thickness on silicon wafers under different sputtering conditions presented in Chapter 2 indicated that the diameter of modified carbon fibers tends to increase with increases in the sputtering time and power. To investigate the effect of the modification process parameters on the carbon fiber diameter, the thickness of the carbon film deposited on the silicon wafer was used to indirectly characterize the carbon

fiber diameter variations under different modification conditions. Assuming that the carbon fiber after surface modification was still a uniform cylinder, the tensile breaking strength of the single carbon fiber was calculated using Equations (3-1) and (3-2), and the tensile properties of the carbon fiber before and after modification are presented in Table 3-2.

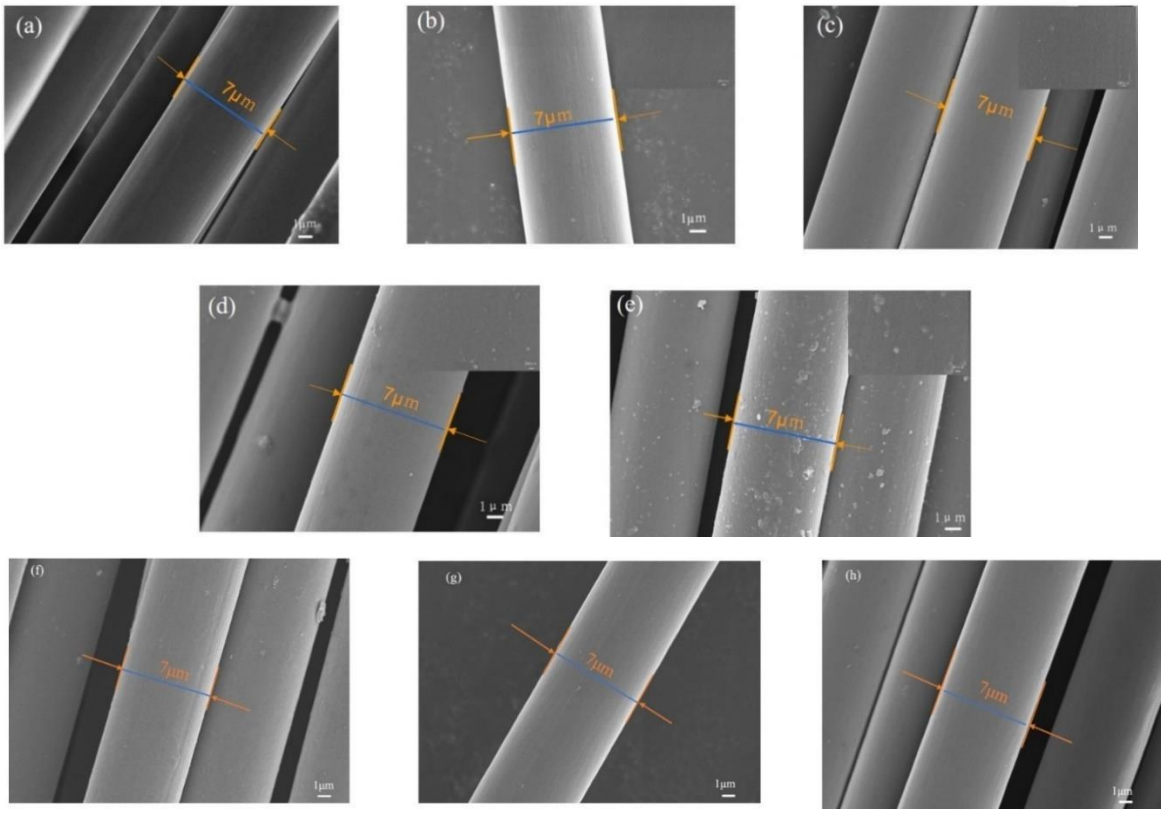

Fig. 3-4 Diameter of carbon fiber before and after Magnetron Sputtering Modification

(a) None (b) 20min (c) 30min (d) 40min (e) 50min (f) 150W (g) 350W (h) 450W

By comparison, the tensile breaking force of the single carbon fiber slightly increased after surface modification. The carbon fibers modified by the 250w,50min magnetron sputtering process showed the largest increase in tensile fracture force, which increased by 9.93%. It was also found that the tensile breaking force of the modified carbon fibers tended to increase with the increase of magnetron sputtering time and magnetron sputtering power.

The calculated tensile breaking strength of the single carbon fibers was improved after the magnetron sputtering, with a maximum increase of 2.82% under the 250 W, 30 min and 450 W, 20 min modification conditions. At a magnetron sputtering power

of 250 W, when the magnetron sputtering time was <30 min, the tensile breaking strength of the single carbon fibers increased with the magnetron sputtering time. The tensile breaking strength of the single carbon fibers treated by magnetron sputtering for 50 min exceeded that of the single carbon fibers treated for 40 min. When the magnetron sputtering time was 20 min, the tensile fracture strength of the single carbon fibers tended to increase with the magnetron sputtering power, but the increase rate gradually decreased. When the magnetron sputtering power was increased from 150 to 450 W, the increase rate in the tensile breaking strength of the single carbon fibers was 3.51%, 0.93%, and 1.23%, respectively. This indicated that the increase in the carbon fiber diameter was conducive to the enhancement of the tensile breaking strength of the single carbon fibers, but it was not the only influencing factor.

Table 3-2 Measured physical and mechanical properties of the single carbon fiber specimens

Sample number	Diameter /μm	Tensile breaking force/CN	Tensile breaking strength/GPa	Breaking force CV/%
1#	3.5	12.29	3.19	13.74
2#	3.524	12.83	3.29	10.93
3#	3.556	13.45	3.39	5.839
4#	3.584	12.72	3.15	12.94
5#	3.597	13.51	3.32	12.64
6#	3.536	12.30	3.13	9.60
7#	3.576	13.14	3.27	11.21
8#	3.590	13.41	3.31	9.07

Fig. 3-5 presents the tensile stress–strain curves of a single carbon fiber before and after modification. As shown in Fig. 3-5(a), the tensile modulus of the single carbon fibers treated with different magnetron sputtering times decreased. For example, the tensile modulus was approximately 1.307 GPa for the unmodified carbon fiber, and it was reduced to approximately 1.159 GPa after magnetron sputtering modification for 20 min. Although the magnetron sputtering modification did not significantly improve

the tensile breaking strength of the single carbon fiber, it significantly improved the tensile fracture toughness. Thus, the magnetron sputtering modification treatment increased the strain and tensile fracture work of the single carbon fiber, and the increase was larger for a longer magnetron sputtering time. The strain of the virgin single carbon fiber was 2.15%, whereas that of the fiber treated by magnetron sputtering for 50 min was 2.55%. The tensile fracture work of the single carbon fiber treated by magnetron sputtering for 50 min increased by 19.73% compared with that of the fiber without modification.

The effects of the sputtering power on the tensile stress–strain characteristics of the carbon fibers were analyzed, as shown in Fig. 3-5(b). The tensile strain and tensile toughness of the carbon fibers modified by different magnetron sputtering powers exhibited improvements, but the changes were small. The single carbon fibers modified at a 450-W magnetron power exhibited the largest change in strain, with only a 9.3% increase. This led to an insignificant increase in the tensile breaking work of the modified single carbon fibers; the largest increase was 14.87%, corresponding to the single carbon fibers modified at 250 W.

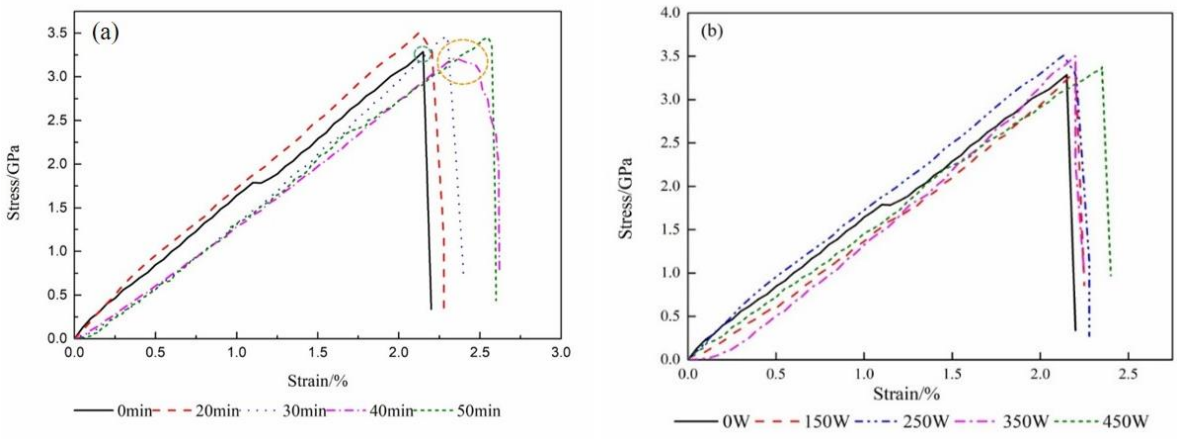

Fig. 3-5 Tensile stress–strain curves of single carbon fibers:
(a) different sputtering times; (b) different sputtering powers

the reason for this phenomenon is ascribed to the load directly acting on the unmodified single carbon fibers when they were stretched, whereas a C/C composite fiber morphology similar to the core structure was formed with the coating of the modified single carbon fibers with a layer of carbon film. In particular, when the

modified single carbon fibers were stretched, the load did not directly act on the carbon fibers to deform them; rather, it acted on the carbon film on the surface of the carbon fibers. The difference in the fracture forms of the single carbon fibers at the tensile limit indicated the influence of the carbon film on their tensile properties. The analysis of the carbon-film morphology presented in Chapter 2 indicated that the densities of the carbon films on the surface of carbon fibers modified at different magnetron sputtering powers differed. When the sputtering power is low, the island structure (aggregated structure) between carbon particles on the surface of the carbon fibers is loose, which prevents force transfer and crack extension when the carbon fibers are subjected to a tensile load and cannot achieve the purpose of effectively improving the mechanical properties of the carbon fibers. With an increase in the magnetron sputtering power, the density of the carbon film increases, improving the tensile load transfer and crack extension. However, owing to the large surface particle size of the carbon film deposited under a high magnetron sputtering power, the film compaction is significant, and the relative slip of cracks between its layers is limited, which affects the increase in the carbon fiber strain.

From the stress–strain curve of the single carbon fiber, the fracture forms of the single carbon fiber before and after modification differed at the tensile limit. Carbon fibers are brittle materials without plastic deformation during tensile fracture. However, when the single carbon fiber surface modified by magnetron sputtering reached the tensile limit, brittle fracture, which is observed for traditional carbon fibers, did not occur; rather, a small amount of tensile yielding occurred. As carbon fibers are brittle materials, the fracture conforms to the Griffith microcrack theory. When the maximum concentrated stress produced by the load at the defect exceeds the inherent tensile strength of the carbon fiber, microcracks occur. With an increase in the tensile strength, the microcracks slowly expand until the carbon fiber is completely broken. Compared with the carbon fiber, the carbon film has a low tensile modulus. Therefore, when bearing a tensile load, the carbon film first deforms and produces microcracks. With an increase in the tensile load, the microcracks expand and are transferred to the surface

of the carbon fiber between the carbon-film layers, resulting in a stress concentration at the defects on the carbon fiber surface. The microcracks continue to expand with the increase in the tensile load until the tensile fracture of the carbon fiber occurs. The specific drawing process of a single carbon fiber is shown in Fig. 3-6.[35].

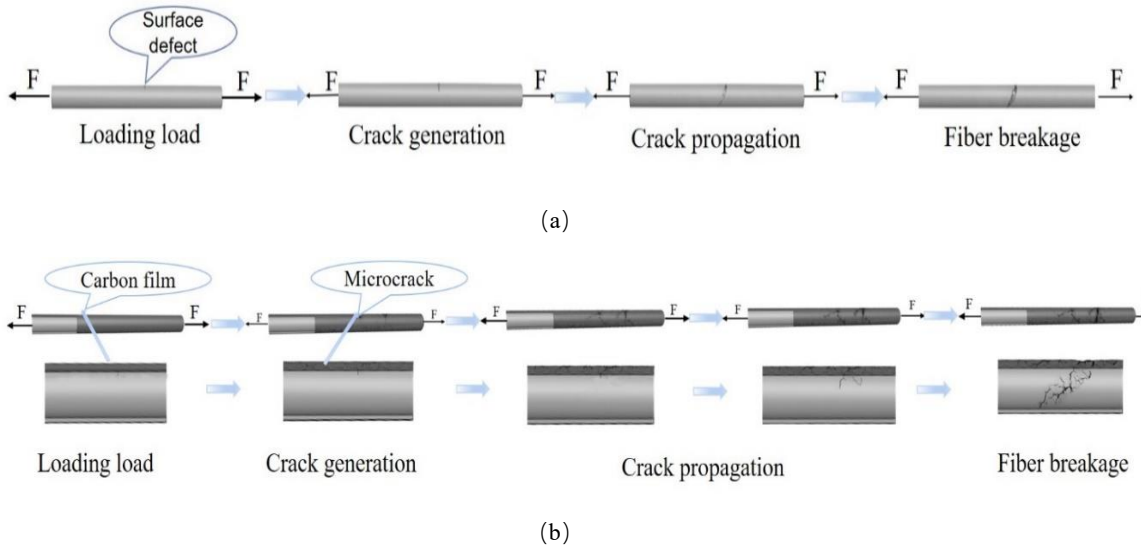

Fig. 3-6 Tensile fracture diagram of the single carbon fiber
(a) raw single carbon fiber (b) single carbon fiber after magnetron sputtering

Traditionally, the strength dispersion of carbon fibers is attributed to the fiber defects. Therefore, the tensile breaking forces of the single carbon fibers before and after modification through CV were compared. The dispersion of the tensile breaking force of the modified carbon fibers significantly improved. After 30 min of magnetron sputtering modification treatment, the tensile breaking force of the carbon fibers exhibited the largest improvement, and the CV value was reduced by 57.5%. The tensile breaking force of carbon fiber monofilaments treated for 40 min exhibited the smallest improvement, with only a 5.8% increase in the CV.

To further investigate the influence of the modification process on the dispersion of the tensile breaking force of the carbon fibers, the Weibull distribution, which is commonly used to study the dispersion characteristics of the fiber force, was used to analyze the tensile breaking force of the single carbon fibers. Fig. 3-7 shows the Weibull distribution linear diagram of the tensile force of the single carbon fibers after different modification processes. The Weibull modulus m of the tensile breaking force of the unmodified single carbon fibers was 7.9903. In comparison, the Weibull modulus m of

the single carbon fibers treated by the modification process was increased, indicating the improved dispersion of the tensile breaking force of the modified carbon fibers.

Under the same magnetron sputtering power, with an increase in the sputtering time, the tensile-strength Weibull modulus of the single carbon fibers increased and then decreased. The Weibull modulus of the single carbon fibers treated for 40 min was the smallest (8.76837), and that of the single carbon fibers modified for 30 min was the largest (15.83). These results were consistent with the variation pattern of the CV value of the tensile breaking force of the carbon fibers. After 50 min of magnetron sputtering modification treatment, the tensile breaking force of the single carbon fibers was significantly increased, and the CV value and Weibull modulus were improved, indicating that the dispersion of the carbon fiber tensile breaking force under this modification condition was relatively poor. This is because when the sputtering time was longer, the carbon particles composing the surface of the carbon film were larger, and the uniformity of the structure was worse, which increased the probability of microcrack generation during stretching and affected the improvement of the discrete tensile fracture force of the modified carbon fibers.

For the same sputtering time, when the sputtering power is not more than 350W, the single carbon fiber tensile fracture force Weibull modulus decreased with an increase in the magnetron sputtering power, and when the magnetron sputtering power reached 450 W, the single carbon fiber tensile fracture force Weibull modulus began to increased. When the sputtering power was 150 W, owing to the low sputtering power and short sputtering time, a dense carbon film was not formed on the surface of the carbon fibers, but no obvious island structure was formed on the carbon fiber surface, which improved the repair of surface defects of the carbon fibers. With an increase in the sputtering power, the size of the deposited particles on the carbon fiber surface increased, the island structure of the carbon fiber surface was enhanced, and the uniformity of the modified carbon fiber surface affected the improvement of the dispersion of the tensile fracture force of the carbon fibers. When the magnetron sputtering power reached 450 W, the increase of carbon fiber diameter and the

improvement of film density have played a positive role in the improvement of the tensile breaking force of modified carbon fibers. This indicated that the increase in the carbon fiber diameter was beneficial to the enhancement of the carbon fiber tensile force and the force dispersion, but the carbon fiber surface carbon film structure morphology also affected the tensile properties of the carbon fibers.

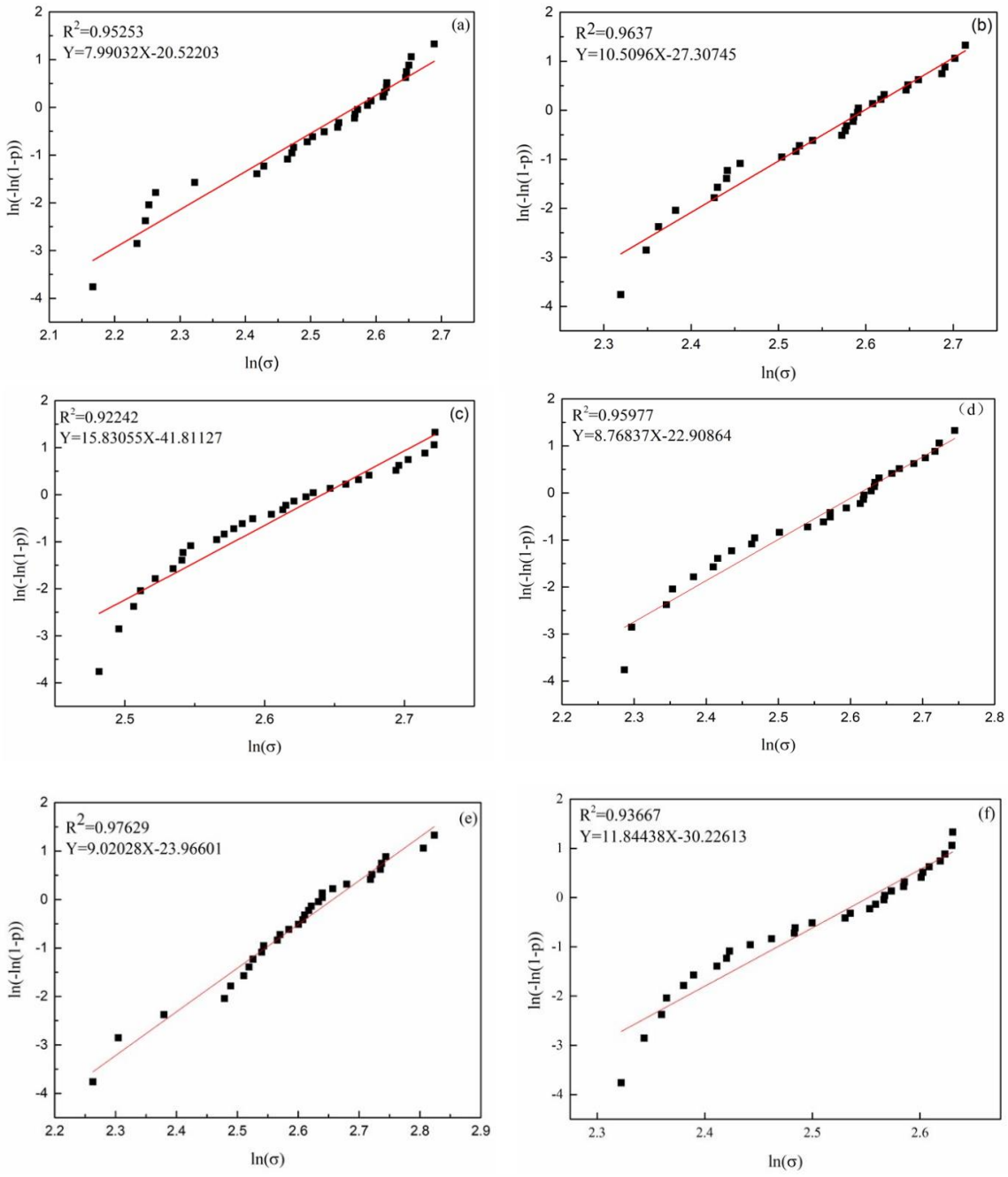

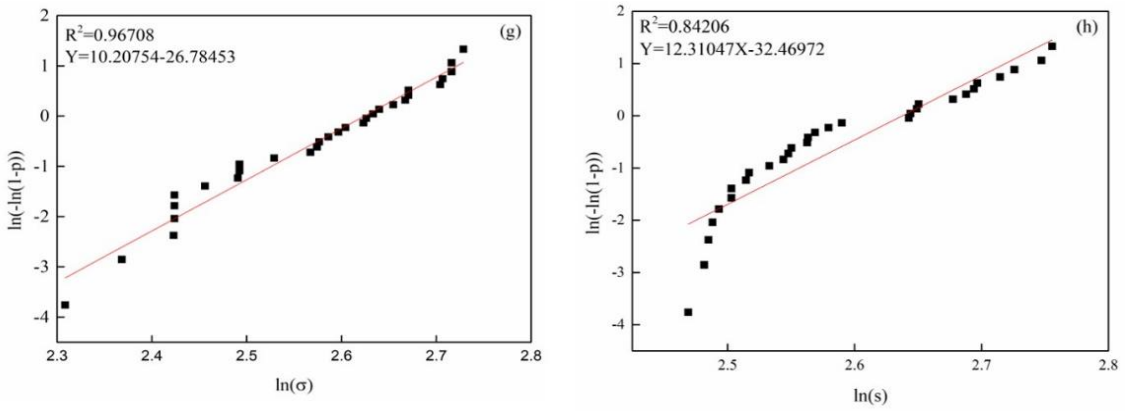

Fig. 3-7 Weibull plots of tensile force of single carbon fiber

(a) raw carbon fiber; (b) 250 W/20 min; (c) 250 W/ 30 min; (d) 250 W/40 min; (e) 250 W/50 min; (f) 150 W/20 min; (g) 350 W/20 min; (h) 450 W/20 min

3.3.1.2 Tensile properties of multifilament carbon fibers

As carbon fibers do not exist as single fibers in practical applications, the tensile properties of multifilament carbon fibers before and after modification were analyzed to further investigate the influence of the magnetron sputtering modification treatment on the mechanical properties of carbon fibers. Fig. 3-8 shows the tensile breaking force/breaking force of the multifilament carbon fibers before and after modification. The tensile breaking force was increased for the modified multifilament carbon fibers. Under the same magnetron sputtering power, the tensile breaking force of multifilament carbon fibers modified for 30 min exhibited the largest increase (7.0%), and that of multifilament carbon fibers modified for 20 min exhibited the smallest increase (4.3%). Under the same magnetron sputtering time, the tensile fracture force of the multifilament carbon fibers increased with the magnetron sputtering power. The multifilament carbon fibers modified at 450 W exhibited the largest increase in the tensile breaking force (4.73%). The tensile breaking force of the multifilament carbon fibers was calculated using Equations (3-3) and (3-4). When the magnetron sputtering power was the same, the tensile breaking force of the multifilament carbon fibers increased slightly with an increase in the magnetron sputtering time when the magnetron sputtering time was not more than 30 min. When the magnetron sputtering time was grater than 30 min, the tensile fracture force of the multifilament carbon fibers

decreased with an increase in the magnetron sputtering time, which differed from the results for single carbon fibers.

With increases in the magnetron sputtering time and power, the thickness of the carbon film deposited on the surface of the multifilament carbon fibers increased, which increased the diameter of the multifilament carbon fibers in disguise, along with their tensile force. Differences in the magnetron sputtering modification process led to differences in the size and structural morphology of the particles on the surface film layer of carbon fibers, which resulted in differences in the tensile properties of the multifilament carbon fibers and single carbon fibers.

The CV value of the tensile breaking force of the multifilament carbon fibers modified by magnetron sputtering was smaller than that of unmodified multifilament carbon fibers, confirming that the surface modification of carbon fibers by magnetron sputtering affects the repair of carbon fiber surface defects. It was also found that the tensile breaking force CV of multifilament carbon fibers was significantly smaller than that of single carbon fibers. The dispersion of the multifilament carbon fibers improved because of their composition of multiple single fibers. Therefore, the tensile breaking force CV value of the multifilament carbon fibers was significantly smaller than that of the single carbon fibers. The tensile breaking force CV value of the multifilament carbon fibers treated with magnetron sputtering for 30 min did not differ significantly from that of single carbon fibers treated under the same magnetron sputtering conditions. This is attributed to the surface of the carbon fibers being effectively covered by the carbon film during the surface modification by magnetron sputtering, whereas the inner fibers were not completely repaired, which resulted in a difference in the repair effect between the surface and inner layers of the multifilament carbon fibers, affecting the improvement of the tensile breaking force CV value. An analysis of the influence of the front surface modification process on the tensile breaking force of single carbon fibers indicated that the greater influence of the modification process on the tensile breaking force of the carbon fibers increased its influence on the tensile breaking force and change in the CV value of the tensile breaking force of the multifilament carbon fiber.

Therefore, as the effect of the magnetron sputtering modification treatment of the single carbon fibers improved, the dispersion of the tensile breaking force of the multifilament carbon fibers increased. When the magnetron sputtering power was 450 W/20min, owing to the enhanced compaction of carbon particles, more carbon particles entered the interior of the bundled carbon fibers through the inter-fiber gap on the surface of the multifilament carbon fibers during the sputtering process, which caused the surface layer of the multifilament carbon fibers to be covered with carbon film and led to repair in the inner layer of the bundled carbon fibers, reducing the difference in properties between the inner and outer layers of the multifilament carbon fibers. Therefore, the CV value of the tensile breaking force of the multifilament carbon fibers treated at 450 W/20min was relatively small.

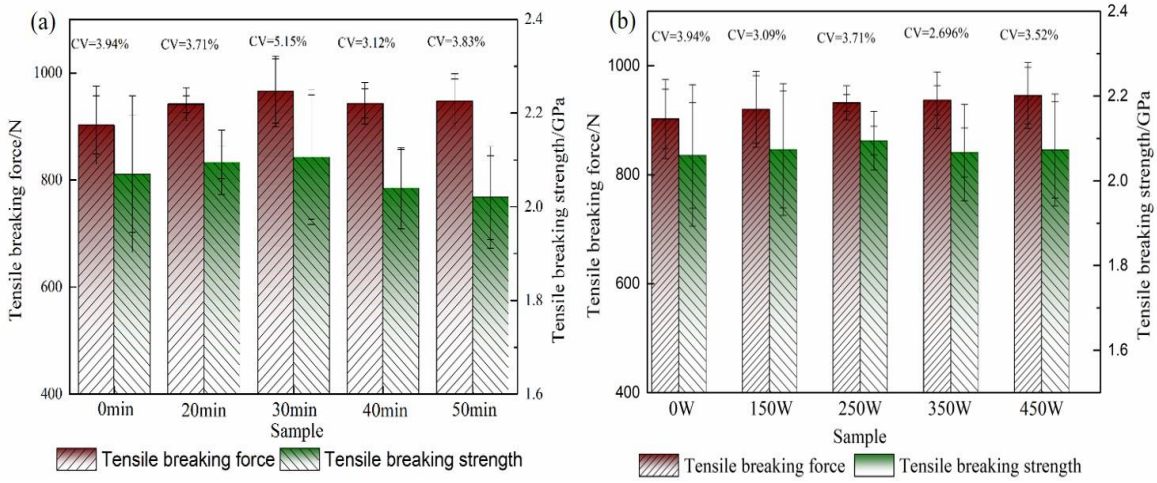

Fig. 3-8Tensile breaking force/strength of the multifilament carbon fibers

(a) Different sputtering time (b) Different sputtering power

An analysis of the stress–strain curves of the multifilamentary carbon fibers, as shown in Fig. 3-9, when the tensile elastic modulus of the multifilament carbon fiber before and after modification was less than 0.5%, the tensile modulus was maintained, and the tensile modulus of the unmodified multifilament carbon fiber was slightly greater than that of the modified carbon fiber. However, when the strain was greater than 0.5%, the tensile elastic modulus of the modified carbon fibers significantly exceeded that of the unmodified carbon fibers, except for the carbon fibers modified for 250W/40 min. Moreover, brittle fracture of the multifilament carbon fibers did not

occur during tensile fracture, which is caused by different fracture times of the multifilament carbon fibers during the tensile process.

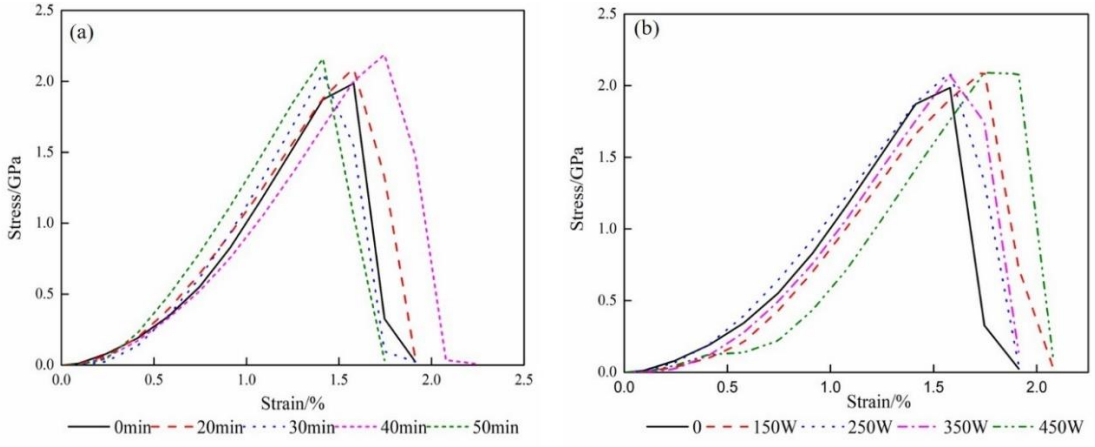

Fig. 3-9 Tensile stress-strain curve of multifilamentary carbon fiber

(a) Different sputtering time (b) Different sputtering power

Because of the uneven relaxation between fibers produced during the treatment of bundle fibers, there are tension-time differences between fibers during stretching; that is, when some fibers reach the tensioned state, others are in the flexed state. As the tensile load increases, the fibers that reach the tensioned state first fracture, and then the fibers in the flexed state also reach the tensioned state and fracture. Therefore, non-brittle fracture occurs in the tensile stress–strain curve. When the modified bundle fibers are subjected to a tensile load, the same phenomenon of inter-fiber tension-time differences occurs owing to the uneven relaxation between fibers. However, the surface treatment of carbon fibers by magnetron sputtering not only deposits a carbon film on the surface of the bundle fibers but also deposits a layer of carbon particles on the internal fibers of the bundle fibers. The magnetron sputtering modification conditions affect the number of carbon particles deposited inside the bundled carbon fibers. When the sputtering power is low and the sputtering time is short, the number of deposited carbon particles is small owing to the small effect of the carbon particle compaction, both of which result in fewer carbon particles being deposited inside the carbon fiber bundle. When the sputtering power is higher and the sputtering time is longer, more carbon particles are deposited inside the fiber bundle. In addition to improving the

surface defects of the carbon fibers and increasing the tensile fracture force of the carbon fibers, this can reduce the differences in mechanical properties between the fibers, improving the overall mechanical properties of the carbon fibers bundle.

3.3.2 Surface energy of carbon fibers

Fig. 3-10 presents the results of contact angle and total surface energy tests of carbon fibers in water and ethylene glycol before and after magnetron sputtering carbon fiber surface treatment. The contact angles of untreated carbon fibers in both different polar solvents were larger, 85.05° (deionized water) and 63.48° (ethylene glycol), while the calculated total surface energy was 25.31 mJ/m^2.

The contact angle of the carbon fibers in deionized water characterizes the wettability between the carbon fibers and a polar solvent. The unmodified carbon fibers had poor wettability in polar solvents, owing to the lack of polar groups on the carbon fiber surfaces. The contact angles of the carbon fibers modified using the magnetron sputtering process were smaller in the two polar solvents, except for slight increases in those of the carbon fibers modified by 150 W/20min in two polar solvents. The contact angle of the carbon fibers modified by 250 W/20min in deionized water was the smallest, with a decrease of 19.18%. The contact angles of the carbon fibers modified using other processes in deionized water were similar, with decreases of approximately 11–12°. The previous analysis indicates that surface modification using magnetron sputtering did not introduce polar groups to the surfaces of the carbon fibers; however, the contact angles of these modified carbon fibers in polar solvents still decreased significantly compared to the untreated fibers.

The contact angles of the carbon fiber in ethylene glycol reflect the dispersion component of the fiber's surface energy, which is mainly related to the surface morphology of the fiber. The surfaces of the untreated carbon fibers are smoother and cleaner; thus, their contact angles in a non-polar glycol solvent are larger. Following surface modification magnetron sputtering, the roughness of the carbon fiber surfaces increased, thereby reducing the contact angles of the fibers in the glycol solvent. After 350W/20min, 450W/20min, and 250 W/30 min, the contact angles of the carbon fibers

in the glycol solvent decreased by 15.48%, 11.3%, and 6.5%, respectively. In contrast, the contact angles of the carbon fibers modified by other magnetron sputtering conditions in the glycol solvent only underwent small changes, unlike the effect of magnetron sputtering modifications on the surface roughness of the carbon fibers. Thus, in addition to the influence of changes in carbon fiber surface roughness on the contact angle in ethylene glycol, other surface morphological changes affect the contact angles of carbon fibers in non-polar solutions.

Fig. 3-10 (c) and (d) show the total surface energies of the carbon fibers before and after magnetron sputtering modification. The total surface energy increased in all carbon fibers modified by magnetron sputtering, including the carbon fibers modified at 150 W/20min conditions, which increased slightly. Their contact angles in two polar solvents also increased. For the same magnetron sputtering duration, the surface energy of the carbon fiber increased with increasing power, which is consistent with the effects of the magnetron sputtering process on the carbon fiber surface roughness. The surface energy of the carbon fiber modified by 350 W/20min exhibited the largest increase (32.12%). The surface energies of carbon fibers modified by the same power at different durations did not increase with increasing magnetron sputtering duration. The carbon fibers modified for 250W/30 min exhibited the largest increases in surface energy (34.65%).

The higher surface roughness of the modified carbon fibers was an important factor that improved the wettability of the fibers. However, since the carbon film deposited on the surfaces of the fibers is a film structure with surface micro-cracks formed by the accumulation of nanometer-size particles (as opposed to a compact structure), the sizes of the particles that comprise the film structure and the microcracked pores will also affect the surface energy of the modified carbon fibers. The presence of micro-cracks improved the surface wettability of the carbon fibers, which indicates that although the magnetron sputtering modification did not introduce polar functional groups to the surfaces of the carbon fibers, the modification process still decreased the contact angles of the carbon fibers in a polar deionized water solvent.

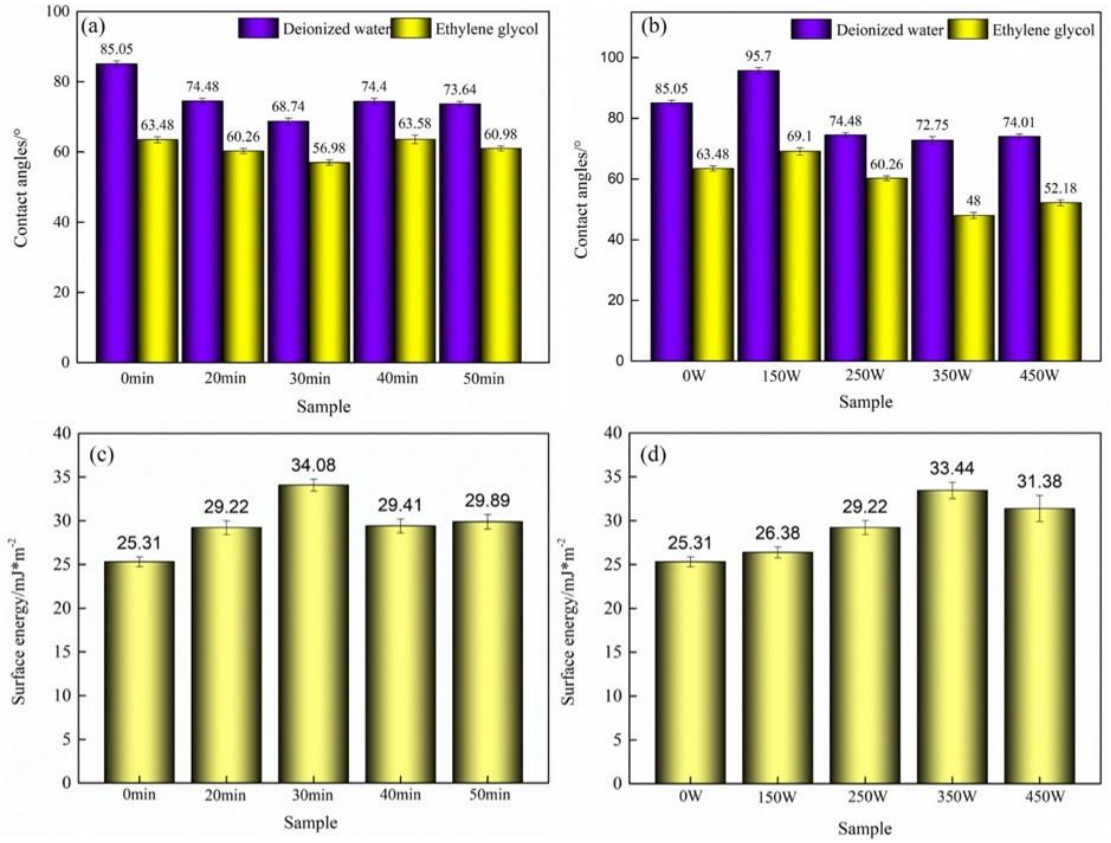

Fig. 3-10 Contact angles and surface energies of carbon fibers

(a) and (b) are contact angle of carbon fiber, (c) and (d) are surface energies of carbon fiber, (a) and (c) Different sputtering time, (b) and (d) Different sputtering power

The increase in the total surface energy of the carbon fibers improved the wettability between the fibers and the resin matrix, which facilitated full contact between the carbon fibers and epoxy resin, increased the probability of physical adsorption and mechanical locking between the fiber and resin, and improved the interfacial properties of the composite. Therefore, surface modification of carbon fibers via magnetron sputtering can be used to form better interfacial bonds between the carbon fibers and resin.

3.3.3 Adhesion strength of carbon film to carbon fibers

Fig. 3-11 shows the adhesion strengths between the carbon films and fibers deposited at different modification conditions. The adhesion strength between the untreated carbon fibers and film was only 2.18 N, while that between the modified fibers and film increased by at least 19.72%. When the sputtering power was 350

W/20min, the adhesion strength was the highest (3.2 N). Under the same magnetron sputtering power, the adhesion strength between the carbon film and carbon fibers increased with the magnetron sputtering time; i.e., when the sputtering time was 50 min, the bond strength between the carbon film and carbon fibers was the highest (3.09 N). The adhesion strengths between the carbon film and carbon fibers for 150 W/20min and 250 W/20min magnetron sputtering powers were comparable with the same sputtering time. The unmodified carbon fibers had a smoother surface, thus, the adhesion strength between them and the tape was lower. After the magnetron sputtering process, the roughness of the fiber surface was increased, thus, the adhesion between the carbon fibers and the tape was stronger, resulting in a higher adhesion strength between the carbon fibers and the tape.

The adhesion between the carbon fibers and carbon film is mainly dependent on diffusion and mechanical bonding, and the interface between the two is "like-diffusion." During the sputtering process, the carbon-film particles bombard the carbon fiber substrate with a high energy, resulting in some of the carbon-film particles remaining inside the substrate and spreading adhesion. As the sputtering time increased, the adhesion strength of carbon nanoparticles to the fibers and the degree of diffusion adsorption between fibers increased; thus, the adhesion strength increased. When the overall growth process of the film was perfect, the surface roughness was small, sufficient strain energy was needed to destroy the film during the adhesion experiment, and the bonding strength between the film and the carbon fibers was high. When the sputtering power was high, i.e., 450 W/20min, the film structure formed a coarse large island; thus, the film surface particle size and roughness increased, and the film had a high internal stress, reducing the film–base interface bond strength.

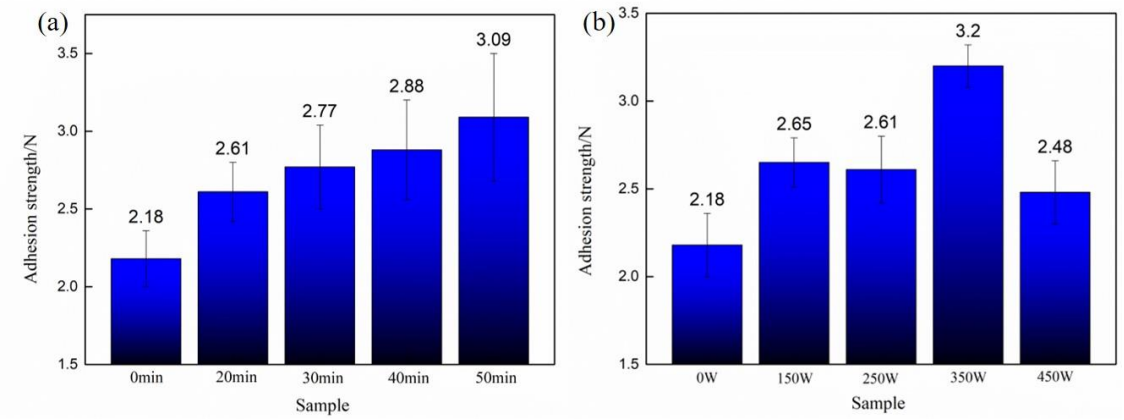

Fig. 3-11 Adhesion strength between the carbon film and carbon fiber

(a) Different sputtering time (b) Different sputtering power

Fig. 3-12 shows the form of the tape after the peeling test with carbon fibers; there was no obvious carbon film on the surface of the tape after the peeling test. After the peeling test, the unmodified carbon fiber had obvious adhered carbon fibers on the tape surface. No obvious carbon films or particles were observed on the tape surfaces after the peeling test of the modified carbon fibers, nor were any obvious adhered carbon fibers observed. When a large amount of carbon film is not observed on the tape surface in this test, the peel strength between the tape and carbon fibers can only indirectly characterize the adhesion between the carbon film and fibers, and does not accurately reflect the adhesion performance between the carbon film and fibers. The actual adhesion strength between the carbon film and the carbon fibers exceeded the adhesion strength between the tape and the carbon fiber. This indicates that there is good adhesion between the carbon film and carbon fibers, which can ensure that the carbon film will not detach from the carbon fibers under a tensile load.

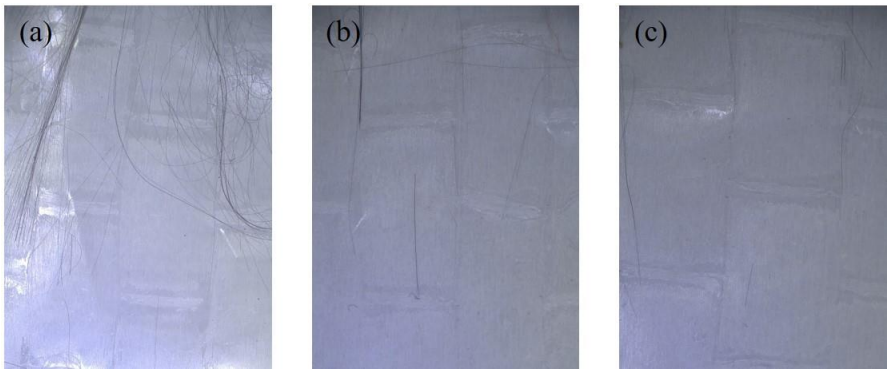

Fig. 3-12 The tape after the peeling test with carbon fibers

(a) unmodified carbon fiber (b) 250W/20min (d) 450W/20min

3.4 Conclusion

The surface of the carbon fibers after magnetron sputtering was covered by a carbon film, which repaired cracks and grooves on the carbon fiber surface. The surface modification of carbon fibers by magnetron sputtering increased the discrete tensile breaking force of the carbon fibers, along with other mechanical properties particularly their tensile toughness. The tensile fracture force CV of carbon fibers modified by magnetron sputtering was reduced by 57.5%, and the tensile fracture force CV of compound filamentary carbon fibers was reduced by 31%. The Weibull modulus of the tensile fracture force of single carbon fibers modified by magnetron sputtering was increased by fitting the Weibull distribution to the tensile fracture force of the single carbon fibers. This indicated the effect of surface modification of the single carbon fibers by magnetron sputtering on the dispersion of the tensile fracture force of the carbon fibers. Under the selected modification conditions, the tensile breaking force of single carbon fibers modified by magnetron sputtering was increased by a maximum of 9.93%, and the tensile breaking force of multifilamentary carbon fibers was increased by a maximum of 6.9%. In addition to the improvement of the tensile properties due to the improvement of the surface defects of the carbon fibers, the tensile properties of the carbon fibers modified by magnetron sputtering were improved by the deposition of a carbon film on the carbon fiber surface, which significantly increased the tensile toughness of the carbon fibers during the tensile process through the crack effect mechanism. The tensile fracture work of single carbon fibers after 50 min of magnetron sputtering treatment was increased by 19.73%, and the tensile fracture work of multifilamentary carbon fibers after 250W/50 min of magnetron sputtering treatment was increased by 23%. The difference of magnetron sputtering on the surface and inner layer fiber repair of compound filamentous carbon fibers is an important reason for further improvement of the repair effect. In future research, it is expected that the consistency of the surface and inner layer modification of compound filamentous carbon fibers can be achieved when surface modification of carbon fibers is performed via magnetron sputtering, so that the tensile dispersion of compound filamentous carbon fibers and their aggregate products can be improved and the tensile mechanical

properties can be enhanced.

The surface energy of the carbon fibers was increased after the magnetron sputtering. The increase in the surface energy provided conditions for the formation of strong interfacial bonds between the carbon fibers and resin matrix, indicating that magnetron sputtering carbon fiber surface modification treatment can improve the interface properties of CFRP composites. However, the magnetron sputtering conditions can affect the carbon fiber surface energy. When the sputtering time was changed and the other sputtering conditions were kept the same, the contact angles of modified carbon fibers in two different polar solvents water and ethylene glycol were reduced compared with those of unmodified carbon fibers in these polar solvents, and the change in the dispersion component of the surface energy was larger. When the sputtering time was ⩽30 min, the surface energy of the modified carbon fibers increased with the sputtering time, and when the sputtering time was >30 min, the surface energy of the modified carbon fibers decreased with an increase in the sputtering time. The contact-angle increase or decrease for carbon fibers modified with a 450W/20min sputtering power in two solvents was small. This indicated that in addition to the surface roughness, the morphological structure of the modified carbon fiber surface influenced the surface energy of the carbon fibers.

The carbon film deposited on the carbon fiber surface magnetron sputtering has strong adhesion to the carbon fiber and will not be peeled off by an applied load such as stretching. Strong adhesion between the modified carbon fibers and carbon film is the basis for the improvement of the mechanical properties of the carbon fibers and is a necessary condition for the improvement of the interface and mechanical properties of carbon fiber composites at a later stage. When all other magnetron sputtering conditions were the same, extending the magnetron sputtering time is beneficial to the adhesion strength between the carbon film and carbon fibers, and the adhesion strength increases with the magnetron sputtering time. Increasing the magnetron sputtering power is also beneficial to the adhesion strength between the carbon film and carbon fibers. However, when the magnetron sputtering power is varied and the other

sputtering conditions are kept the same, differences in the sputtering power lead to differences in the sputtered carbon particle size and the carbon-film structure. When the particle size and roughness of the carbon film surface increase, the adhesion strength between the carbon film and carbon fibers is affected owing to the higher internal stress in the carbon film.

References

[1] D. Jang, M.E. Lee, J. Choi, S. Y. Cho, S. Lee. Strategies for the production of PAN-Based carbon fibers with high tensile strength. Carbon. 2022(186):644-677

[2] B.A Newcomb. Processing, structure, and properties of carbon fibers. Composites Part A. 2016(91):262-282

[3] Y. Zhang, J. Zhao, D. Pan. Defects of carbon fibers and its modification methods. New Chemical Materials. 2003(31):25-27

[4] J. Yao, Z. Zou. Effect of anodic oxidation treatment on strength dispersion of carbon fiber and its characterization. Synthetic Fiber in China. 2017(46):26-29

[5] H. Zhu, X. Li, F. Han, Z. Dong, G. Yuan, G. Ma, A. Westwood, K. He. The effect of pitch-based carbon fiber microstructure and composition on the formation and growth of SiC whiskers via reaction of such fibers with silicon sources. Carbon. 2016(99):174-185

[6] B. Dharmasiri, J. Randall, Y. Yin, G. G. Andersson, E. H. Doeven, P. S. Francis, L. C. Henderson. Carbon reinforced carbon fibers: Using surface modification as a route to enhanced physical performance. Compos. Sci. Technol.. 2022(218):109217

[7] C. Wang, Y. Li, L. Tong, Q. Song, K. Li, J. Li, Q. Peng, X. He, R. Wang, W. Jiao, S. Du. The role of grafting force and surface wettability in interfacial enhancement of carbon nanotube/carbon fiber hierarchical composites. Carbon. 2014(69):239-246

[8] S. Soulis, G. Konstantopoulos, E. P. Koumoulos. C. A. Charitidis. Impact of alternative stabilization strategies for the production of PAN-Based carbon fiber with high performance. Fibers. 2020(33):1-25

[9] S. Nunna, M. Naebe, N. Hameed, B. L. Fox, C. Creighton. Evolution of radial heterogeneity in polyacrylonitrile fibres during thermal stabilization : an overview. Polym. Degrad. Stab.. 2017(136):20-30

[10] J. Nasser, L. Zhang, H. Sodano. Aramid nanofiber interlayer for improved interlaminar properties of carbon fiber/epoxy composites. Composites Part B. 2020(197):108130

[11] J. K. Kocsis, H. Mahmood, A. Pegoretti. All-carbon multi-scale and hierarchical

fibers and related structural composites: A review. Compos. Sci. Technol.. 2020(186):107932

[12] N. H. Ismail, J. O. Akindoyo, M. Mariatti. Solvent mediated dispersion of carbon nanotubes for glass fibre surface modification -suspensions stability and its effects on mechanical, interlaminar and dynamic mechanical properties of modified glass fibre reinforced epoxy laminates. Composites Part A. 2020(139):106091

[13] P. Zhu, F. Ruan, L. Bao. Preparation of polyetherimide nanoparticle on carbon fiber surface via evaporation induced surface modification method and its effect on tensile strength and interfacial shear strength. Appl. Surf. Sci.. 2018(454):54-60

[14] Z. Zhao, K. Teng, N. Li, X. Li, Z. Xu, L. Chen, J. Niu, H. Fu, L. Zhao, Y. Liu. Mechanical, thermal and interfacial performances of carbon fiber reinforced composites flavored by carbon nanotube in matrix/interface. Compos. Struct.. 2017(159):761-772

[15] B. Dharmasiri, J. D. Randall, M. K. Stanfield, Y. Ying, G. G. Andersson, D. Nepal, D. J. Hayne, L. C. Henderson. Using surface grafted poly(acrylamide) to simultaneously enhance the tensile strength, tensile modulus, and interfacial adhesion of carbon fibres in epoxy composites. Carbon. 2022(186):367-379

[16] M. Kikuchi, K. Nakaso, A. Murate, A. Hosoi, H. Kawada. Influence of covalently-bound graphene oxide on the mechanical properties of carbon fiber composites materials. Diamond Relat. Mate.. 2022(121):108730

[17] A. Anders. Tutorial: Reactive high power impulse magnetron sputtering (R-HiPIMS). J. Appl. Phys.. 2017(121):171101

[18] J. T. Gudmundsson. Physics and technology of magnetron sputtering discharges. Plasma Sources Sci. Technol.. 2020(29):113001

[19] S. Xu, X. Ma, G. Tang, M. Sun. Effect of deposition parameters on deposition rate of B-C-N film prepared by magnetron sputtering. Heat treatment of metals. 2009(34):31-33

[20] C.R. Lu, J. Wang, X. Lu, T. Zheng, Y.Y. Liu, X.D. Wang, D.X. Zhang, D. Seveno. Wettability and interfacial properties of carbon fiber and poly (etherether ketone) fiber

hybrid composite. Applied Materials Interfaces.2019. 11:31520-31531

[21] P. Chen, C. Lu, Q. Yu, Y. Gao, J.F. Li, X.L. Li. Influence of fiber wettability on the interfacial adhesion of continuous fiber-reinforced PPESK composite. Journal of Applied Polymer Science. 2006.102:2544-2551

[22] J.J. Sha, Z.Z. Lu. R.Y. Sha, Y.F. Zu, J.X. Dai, Y.Q. Xian, W. Zhang, D. Cui, C.L. Yan. Improved wettability and mechanical properties of metal coated carbon fiber-reinforced aluminum matrix composites by squeeze melt infiltration technique. Metals Society of China. 2021. 31:317-330

[23] ASTMD3379-75 Standard test method for tensile strength and Young's modulus for high-modulus single-filament materials

[24] JISR7601 Testing methods for carbon fibers

[25] M. Wang, W. Bian. The relationship between the mechanical properties and microstructures of carbon fibers. New Carbon Materials. 2020(35):42-49

[26] ASTMD 4018 Standard test methods for properties of continuous filament carbon and graphite fiber tows

[27] JISR 7608-2007 Carbon fiber-Determination of tensile properties of resin-impregnated yarn

[28] F. Mesquita, S. Bucknell, Y. Leray, S. V. Lomov, Y. Swolfs. Single carbon and glass fibre properties characterised using large data sets obtained through automated single fibre tensile testing. Composites Part A. 2021(145):106389

[29] F. He, S. Wang, Y. Yang. Evaluation of the dispersity of carbon fiber tensile strength by Weibull theory. Hi-Tech Fiber & Application. 2001(26):29-31

[30] Z. Meng, Z. Tan, Y. Zhou, Y. Zhang, Y. Lu, K. Wu. Influence of surface treatment on tensile properties and strength distribution of carbon fiber bundles. Contemporary Chemical Industry. 2020(49):1561-1565

[31] J. Lamon, M. R. Mili. Investigation of flaw strength distributions from tensile force-strain curves of fiber tows. Composites Part A. 2021(145):106262

[32] O. Benjeddou. Weibull statistical analysis and experimental investigation of size effects on tensile behavior of dry unidirectional carbon fiber sheets. Polym. Test..

2020(86):106498

[33] ASTMD3330 Standard test method for peel adhesion of pressure-sensitive tape

[34] S. Qiu, C.A.F. Rojas, D.X. Zhang, A.W.V. Vuure, D. Seveno. Wettability of a single carbon fiber. Langmuir: The ACS journal of surfaces and colloids. 2016. 32:9697-9705

[35] W. Zhou, L. Long, Y. Li. Mechanical and electromagnetic wave absorption properties of Cf-Si3N4 ceramics with PyC/SiC interphases. J. Mater. Sci. Technol.. 2019(35):2809-2813

Chapter 4

Effect of magnetron sputtering modification on mechanical properties of CFEP composites

Chapter 4： Effect of magnetron sputtering modification on mechanical properties of CFEP composites

4.1 Introduction

Carbon fibers have excellent mechanical properties [1-3], but their production process requires high temperature carbonization, graphitization process, which makes the surface of carbon fiber very smooth. In addition, the lack of surface active functional groups, poor wettability, and low interfacial bonding properties greatly weaken the application of high-performance carbon fiber resin-based composites [4,5]. Weak interfacial bonding creates unstable cracks, yet defects within the material are difficult to detect, which is extremely harmful in practice. Therefore, it is necessary to modify carbon fibers to optimize their interfacial structures and improve the interfacial bonding between the carbon fibers and resin to obtain high performance composites [6-11]. Currently, nanomodification methods have received a lot of research attention [12-14]. The introduction of nanoparticles not only improves the roughness of the carbon fiber surface, but also changes the direction of crack expansion, which can improve the mechanical properties of carbon fibers to a certain extent. However, conventional nanoparticles usually need to be pre-treated chemically and introduced onto the carbon fiber surface via physical or chemical grafting methods, and these processes may damage the mechanical properties of the carbon fibers [15-19]. Besides, the disadvantages of nanoparticles, such as poor dispersion, high cost, and even carcinogenicity, greatly limit the industrial applications of this method. Some flexible nanoparticles collapse when the resin is infiltrated into the carbon fiber surface, weakening its ability to improve the mechanical engagement. Recently, a new method of introducing nanoparticles has been discovered by researchers, i.e., in situ growth of nanowires or nanowhiskers on the surface of carbon fibers, which overcomes the disadvantages of conventional nanoparticle modification of non-uniformity and easy agglomeration, and at the same time, uses relatively mild growth conditions that are not detrimental to the properties of the carbon fibers themselves. At present, copper oxide nanosheets (CuO), zinc oxide (ZnO), and titanium dioxide (TiO_2) nanowhiskers have

been successfully grown on the surface of carbon fibers [20-28]. However, the addition of nanoparticles changes the chemical composition of the resulting carbon fiber composites, causing changes in the structural composition of the carbon fibers, which affect the properties of the carbon fibers themselves. Therefore, using the magnetron sputtering process introduced in Chapter 2 to treat the surface of carbon fibers, the carbon film constructed via magnetron sputtering also has the characteristics of nano structural properties, increasing the surface roughness of the carbon fibers, and changes the direction of crack expansion during load loading to improve the comprehensive mechanical properties of carbon fiber composites. Magnetron sputtering surface modification of carbon fibers not only does not cause pollution to the environment, but also does not affect the chemical structure of the carbon fibers themselves.

Magnetron sputtering is a physical vapor deposition method, which mainly involves the ionization of an inert gas using DC or a high frequency electric field. The target atoms or molecules are sputtered out under the bombardment of high speed electrons and ions, and then deposited onto the substrate to form a thin film. When compared with other film-forming technologies, magnetron sputtering has the advantages of fast sputtering speed, uniform film formation, strong process controllability, and good adhesion performance, while causing no damage to the substrate properties. Based on our studies on the effects of the magnetron sputtering process and process parameters on the structural morphology and properties of carbon films, and the modification process on the surface energy and mechanical properties of carbon fibers described in the previous two chapters, we have further analyzed the effects of the magnetron sputtering process and process parameters on the mechanical properties of carbon fiber composites and discuss the damage mechanism of carbon fiber composites after the magnetron sputtering modification process.

Epoxy resin is an excellent thermosetting resin. Due to its excellent physical, electrical insulation, chemical corrosion resistance, heat resistance, and adhesion properties, it has become an irreplaceable matrix material in the field of fiber reinforced composites. To date, many researchers have modified epoxy resin to improve its

properties [29–31]. Therefore, in this chapter, carbon fiber epoxy polymer (CFEP) have been prepared using epoxy resin as the matrix. The effects of the surface modification of carbon fibers using magnetron sputtering technology on the mechanical and interfacial properties of carbon fiber composites have been analyzed by examining the mechanical properties of the carbon fiber composites before and after the modification process.

4.2 Experiments part

4.2.1 Experimental materials

Carbon fiber (T700, 12 K, and diameter ~7 μm) was purchased from Toray Industries, Japan. Carbon fibers modified via magnetron sputtering were self-made in our laboratory. Epoxy resin (JL-235) and the epoxy curing agent (JH-242) were provided by Changshu Jiafa Chemical Co., Ltd of China.

4.2.2 Preparation of CFEP composite materials

Carbon fiber epoxy resin-based (CFEP) composites were prepared via an injection molding-like composite method using compound filamentary carbon fibers as the reinforcement and epoxy resin (Changshu Jiafa Chemical Co., Ltd., China) as the matrix before and after modification via the magnetron sputtering process described in Chapter 2. The CFEP composites were prepared by placing the magnetron sputtered carbon fiber bundle between two molds and injecting vacuum-treated epoxy resin into the mold using a homemade mold with a thickness of 1.5 mm PTFE film sheet. In order to avoid the influence of the carbon particle deposition film size on the carbon fiber composites, the composites were prepared for tensile and flexural properties testing with reference to the fracture test method for single fiber composites. According to the ISO527-3 standard [32] test standard, composite shear samples were prepared using three bundles of carbon fibers as reinforcement due to the difference in size of the different mechanical properties test samples, whereas only one bundle of carbon fibers was used as the reinforcement for the composite tensile and flexural properties test samples. The mass ratio of epoxy resin to curing agent was 100:27, which was cured at room temperature for 48 h. The size of the composite samples and preparation process

are shown in Fig. 4-1.

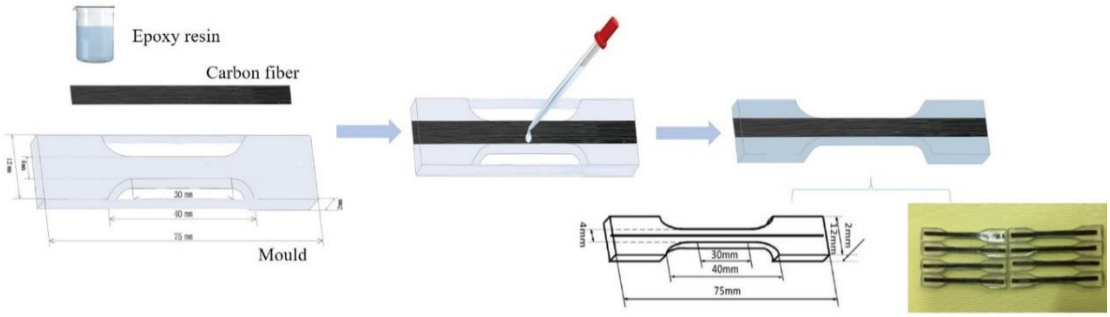

Fig. 4-1 Preparation method and specimen size of carbon fiber epoxy resin composite

4.2.3 Surface morphology analysis

Low-vacuum scanning electron microscopy (SEM) was used to characterize the surface morphology of the CFEP composites in the tensile and flexural damage sections and cross-sections, and to observe the damage pattern of the composites under external loading, as well as the bonding between the resin and carbon fiber interface at the cross-sections.

4.2.4 In-plane shear performance test

Shear testing is an important tool used to characterize the mechanical properties of reinforced fiber composites from a macroscopic perspective. In this paper, the V-notch shear test was used to illustrate the in-plane shear performance between the carbon fibers and resin matrix. The V-notched beam shear test method, also known as the Iosipescu shear test method, was proposed by Iosipescu in 1967 as an experimental method to measure the shear properties of metals. This method was subsequently developed and applied to composites by Walrath and Adams et al. These scholars have agreed and suggested that a double V-notched sample subjected to two mutually canceling bending moments will ensure a homogeneous pure shear region in the sample [33,34]. The shear properties of the composite materials were studied on a LE5105 microcomputer-controlled electronic compound material special tester (Force Test Shanghai Scientific Instruments Co., Ltd.) according to the ASTMD5379/D5379M-05 standard [35], and the sample size and loading method shown in Fig. 4-2.

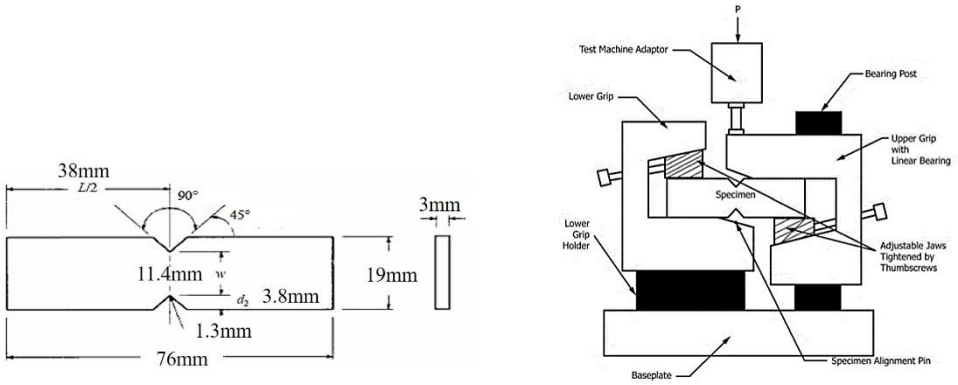

Fig. 4-2 Loading method for in-plane shear test of composite materials

The loading speed was 1 mm/min and five valid measurements were recorded for each sample. The in-plane shear strength of the composite was calculated according to Equation 4-1

$$F^u = \frac{P^u}{A} \tag{4-1}$$

Where F^u is the ultimate strength (MPa), P^u is the lower ultimate load and load at a shear strain equal to 5% (N), and A is cross-sectional area of the material (mm^2).

4.2.5 Tensile performance test

The tensile properties of composite materials are an important criteria used to evaluate their mechanical properties. The tensile properties of the composites were tested on a CSS-88100 universal testing machine according to the ASTMD638 standard [36] at a loading speed of 2 mm/min and five valid measurements for each specimen, and the tensile strength of the composites was calculated according to Equation 4-2.

$$\sigma = \frac{P_r}{bh} \tag{4-2}$$

Where σ is the tensile strength (MPa), P_r is the maximum load before damage (N), and A is the cross-sectional area of the composite material (mm^2).

4.2.6 Bending performance test

In practical industrial applications, the flexural strength of a composite material can be used to assess the flexural performance of the entire material. In addition, the bending strength is also determined to some extent by the interfacial bonding of the composite material. Although positive bending stress is the main factor for material failure, fiber composite materials are also subject to internal shear damage, external

surface pressure damage, and fiber pressure damage under loading. In this paper, the composite was tested under bending according to the three-point bending test of the ASTMD790 [37] standard. The loading speed was 2 mm/min and the span-thickness ratio was 32:1. The test data were obtained for five valid samples. The bending strength of the composite material was calculated according to Equation 4-3.

$$\sigma_f = \frac{3PL}{2bd^2} \tag{4-3}$$

Where σ_f is the bending strength (MPa), P is the maximum load at which the specimen is damaged (N), L is the span distance (mm), B is the width of the sample (mm), and d is the sample thickness (mm).

4.3 Experimental results and discussion

4.3.1 In-plane shear performance analysis

4.3.1.1 In-plane shear strength analysis

In-plane shear strength is one of the criteria used to evaluate the mechanical properties of composite materials, as well as the interfacial bond strength. After the magnetron sputtering carbon fiber surface treatment process, the surface roughness of the carbon fibers increases, and the surface properties change, resulting in changes in the interfacial properties of the resulting composite material. As the CFEP samples do not undergo fracture damage in the shear test, but rather torsional deformation, the maximum shear force within 5% of the shear strain was taken as the maximum shear force of the samples, and the in-plane shear strength of the carbon fiber composites was calculated according to Equation 4-1.

Fig. 4-3 shows the in-plane shear strength of the CFEP samples. The in-plane shear strengths of the modified CFEP samples were increased. The CFEP modified under 250 W and 30 min conditions show the largest increase in the in-plane shear strength of 39.02%. When the magnetron sputtering time power was small and the sputtering time was short, the in-plane shear strength of the CFEP improved the least, e.g., the in-plane shear strength of CFEP modified under 250 W/20 min and 150 W/20 min conditions only increase by 10.22% and 10.24%, respectively.

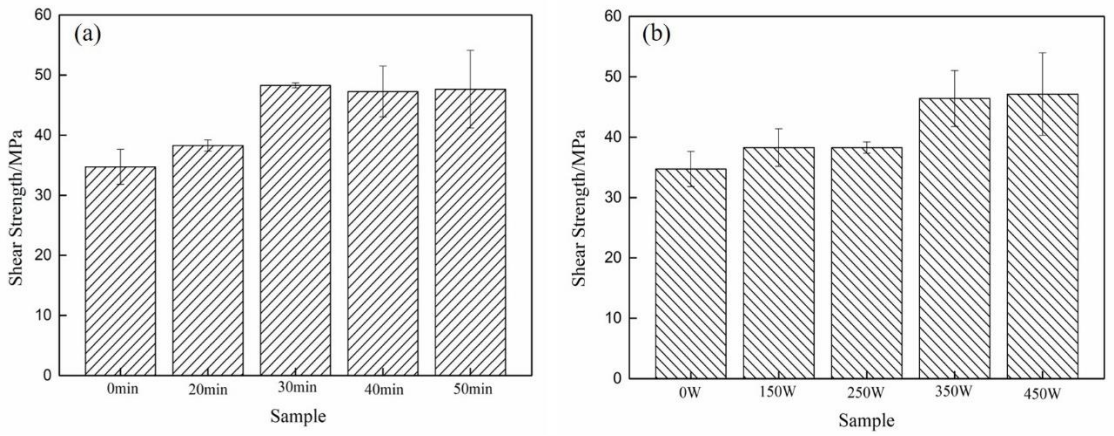

Fig. 4-3 In-plane shear strength of CFEP composites

(a) Different sputtering time (b) Different sputtering power

The shear stress-strain curve obtained for CFEP is shown in Fig. 4-4. Usually, the crack damage of the composite material initially appears at the root of the notch of the sample and this was also true for the actual test (Fig. 4-5). In addition, when crack damage occurs in the composite, it leads to a small load drop in the curve, which means that the initial load drop in the stress-strain curve was the first crack damage that occurs in the composite. Based on a comparison of the stress-strain curves obtained for CFEP before and after the modification process, it was found that the unmodified CFEP showed the earliest cracking damage. It was also found from the stress-strain curves that the shear modulus of CFEP increases significantly when the sputtering time exceeds 20 min or the sputtering power exceeds 250 W.

The surface of the untreated carbon fiber was smooth and the interfacial bonding performance between the carbon fibers and resin was poor. When an external load is applied, the interface between the fibers and resin was prone to cracking phenomenon, so crack damage occurs at the earliest stage. After the surface modification of the carbon fibers via magnetron sputtering, the constructed carbon film forms an island structure with high and low surface morphologies on the surface of the carbon fibers, which increases the surface roughness and is conducive to the enhancement of the physical engagement properties between the carbon fibers and epoxy resin. Meanwhile, after the modification process, the increase in the surface energy of the carbon fibers improves the wettability of epoxy resin to the carbon fibers, which further improves the interfacial

properties between fibers and resin. Therefore, when an external load is exerted, it will be transmitted between the interface layers, and the carbon film layer on the fiber surface will hinder the load propagation in the interface region, changing the pathway of external load propagation, forming a certain reaction force, and thus, greatly reduce the possibility of the cracking of the interface by external forces, delaying CFEP shear damage, and increasing the shear modulus.

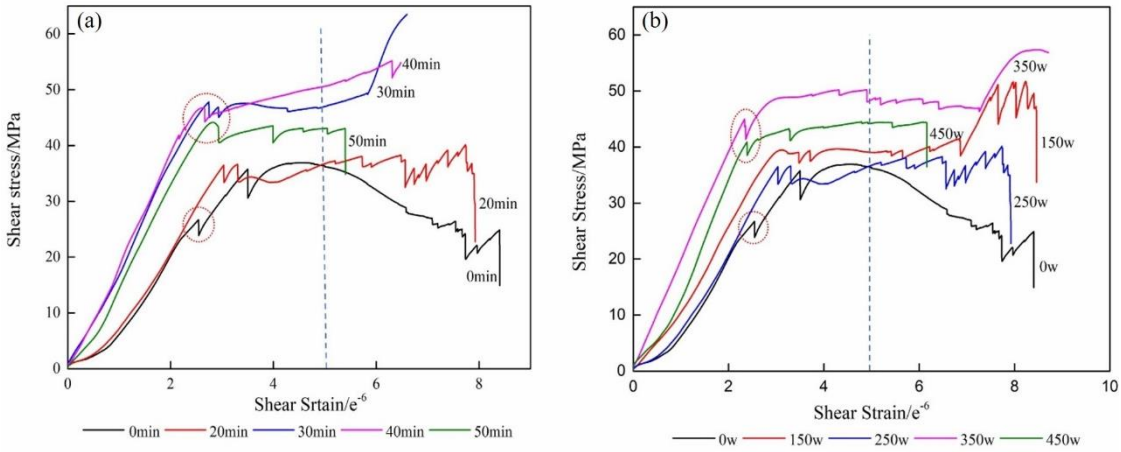

Fig. 4-4 Shear stress-strain curve of CFEP composite

(a) Different sputtering time (b) Different sputtering power

4.3.1.2 CFEP composite material shear damage morphology

The morphology of the CFEP composites after shear damage is shown in Fig. 4-5, which reveals that although the crack damage of the unmodified treated CFEP composite was also transmitted on the resin surface, it can be observed that the crack damage occurs at the edge contact interface bond formed between the carbon fibers and resin, which propagates laterally along the interface, and was accompanied by the phenomenon of carbon fiber damage. In contrast, although the crack damage of the modified CFEP composite also occurs at the root of the specimen notch, it can be found that the crack propagates at the contact interface formed between the carbon fibers and resin, and there were obvious traces of interfacial debonding, and no obvious carbon fiber damage in all forms of the damage observed in the modified CFEP.

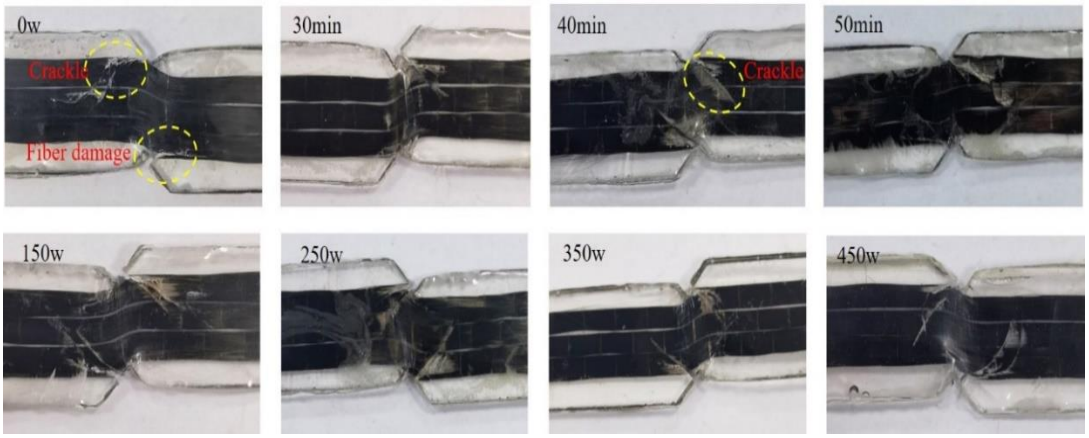

Fig.4-5 Morphology of CFEP composite after shear damage

Due to the poor interfacial bonding between the untreated carbon fibers and resin matrix, cracks were generated at the edge of the contact between carbon fibers and resin under the action of an applied load, and when the cracks reach the interface, they extend directly along the interface side, followed by debonding failure, resulting in fiber damage and destruction. After the carbon fibers were modified via magnetron sputtering, the interfacial bonding performance between the carbon fibers and resin matrix was improved, and the CFEP composite interfacial system consisting of the carbon film layer constructed on the surface of carbon fiber hinders the occurrence of cracks, changes the aspect of crack propagation, and absorbs most of the fracture energy in the form of energy sharing and redistribution. These effects result in the improvement in the interfacial bonding performance between the carbon fibers and resin. Therefore, the surface modification of magnetron sputtered carbon fibers makes the CFEP composites exhibit an enhanced in-plane shear strength.

4.3.2 Tensile performance analysis

4.3.2.1 Tensile strength analysis

The tensile strengths of CFEP composites are shown in Fig.4-6. The tensile strengths of the CFEP composites modified by the carbon fiber surface were all enhanced and the minimum increase was 13.71%. The tensile strength of the CFEP composites modified using different magnetron sputtering powers with the same magnetron sputtering time increases upon increasing the magnetron sputtering power. The tensile strength of the CFEP composites modified at 450 W increased the most

(26.16%). The tensile strengths of the CFEP composites modified at 150 and 250 W were basically the same. The tensile strength of the CFEP composites modified using the same magnetron sputtering power and different magnetron sputtering times did not increase gradually with the extension of the sputtering time, and the tensile strength of the CFEP composites treated under sputtering conditions of 250 W and 30 min increased the most. The tensile strength was increased by 22.20% when compared to the unmodified CFEP composite.

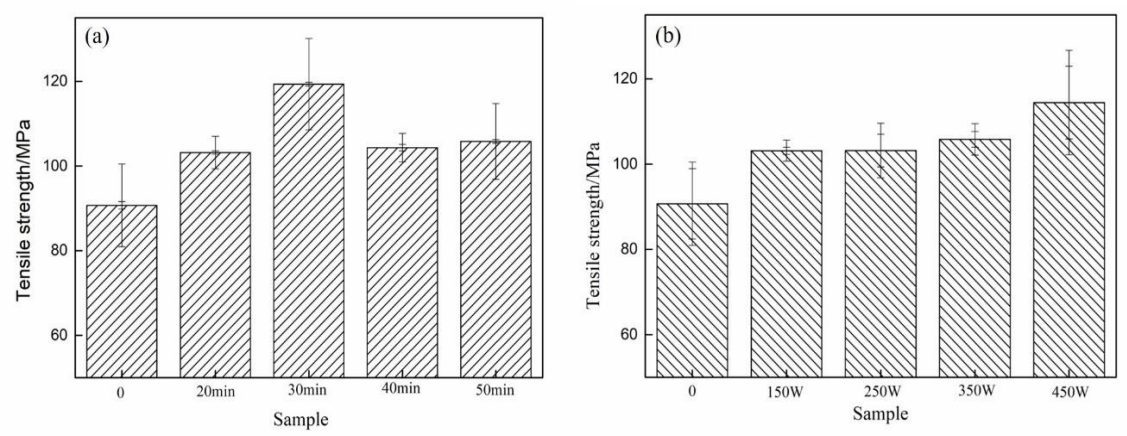

Fig. 4-6 Tensile strength of CFEP composites

(a) Different sputtering time (b) Different sputtering power

The main reasons affecting the tensile strength of the CFEP composites after modification via the magnetron sputtering process are as follows. Firstly, the surface modification of the carbon fibers via magnetron sputtering plays a role in repairing the defects on the surface of the carbon fibers, so that the mechanical properties of carbon fiber itself are improved. Secondly, the magnetron sputtering modification process also increases the surface roughness of the carbon fibers, which is beneficial to the physical engagement between the carbon fibers and resin, so that the interfacial bonding performance was improved. Finally, it was due to the presence of the carbon film on the surface of the carbon fibers that a composite interface layer was formed between carbon fibers and carbon film, and between the carbon film and resin matrix. The construction of the CFEP composite interface layer system effectively improves the transmission of cracks between the interface layers under tensile loading, so that the tensile strength of the CFEP composite was effectively improved. However, there are

differences in the structure of the carbon film layers constructed using the different magnetron sputtering modification conditions studied. Our analysis of the morphological structure of the deposited carbon films under different magnetron sputtering process conditions described in Chapter 2 shows that when the same magnetron sputtering power conditions were applied, the size of the sputtered carbon particles and compaction effect on the carbon film were the same. Therefore, the carbon films on the carbon fiber surface only differ in terms of their thickness and surface morphology. Under the different sputtering power conditions, the size of the sputtered carbon particles and compaction effect on the carbon film differ greatly, resulting in the different thickness of the carbon films, but also the different structures of the carbon film. Therefore, the tensile processes of the CFEP composites treated using the different magnetron sputtering modification processes are also different.

The tensile stress-strain tests of the CFEP composites are shown in Fig. 4-7. The tensile fracture of the unmodified CFEP composite was a brittle fracture and there is no yielding during the tensile fracture, whereas the CFEP composite modified via magnetron sputtering has stress yielding during the tensile process. The stress yielding phenomenon observed for the CFEP composites modified using the same magnetron sputtering power becomes more and more obvious with an increase in the magnetron sputtering time, and the strain also increases with an increase in the sputtering time. Similarly, the CFEP composites modified using different magnetron sputtering power also show stress yielding during the tensile process, but the stress yielding of the CFEP composites modified at 150 and 250 W was not particularly obvious, and gradually became obvious when the sputtering power exceeds 250 W. When the magnetron sputtering power was <250 W, the tensile modulus of the modified CFEP composites was comparable to that of the unmodified CFEP composite. When the magnetron sputtering power was >250 W, the tensile modulus of the modified CFEP was significantly smaller than that of the unmodified CFEP composite, and the strain of the modified CFEP composite gradually increases with an increase in the sputtering power.

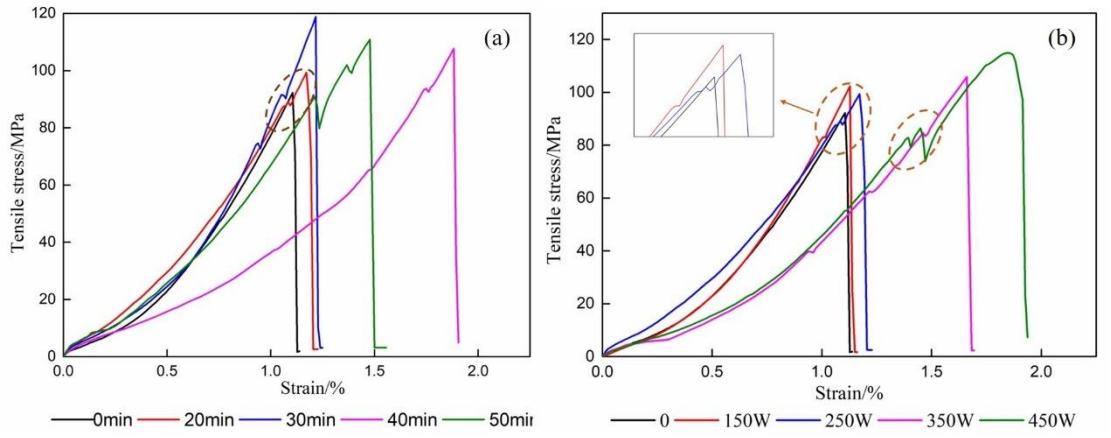

Fig. 4-7 Tensile stress-strain curves of CFET composites

(a) Different sputtering time (b) Different sputtering power

The most obvious improvement in the CFEP composites with carbon fibers modified via magnetron sputtering was observed for the tensile toughness. Under the same magnetron sputtering power conditions, the tensile fracture work of the CFEP composites gradually increases with an increase in the magnetron sputtering time. Although the CFEP composites modified for 30 min had the maximum tensile strength, the CFEP composites modified for 40 min obtained a higher tensile fracture work, which increased by 94.8% when compared with the unmodified CFEP composite. The tensile fracture work of the CFEP composite treated at 150 W increased by 30.58% although the increase was small. The tensile fracture work of the CFRP composite modified at 450 W was the largest increase of all of the modification processes studied with an increase of ~1.44 times. The stress yielding phenomenon presented during the tensile process of the CFEP composites indicates that the tensile toughness of the CFEP composites modified via magnetron sputtering was improved, but when the sputtering time was short and sputtering power was small, it was not conducive to an improvement in the tensile toughness of the CFEP composite.

4.3.2.2 Tensile section morphology of CFEP composite

Optical microscopy of the CFEP composite tensile section is shown in Fig. 4-8. The CFEP composite tensile section without the carbon fiber surface treatment has obvious cracks and the tensile fracture was untidy and toothed. In contrast, the tensile sections of the CFEP composites modified via magnetron sputtering were crack-free

under optical microscopy and the tensile fractures were neat, but there was slight fiber extraction at the fracture sites.

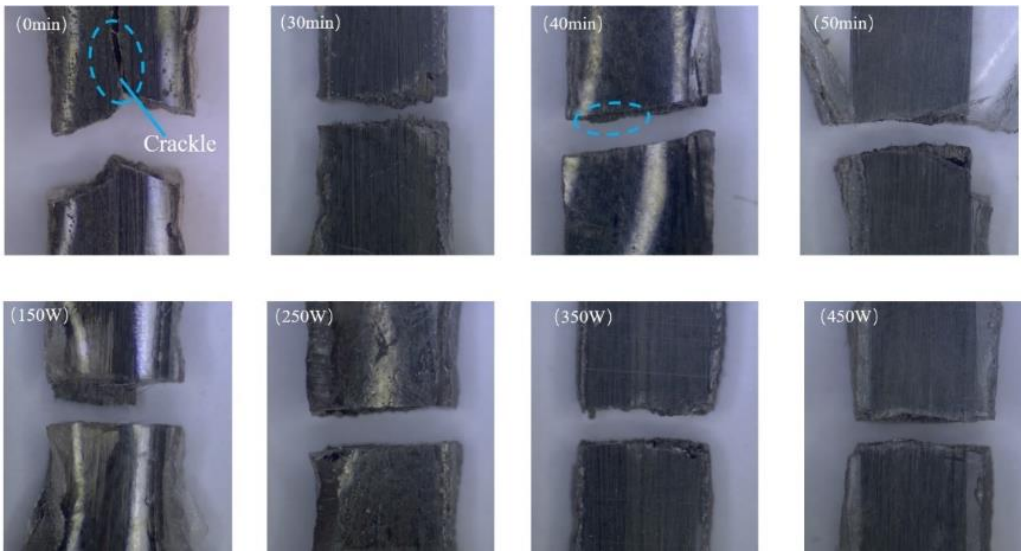

Fig. 4-8 Optical morphology of tensile fracture damage of CFEP composites

To further characterize the CFEP composites tensile damage, the tensile section of the CFEP composites was further characterized using SEM, as shown in Fig. 4-9. Fig. 4-9(a) shows the tensile section of the unmodified CFEP composite exhibits obvious cracks on the resin in the tensile section, and the carbon fibers have obvious traces of debonding and dissociation from the resin. Fig. 4-9(b) shows the tensile section of the CFEP composites modified at 250 W and 30 min. The modified carbon fibers were fully infiltrated and coated by epoxy resin, and there were no cracks and fiber extraction traces after tensile damage.

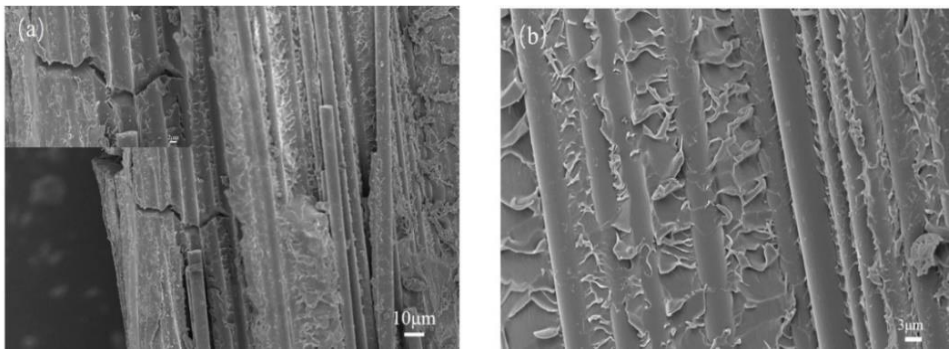

Fig. 4-9 Tensile cross-sectional morphology of CFEP composites

(a) Unmodified CFEP composite (b) Modified CFEP composited by 250w and 30min

Fig. 4-10 shows the tensile section SEM images of CFEP composite. In the tensile

fracture section of the unmodified CFEP composite, there are obvious pores between carbon fibers and resin, the pores are large, and the tensile fracture of the composites were all fiber pullout fractures. In the tensile fracture section of the modified CFEP composite, there were no obvious pore spaces between the carbon fibers and resin, and the tensile fracture damage of the composite was no longer the debonding and pulling of the fibers.

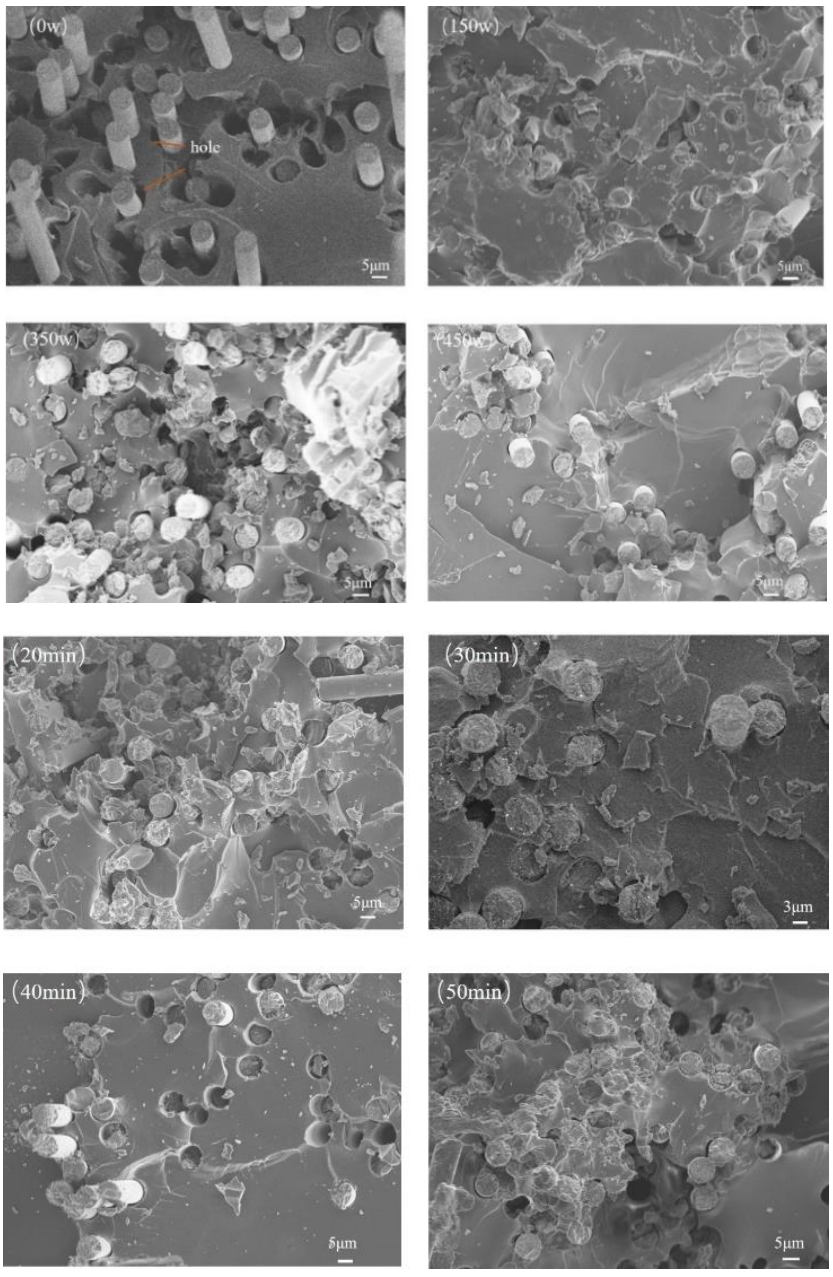

Fig. 4-10 Tensile fracture section morphology of CFEP Composite

There are three forms of tensile damage in the modified CFEP composites during the tensile process due to the presence of the interfacial system. The first is that the

CFEP composites have excellent interfacial bonding properties and carbon fiber fracture occurs during tensile damage. The second is that the carbon fiber coated with carbon film has excellent interfacial bonding properties with the resin matrix, and the bonding strength between the carbon film and carbon fibers was much stronger than the matrix phase, and the carbon fiber with the carbon film was pulled out from the polymer matrix at the tensile section, and the debonding and dissociation process occurs between the film coating layer and the matrix phase. In the other case, the carbon film was debonded from the matrix resin during the extraction process and the fibers were extracted (Fig. 4-11).

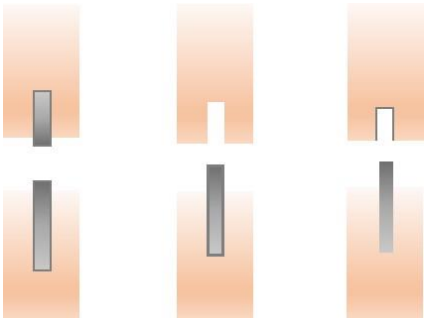

Fig. 4-11 Tensile failure mode of composite materials

Fig. 4-12 shows the cross-section of the stretched CFEP composites modified at 250 W and 30 min. The presence of the carbon film layer on the fibers after the CFEP composites were stretched can be clearly seen in Fig. 4-12 (b). This indicates that the first and second forms of the CFEP composite tensile damage are mainly dominated by the modified CFEP composites.

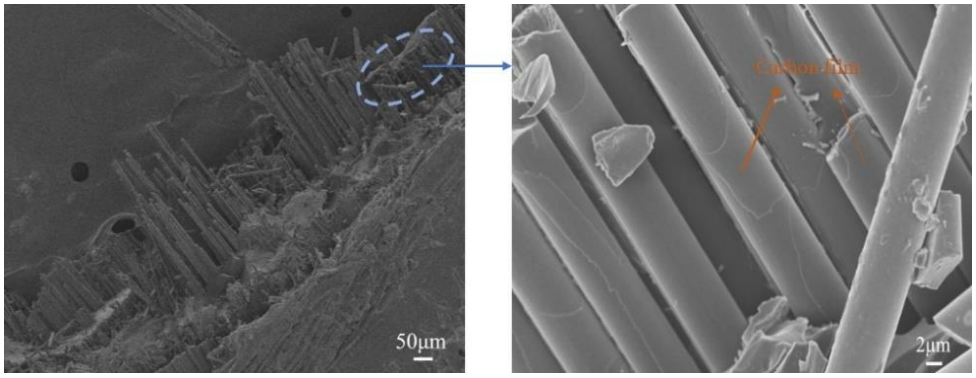

Fig. 4-12 Tensile fracture surface morphology of modified CFEP composites (250w,30min)

4.3.2.3 Tensile fracture mechanism of CFEP composite

Under tensile loading, the epoxy resin in the unmodified CFEP composite first

fractures and then cracks. The load is then transferred to the interface. With an increase in the tensile load, the cracks expand, and the adhesive between carbon fibers and matrix resin produces stress concentration. The carbon fibers were pulled out and fractured by the tensile load. As a result, the fibers pulled out in the tensile section of the CFEP composites and there are obvious cracks on the CFEP composites. Under the tensile load, the modified CFEP composites undergo epoxy resin fracture and cracking. The generated cracks are transferred to the interfacial system of the CFEP composites and transmitted on the interfacial layer, and the crack transfer process in the interfacial layer effectively improves the tensile toughness and stress concentration of the CFEP composite. The slip of the carbon film layer occurs when the crack passes through the interface layer. When debonding occurs between the carbon film and carbon fibers or between the carbon film and matrix, the carbon fibers break and the CFEP composite disintegrates. A schematic diagram of the tensile mechanism of the specific CFEP composite is shown in Fig. 4-13.

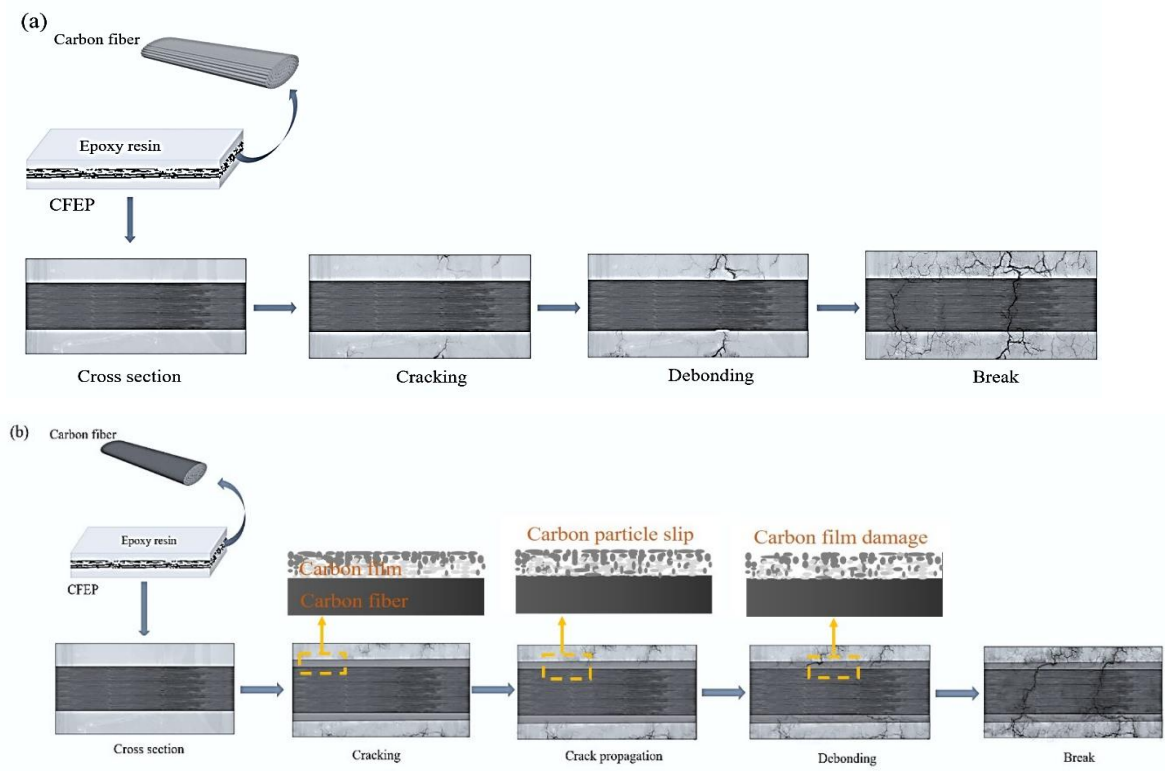

Fig. 4-13 Schematic diagram of the tensile fracture mechanism of CFEP composites

(a) The tensile fracture unmodified CFEP composited (b) The tensile fracture modified CFEP composited

4.3.3 Bending performance analysis of CFEP composite

4.3.3.1 Bending strength analysis

Fig. 4-14 shows the bending strength of the CFEP composites. The bending strength of the CFEP composites modified via magnetron sputtering increased when compared with the unmodified composite, in which the bending strength of the CFEP composites modified at 250 W and 30 min exhibits the largest increase (28.62%) and the bending strengths of the CFEP composites modified using the same magnetron sputtering power tend to increase with an increase in the sputtering time. The bending strength of the CFEP composite modified at 150 W and 20 min exhibits the smallest increase (4.96%). Although positive bending stress is the main cause of composite failure, the bending strength was also determined to some extent by the interfacial bonding properties of the composite under loading. By analyzing the bending strength of the CFEP composites, it was found that the change in the bending strength of the modified CFEP composites was consistent with the trend observed for the effect of the modification process on the surface energy of the carbon fibers. This further illustrates that the surface modification of carbon fibers via magnetron sputtering was beneficial to improving the bonding properties between the carbon fibers and resin matrix, and plays a positive role in the improvement of the mechanical properties of CFEP composites.

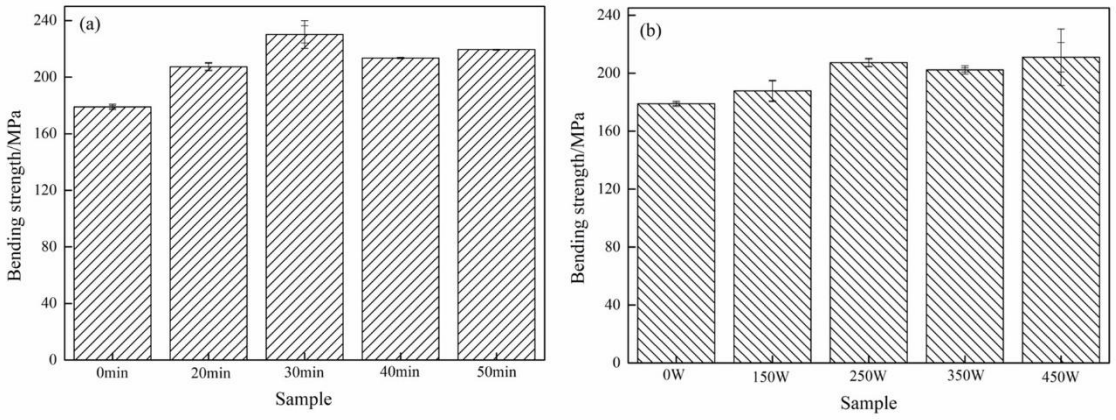

Fig. 4-14 Bending strength of CFEP composite

(a) Different sputtering time (b) Different sputtering power

The bending stress-strain curves obtained for the CFEP composites are shown in Fig. 4-15. The bending stress-strain curve of the unmodified CFEP composite shows

instantaneous damage and disintegration of the CFEP composite when the bending load stress limit was reached, which was brittle damage failure. The bending stress-strain curves of CFEP composites modified using different magnetron sputtering conditions differ depending on the conditions used. When compared with the bending stress-strain curve obtained for unmodified CFEP composites, there are two main changes. The first one is that there is a small bending yielding phenomenon in the modified CFEP composites during the loading process, such as bending damage of the CFEP composite modified at 250 W/20 min and 250 W/40 min. The second is that when the maximum bending load reaches the limit, the modified CFEP composites do not undergo brittle damage fracture. Instead, the CFEP composites undergo continuous deformation during the loading process, followed by damage failure, such as the bending damage observed for the CFEP composites modified at 250 W/30 min, 250 W/50 min, and 350 W/20 min. By comparing the effects of the different modification process conditions on the bending properties of the CFEP composites, it was found that these phenomena were more pronounced when the sputtering time changes, whereas they were relatively less affected upon variation of the magnetron sputtering power. The bending damage of the composite materials is a complex process. When the composite material was subjected to a bending load, it was also subjected to in-plane shear failure and external surface pressure, and the yielding phenomenon reflected in the bending stress-strain curves of the CFEP composites is an embodiment of tensile failure.

This comparison also reveals that the bending modulus of the CFEP composites modified at the other sputtering times was larger than the unmodified CFEP composites, except for the bending modulus of the CFEP composites modified for 20 min, which was similar to the unmodified CFEP composite. The bending modulus of the CFEP composites modified for 30 and 50 min increases significantly, especially the CFEP composite modified for 30 min, which exhibits the largest increase in the bending modulus among all of the modified specimens with an increase of 1.18 times. This was attributed to the fibers in the CFEP composites modified for 30 and 50 min having the best interfacial bonding properties with the resin matrix, and therefore exhibit stronger

integrity when the CFEP composites are subjected to bending loads, which enhances the bending modulus of the CFEP composites.

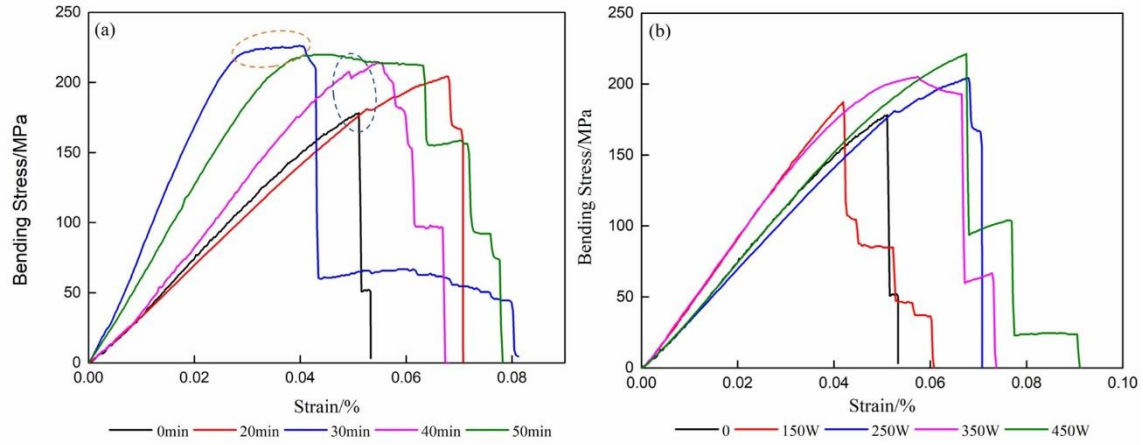

Fig. 4-15 Bending stress-strain curve of CFEP composite

(a) Different sputtering time (b) Different sputtering power

The thickness of the carbon film was favorable toward the transfer of cracks generated by the force load between the interfaces, which is conducive to the delay of the damage and destruction of the CFEP composites. Therefore, this can effectively improve the toughness and increase the damage tolerance of CFEP composites. For example, although the bending modulus of the CFEP composite modified for 20 min did not significantly improve, the energy absorbed by bending fracture increased by 65.65% when compared to the unmodified CFEP composite.

Due to their low surface energy and poor wettability with the resin matrix, the unmodified carbon fibers easily form defects, such as pores and cracks, at the interface. When the composite was subjected to a small bending load, the interface will crack. Due to the lack of an interfacial layer between the two phases, the crack peak expands in a direction directly perpendicular to the fiber reinforcement, allowing the composite to break through the physical adhesion barrier without absorbing much energy.

Carbon fibers modified via magnetron sputtering improve the surface energy of the carbon fibers due to the construction of nano-sized carbon films on the surface of the carbon fibers, which improves the wettability between the epoxy resin and surface of the carbon fibers. Moreover, the surface roughness of the carbon fibers increases after surface modification magnetron sputtering process, which increases the interfacial

engagement effect between the carbon fibers and resin, and is conducive to an enhancement in the interfacial bonding performance of the composite material.

When the composite material was subjected to an external load, the crack first reaches the interface layer from the matrix and the existence of the interface layer will cause the crack expansion direction to change from the original perpendicular to the carbon fiber direction to a more complex propagation pathway when the crack peak touches the interface phase due to the existence of the weak interface between the fibers and matrix. Consequently, more and new tiny cracks will be formed around it, more cracks will move forward, thus producing more tiny cracks. The crack propagation direction will constantly change and become more complex with the expansion and propagation of the crack, and the energy will be gradually consumed, which can effectively delay the damage to the CFEP composite. Therefore, the interface formed between the two phases modified via magnetron sputtering can slow down the crack expansion and increase the crack expansion pathway, so that the energy consumed by the composite for interfacial debonding and bending fracture increases, so the bending strength and bending modulus of the composite increases.

4.3.3.2 Bending section morphology of CFEP composite

Fig. 4-16 shows there are many microcracks on the resin matrix in the bending section of the unmodified CFEP composite and the fracture of CFEP composite has an irregular morphology, mainly via fiber delamination fracture damage. The modified CFEP composites have no obvious microcracks on the bending damage section of CFEP composite treated using the other modification conditions with the exception of the obvious resin damage on the bending damage section of CFEP modified at 250 W and 20 min. The fracture morphology of the modified CFEP composites changes significantly, but there are also slight differences depending on the magnetron sputtering modification process used. The bending fracture surface of the modified CFEP composites was mostly linear fracture, but the bending fracture of the CFEP composite treated at 250 W and 50 min showed obvious irregular fractures, but no carbon fibers were pulled out of the resin matrix, and the fibers were mainly damaged

by fracture. Meanwhile, there were obvious traces of fiber and resin gluing on the surface of the modified CFEP composites, which further indicate that the interfacial bonding properties of the CFEP composites were improved.

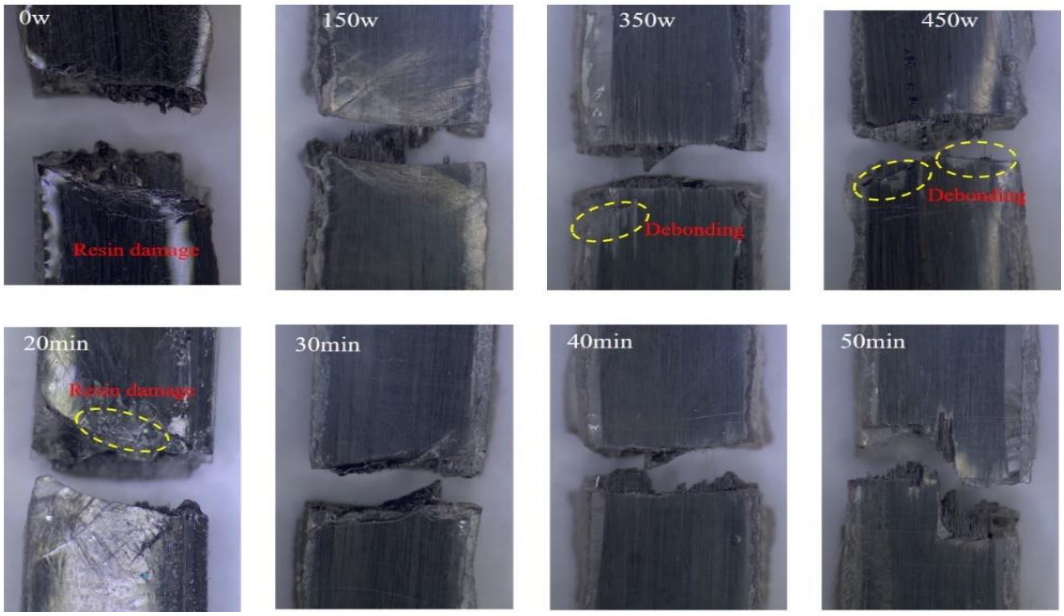

4-16 Bending damage forms of CFEP composites

Further characterization of the bending section of the CFEP composite using SEM was carried out. Fig. 4-17 shows after bending damage of the unmodified CFEP composite, a large number of carbon fibers were pulled out from the resin matrix, the surface of the pulled out carbon fibers was smooth and clean, there was no obvious residue of the matrix resin, and there were many holes left in the resin matrix at the fracture site after the fibers were completely pulled out, which indicate that the interfacial bonding between the fibers and resin was poor, and the CFEP composite could crack under a small bending load.

After the bending damage of the modified CFEP composite, the damaged fiber surface was covered by resin and carbon film. This is because after the modification of the carbon fiber via magnetron sputtering, a better mechanical engagement between the carbon fibers and matrix resin was formed, and the interfacial bonding performance was greatly enhanced. Moreover, the composite interface area between the two phases will induce and disperse cracks, thus forming a network structure of cracks in different directions. When the composite material was subjected to an applied bending load, the

cracks were transmitted between the composite interfacial layer system, and a large amount of energy was consumed as a result, thus improving the bending resistance of the composite material.

However, it was also found that the bending section of the modified CFEP composites also exhibit this fiber pullout phenomenon, which is because the surface carbon fibers and internal carbon fibers cannot obtain a uniform modification effect during the magnetron sputtering modification process of the multifilament carbon fibers, which thus affects the interfacial bonding between the internal fiber layer and resin, and when subjected to a bending load, delamination damage occurs. It can be observed from Fig. 4-17(c) and (d) that the bending fracture surface of the CFEP composites modified at 250 W and 30 min was relatively flat, and only a small amount of carbon fibers were pulled out. There was no obvious dispersion of the carbon fibers and resin fragments, which indicates the enhanced encapsulation of the carbon fibers by the resin.

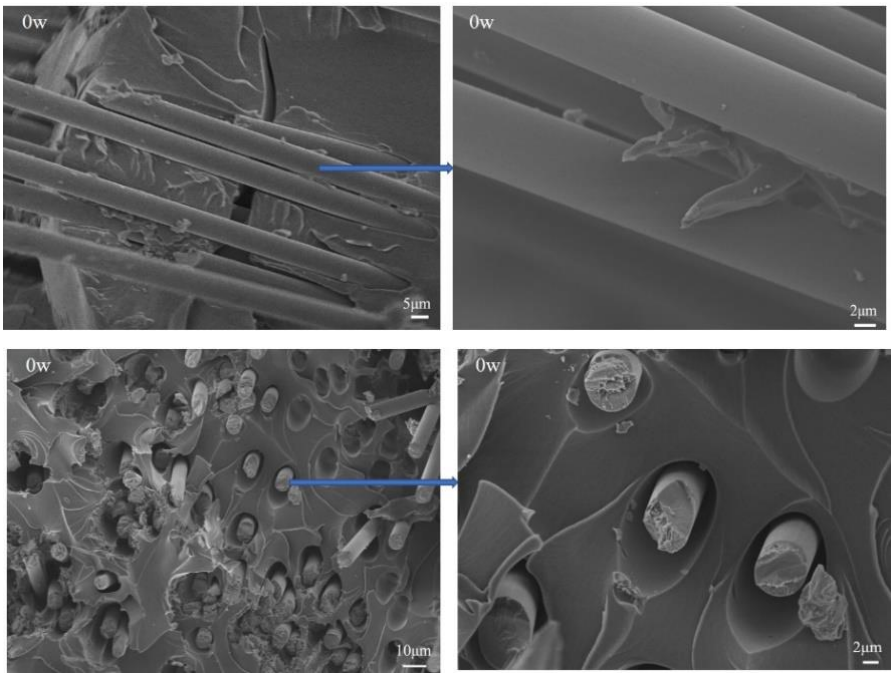

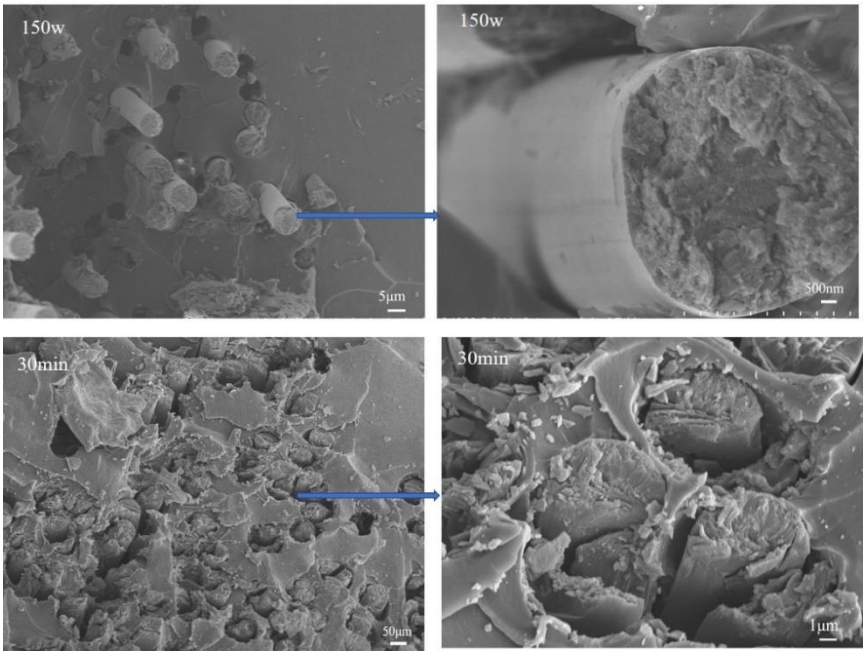

Fig. 4-17 SEM image of bending section of CFEP composite

4.3.3.3 Analysis of the bending mechanism of CFEP composite

Unmodified carbon fibers have low surface energy and poor wettability with the resin matrix due to their carbonaceous graphite structure. Defects such as pores and cracks are easily formed at the interface, and the interface bonding is poor due to the physical adsorption between the two phases. When the CFEP composite was subjected to a small bending load, cracking occurs at the interface and the load reaches the fibers directly. Due to the lack of an interfacial layer between the two phases, the crack peak expands in the direction directly perpendicular to the fiber reinforcement, making it possible for the composite to break through the physical adhesion barrier and fracture without absorbing much energy.

When the carbon fibers were modified via magnetron sputtering, the roughness and surface energy of the carbon fibers are improved due to the construction of a carbon film layer on the surface of carbon fibers. The wettability of the epoxy resin to the fibers was improved and the interfacial bonding performance of the CFEP composites was significantly enhanced. When the CFEP composite was subjected to an external load, the crack first reaches the interface layer from the matrix, and the existence of the interface layer will make the crack expansion direction change from the original perpendicular to the carbon fiber direction to a more complex propagation pathway, and

when the crack peak touches the interface layer system, more tiny cracks will be formed around it, more cracks will move forward. The crack propagation process continues, the propagation direction constantly changes, and as the cracks expand and propagate, the energy will be consumed gradually, unlike the unmodified carbon fiber reinforced dimensional composites, in which the cracks can advance unhindered and directly impact the carbon fiber, leading to the destruction of the fiber and the whole composite material because of the existence of the interfacial layer. Therefore, the interface formed by the constructed carbon film between the two phases can slow down the expansion of the cracks and increase the crack expansion pathway, making the energy consumed in the interface debonding and bending fracture of the composite increase, so the bending strength and bending modulus of the composite increases. However, due to the different magnetron sputtering process conditions, the structure of the carbon film built on the interface layer varies. When the carbon film layer is thinner, the effect of the load in slowing down the crack propagation and expansion between the interface layers is weakened, the complexity of the crack propagation direction and propagation pathway is weakened, and the energy consumed by the crack expansion is reduced. When the thickness of the two-phase interface layer decreases, the energy absorbed by the debonding and fracture of the composite interface decreases when subjected to an applied bending load, resulting in a decrease in the bending properties of the CFEP composite and a decrease in the bending strength and bending modulus values. The mechanism is shown in the Fig.4-18.

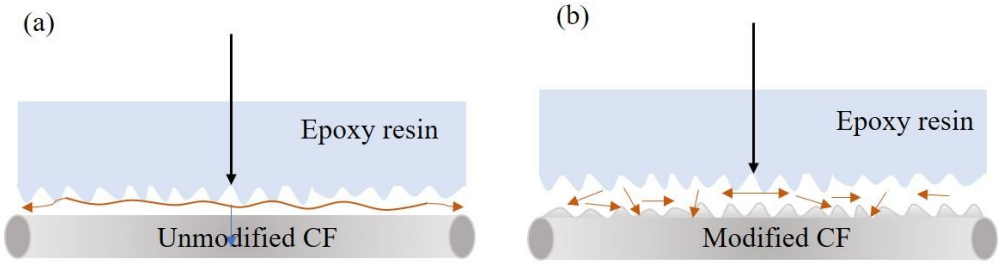

Fig. 4-18 Bending fracture mechanism of CFEP composites

4.4 Conclusion

After the surface modification of carbon fibers via magnetron sputtering, the interfacial bonding between the carbon fibers and resin matrix is improved. The

mechanical properties of the resulting CFEP composites are improved and the mechanical damage mechanism changed due to the construction of a carbon film on the surface of the carbon fibers, which not only improves the mechanical damage strength, but also improves the toughness of the CFEP composites. The specific conclusions are as follows:

The in-plane shear strength of the CFEP composites modified via magnetron sputtering increased, and the CFEP composite modified at 250 W/30 min exhibited the largest increase in-plane shear strength with an increase of 39.02%. When the magnetron sputtering power is low and the sputtering time is short, the increase rate is small due to the small increase in the carbon fiber surface energy, such as the in-plane shear strength of CFEP composites modified at 250 W/20 min and 150 W/20 min only increased by 10.22% and 10.24%, respectively. The shear modulus of the CFEP composites modified via magnetron sputtering was also significantly improved.

When the modified CFEP composites were subjected to shear load, the time of crack damage was delayed, and the cracks produced by the modified CFEP composites propagated along the interface of carbon fiber and resin contact to produce interfacial debonding, but no obvious carbon fiber damage occurred during shear loading. After modification of the carbon fibers via magnetron sputtering, the tensile properties of the resulting CFEP composites are greatly improved due to the increase in the surface roughness and improvement in the intrinsic properties, as well as the role of the composite interface layer between the carbon fiber composites.

After the modification of carbon fiber by magnetron sputtering, the tensile properties of CFEP composites are greatly improved due to the increase of surface roughness and the improvement of intrinsic properties, as well as the effect of the composite interfacial layer between the interfaces of CFEP composites. Firstly, the tensile strength of the modified CFEP composites increased significantly when compared with the unmodified CFEP composite; the tensile strength exhibited a minimum increase of 13.71% and maximum increase of 31.54%. Secondly, the tensile fracture toughness of the CFEP composites modified via magnetron sputtering was

greatly improved, and the tensile fracture work of the modified CFEP composites increased by a maximum of about 1.44 times when compared to the unmodified CFEP composite. In addition, the modified CFEP composites exhibit stress yielding phenomenon in the tensile tests, which avoids the brittle damage of the CFEP composites.

The bending strengths of the CFEP composites modified via magnetron sputtering has not been significantly improved with a maximum increase of 28.62% and the minimum increase is only 4.96%. However, the bending modulus of the modified carbon fiber composites has been greatly improved, and the bending modulus of the carbon fiber composites modified at 250 W for 30 min was increased by 1.18 times.

Similarly, the bending damage form and damage mechanism of the CFEP composites prepared using the carbon fibers modified via magnetron sputtering are also changed. As the interface meshing performance between the modified carbon fibers and resin matrix is improved, the carbon fibers are effectively covered and bonded together by the resin after modification, and the pore space between the carbon fiber and resin matrix is significantly reduced; even after damage fracture under a bending load, it will not show the appearance of larger pore space between the carbon fibers and resin matrix. According to the different magnetron sputtering processes studied, the phenomenon of internal fiber damage will occur in the CFEP composite during bend loading.

References

[1] T. K. Das, P. Ghosh, N. C. Das. Preparation, development, outcomes, and application versatility of carbon fiber-based polymer composites: a review. Adv. Compos. Hybrid Mater.2019(2):214-233

[2] N. Forintos, T. Czigany. Multifunctional application of carbon fiber reinforced polymer composites: electrical properties of the reinforcing carbon fibers-a short review. Composites Part B. 2019(162): 331–343

[3] N. Hiremath, S. Young, H. Ghossein, D. Penumadu, U. Vaidya, M. Theodore. Low cost textile-grade carbon fiber epoxy composites for automotive and wind energy applications. Composites Part B. 2020(198):108156

[4] J.D. Schaefer, A.J. Rodriguez, M.E. Guzman, C.S. Lim, B. Minaie, Effects of electrophoretically deposited carbon nanofibers on the interface of single carbon fiber embedded in epoxy matrix. Carbon. 2011. 49: 2750–2759

[5] Schaefer J D, Guzman M E, Lim C S, Rodriguez A J and Minaie B. Influence of functionalized carbon nanofibers on the single carbon fiber–epoxy matrix interface Composites Part B: Engineering. 2013,55 41–47

[6] B.W. Qiu, M.X. Li, X.Q. Zhang, Y. Chen, S.T. Zhou, M. Liang, H.W. Zou. Carboxymethyl cellulose sizing repairs carbon fiber surface defects in epoxy composites. Materials Chemistry and Physics. 2021.258:123677

[7] Yao S S, Jin F L, Rhee K Y, Hui D and Park S J. Recent advances in carbon fiber reinforced thermoplastic composites: a review. Composites Part B: Engineering. 2018,142 241–50

[8] Liu Y, Zhang X, Song C, Zhang Y, Fang Y and Yang B 2015 An effective surface modification of carbon fiber for improving the interfacial adhesion of polypropylene. Composites Material Design. 88 810–9

[9] S.B. Zhang, Q.L. Dai. The surface modification of carbon fiber for thermoplastic HDPE composites. Surface Interface Analysis. 2018.51: 184–189

[10] G.J. Yang, M. Park, S.J. Park. Recent progresses of fabrication and characterization of fibers-reinforced composites: A review. Composites Communication. 2019. 14:34-

42

[11] M.W. Ren, L.Y. Liu, G.H. Fan, Y.B. Chen, K.W. Gao, Y.S. Zhou. Recent research of surface modification and reconstruction of carbon fiber. New Chemical Materials. 2018. 46: 40–3

[12] H. Manwar, N. Atsushi, N. Koichi, Mechanical property improvement of carbon fiber reinforced epoxy composites by AL_2O_3 filler dispersion. Materials Letters. 1996. 26: 185–191

[13] T. M. Loganathan, M. T. A. Sultan, M. Jawaid, Q. Ahsan, J. Naveen, A. U. M. Shan, A. R. A. Talib, A. A. Basri. Physical, mechanical, and morphological properties of hybrid cyrtostachys renda/kenaf fiber reinforce with multi-walled carbon nanotubes (MWCNT)-phenolic composites Polymers. Polymers. 2021. 19:3448

[14] S.P. Sharma, S.C. Lakkad. Effect of CNTs growth on carbon fibers on the tensile strength of CNTs grown carbon fiber reinforced polymer matrix composites. Composites Part A: Applied Science and Manufacturing. 2011. 42: 8–15

[15] X.M. Yao, X.Y. Gao, J.J. Jiang, C.M. Xu, C. Deng, J.B. Wang. Comparison of carbon nanotubes and graphene oxide coated carbon fiber for improving the interfacial properties of carbon fiber/epoxy composites. Composites Part B: Engineering. 2018. 132:170-177

[16] S.J. Shen, L.W. Yang, C.Y. Wang, L.M. Wei. Effect of CNT orientation on the mechanical property and fracture mechanism of vertically aligned carbon nanotube/carbon composites. Ceramics International. 2020. 46: 4933–4938

[17] R.H. Zhang, X.T. Shi, L. Tang, Z. Liu, J.L. Zhang, Y.Q. Guo, J.W. Gu. Thermally conductive and insulating epoxy composites by synchronously incorporating Si-sol functionalized glass fibers and boron nitride fillers Chinese Journal of Polymer Science. 2020. 38: 730–739

[18] L. Tang, M.K. He, X.Y. Na, X.F. Guan, R.H. Zhang, J.L. Zhang, J.W. Gu. Functionalized glass fibers cloth/spherical BN fillers/epoxy laminated composites with excellent thermal conductivities and electrical insulation properties. Composites Communications 2019.16: 5–10

[19] H.L. Cao, Y.C. Shi, H. Shen, H.D. Zhan, J.R. Liu. The production of core–shell structure carboxylated carbon nanotubes/polypyrrole composite materials in different reaction media and further investigation on their core–shell structure. Key Eng. Mater. 2017.730: 37–41

[20] B.K. Deka, K. Kong, J. Seo, D.Y. Kim, Y.B. Park, H.W. Park. Controlled growth of CuO nanowires on woven carbon fibers and effects on the mechanical properties of woven carbon fiber/polyester composites. Composites Part A: Applied Science and Manufacturing. 2015. 69:56-63

[21] W. Yuan, J. Luo, B.Y. Pan, Z.Q. Qiu, S.M. Huang, Y. Tang. Hierarchical shell/core CuO nanowire/carbon fiber composites as binder-free anodes for lithiumion batteries. Electrochimica Acta. 2017. 241:261-271

[22] N. Zheng, Y.D. Huang, W.F. Sun, X.S. Du, H.Y. Liu, S. Moody, J.F. Gao, Y.W. Mai. In-situ pull-off of ZnO nanowire from carbon fiber and improvement of interlaminar toughness of hierarchical ZnO nanowire/carbon fiber hydrid composite laminates. Carbon. 2016. 110:69-78

[23] M. Parisa, M. Abshirini, M. Saha, L.L. Huang, Y.T. Liu. Interfacial properties of ZnO nanowire-enhanced carbon fiber composites: A molecular dynamics simulation study. Langmuir. 2021.37:7138-7146

[24] G.J. Ehlert, U. Galan, H.A. Sodano. Role of surface chemistry in adhesion between ZnO nanowires and carbon fibers in hybrid composites. The Journal of Physical Chemistry. 2013. 5: 635-645

[25] Y.R. Lin, G. Ehlert, H.A. Sodano. Increased interface strength in carbon fiber composites through a ZnO nanowire interphase. Advanced Functional Materials. 2009. 19:2654-2660

[26] L. Xiong, F. Zhan, H.B. Liang, L. Chen, D.S. Lan. Chemical grafting of nano-TiO_2 onto carbon fiber via thiol-ene click chemistry and its effect on the interfacial and mechanical properties of carbon fiber/epoxy composites. Composites. 2018. 53:2594-2603

[27] B. Pant, G.P. Ojha, Y.S. Kuk, O.H. Kwon, Y.W. Park, M. Park. Synthesis and

characterization of ZnO-TiO2/carbon fiber composites with enhanced photocatalytic properties. Nanomaterials. 2020.10:1960

[28] L.C. Ma, N. Li, G.S. Wu, G.J. Song, X.R. Li, P. Han, G. Wang, Y.D. Huang, Interfacial enhancement of carbon fiber composites by growing TiO2 nanowires onto amine-based functionalized carbon fiber surface in supercritical water. Applied Surface Science. 2018.433: 560-567

[29] J. Misumi, T. Oyama. Low viscosity and high toughness epoxy resin modified by in situ radical polymerization method for improving mechanical properties of carbon fiber reinforced plastics. Polymer. 2018. 156:1-9

[30] X.Q. Mi, N. Liang, H.F. Xu, J. Wu, Y. Jiang, B. Nie, D.H. Zhang. Toughness and its mechanisms in epoxy resins. Progress in Materials Science. 2022. 130:100977

[31] J.C. Capricho, B. Fox, N. Hameed. Multifunctionality in epoxy resins. Polymer Reviews. 2020.60:1-41

[32] ISO 527-3 Plastics -determination of tensile properties -Part 3: Test conditions for films and sheets

[33] N. Saba, M. Jawaid, M.T.H. Sultan. An overview of mechanical and physical testing of composite materials. Mechanical and Physical Testing of Biocomposites, Fibre-Reinforced Composites and Hybrid Composites. 2019.1-12

[34] B. Gregory, Mckenna. Interlaminar effects in fiber-reinforced plastics- A review. Polymer-Plastics Technology and Engineering. 1975. 5: 23-53

[35] ASTMD5379/D5379M-05: Standard test method for shear properties of composite materials by the V-notched beam method

[36] ASTMD3039-08:2008 Standard test method for tensile properties of polymer matrix composites materials

[37] ASTMD790-10: 2010 Standard test method for flexural properties of unreinforced and reinforced plastics and electrical insulating materials.

[38] L.Y. Han, K.Z. Li, J.J. Sun, Q. Song, Y.W. Wang. Reinforcing effects of carbon nanotube on carbon/carbon composites before and after heat treatment. Materials Science and Engineering A. 2018. 735: 10-18

Chapter 5

Conclusion

Chapter 5: CONCLUSION

The mechanical properties of carbon fibers are affected by surface defects. Additionally, the smooth surface of carbon fibers and the lack of surface active functional groups leads to weak interfacial bonding between carbon fibers and the resin matrix, which affects the performance of the CFRP composite. To improve the mechanical properties of carbon fibers and enhance the interfacial bonding properties between carbon fibers and the resin matrix, magnetron sputtering technology was used to modify the carbon fiber surface and repair the surface defects by exploiting the homogeneity of the sputtering target and carbon fibers. Owing to the carbon film constructed on the carbon fiber surface, the interfacial bonding between the carbon fibers and resin matrix is strengthened, which provides a new method for carbon fiber surface repair and interfacial modification of carbon fiber-reinforced resin matrix composites.

In Chapter 1, an overview of the interface mechanism of carbon fiber composites and carbon fiber surface modification technology was presented, and the magnetron sputtering process and film-formation process were described. Additionally, the reasons why magnetron sputtering was selected for the surface modification of carbon fibers were explained.

In Chapter 2, the morphology and structural properties of carbon films deposited via magnetron sputtering were analyzed, and the effects of different substrates and magnetron sputtering process parameters on the structural properties of carbon films were discussed.

Magnetron sputtering deposited carbon films on different substrates exhibit a surface morphology with microcracks and a cross sectional morphology with a columnar structure, but owing to the curved morphology of carbon fibers, the surface morphology of carbon fibers differs slightly from the morphology of carbon films deposited on silicon wafers with regard to microcrack and pores. The magnetron sputtering modification method has no obvious effect on the microstructure or phase composition of carbon fibers and does not affect the physicochemical properties of

CFRP composites. Heat treatment changes the surface morphology and cross-sectional morphology of the carbon film. The surface of the carbon film changes from a particle stacking structure to a sheet-like crystal structure, the cross-sectional columnar structure disappears, the structure becomes more ordered, and the mechanical properties are enhanced.

In Chapter 3, the effects of the magnetron sputtering modification process on the mechanical properties and surface properties of carbon fibers were examined. After the modification of carbon fibers by magnetron sputtering, a carbon film was deposited on the carbon fiber surface. The carbon nanoparticles repaired the surface defects of the carbon fibers, and the mechanical properties of the carbon fibers were improved—particularly the tensile fracture work and tensile fracture strength dispersion. Among the magnetron sputtering modification conditions used in this study, the maximum increase in the tensile fracture work of the carbon fibers was 23%. The surface energy of the carbon fibers was also improved by magnetron sputtering modification, indicating that this treatment is suitable for improving the interfacial bonding properties of carbon fiber composites.

In Chapter 4, the in-plane shear properties, tensile properties, and bending properties of CFRP composites modified by the magnetron sputtering process were discussed, and the effects of the magnetron sputtering process on the mechanical properties of CFRP composites were analyzed, as well as the damage mechanism. The surface modification of carbon fibers by magnetron sputtering can increase the surface roughness and surface energy of the carbon fibers, which is conducive to mechanical engagement between the modified carbon fibers and the resin matrix. After the surface modification of the carbon fibers by magnetron sputtering, a composite interface layer with a carbon film structure was formed in the interface layer of the CFRP composites, and the composite interface layer effectively transmitted the cracks produced by the composite during load loading, which delayed the mechanical damage of the modified CFRP composites, improving their toughness.

In Chapter 5, the effects of the magnetron sputtering process on the surface

morphology and microstructure properties of carbon fibers were investigated, and the feasibility of magnetron sputtering carbon fiber surface modification for the repair of carbon fiber surface defects and improvement of the mechanical properties, as well as the interfacial properties and mechanical properties of CFRP composites, was confirmed.

The successful implementation of interfacial modification of CFRP composites by magnetron sputtering provides a new method for undamaged interface modification, and also provides a theoretical basis for the construction of nanocomposite interfaces and a new idea for the subsequent construction of multi-scale layer interfaces of CFRP composites.

ACCOMPLISHMENTS

LIST OF PUBLICATION

Journal Publications

[1] Li Yang, Hong Xia, Zhenzhen Xu, LiHua Zou, Qingqing Ni. Influence of surface modification of carbon fiber based on magnetron sputtering technology on mechanical properties of carbon fiber composites. Materials Research Express. 7 (2020) 105602

[2] Li Yang, Yuan Chen, Zhenzhen Xu, Natuski Toshiaki, Yusong Xi, Qingqing Ni. Effect of heat treatment on mechanical property of amorphous carbon films by magnetron sputtering. Diamond & Related Materials. 129 (2022)109328

[3] Li Yang, Yuan Chen, Zhenzhen Xu, Hong Xia, Toshiaki Natuski, Yusong Xi, Qingqing Ni. Effect of surface modification of carbon fiber based on magnetron sputtering technology on tensile properties. Carbon. 204(2023)377-386

ACKNOWLEDGMENTS

First and foremost, I would like to express my sincere gratitude to my supervisor Prof. Qing-Qing Ni for providing me the opportunity to study in Shinshu University, and I also thankful for his support and guidance throughout my PhD period. The knowledge and assistance given by him from time to shall carry me a long way in the journey of life on which I am about to embark.

I am also grateful to Prof. Toshiaki Natsuki as my co-supervisor and co-referee, for his valuable and constructive suggestions during the development of this research work. Without his enthusiastic encouragement and useful critiques, this research would not have been successful.

Meanwhile, I like to express my gratitude to Dr. Hong Xia for her continuous guidance and support to my research work. Special thanks to all former and current members of Ni Lab (Dr. Jun Hong, Dr. Yajun Liu, Dr. Hao Wang, Dr. Jingyan Qu,) for their assistance and suggestions on my research.

I want to express my special thanks to Prof. Zhenzhen Xu at Anhui Polytechnic University for their suggestions and warm encouragement, which have boosted my research work.

Finally, I would like to thank my beloved families for their support, understanding and concern during my PhD period. I also want to thank all my friends at Shinshu University.

Thank you

Yang Li